

L

Lac Carrier Protein

- ▶ [H⁺-Lactose Membrane Transport Protein, LacY](#)

Lactate Dehydrogenase

- ▶ [Protein Dynamics: Time-Resolved Spectroscopic Studies](#)

Lactate Dehydrogenase – Computational Studies

Marc Willem van der Kamp
Centre for Computational Chemistry, School of
Chemistry, University of Bristol, Bristol, UK

Synonyms

[LDH](#)

Definition

An enzyme that catalyzes the interconversion of pyruvate and lactate.

Basic Characteristics

Several classes of lactate dehydrogenases exist, dependent on whether NAD(P)H or cytochrome *c* is used as cofactor and whether the enzyme acts on D-lactate or L-lactate. The most widely studied class is the NAD(P)H dependent enzyme that catalyzes conversion of pyruvate (the final product of glycolysis) into lactate in animal tissues when oxygen is limited, and the reverse reaction in the liver (in the so-called Cori cycle, or lactic acid cycle). Computer molecular simulation and modeling studies of the reaction have been used to investigate and illustrate general catalytic principles (Yadav et al. 1991; Wilkie and Williams 1992). LDH has also been used as a test system in development of new methods for modeling enzyme reactions (such as QM/MM transition state optimization (Turner et al. 1999)). Ferrer et al. calculated two-dimensional potential energy profiles at the AM1/CHARMM22 level, with energy corrections at the MP2 ab initio level (Ferrer et al. 2005): They modeled the hydride transfer from the dihydronicotinamide ring of NADH to the carbonyl C atom of pyruvate, as well as the proton transfer to the carbonyl O atom from a protonated catalytic histidine. As well as pointing out the importance of considering multiple protonation states of active site residues in QM/MM modeling, they established that the reaction probably occurs through an asynchronous concerted reaction pathway in which hydrogen transfer precedes proton transfer. This picture may change, however, when active site residues are mutated: They also modeled the effects of mutations (Ferrer et al. 2008).

Cross-References

► [QM/MM Methods](#)

References

- Ferrer S, Silla E, et al. Dependence of enzyme reaction mechanism on protonation state of titratable residues and QM level description: lactate dehydrogenase. *Chem Commun.* 2005; (47):5873–5
- Ferrer S, Tunon I, et al. Theoretical site-directed mutagenesis: Asp168Ala mutant of lactate dehydrogenase. *J R Soc Interface.* 2008;5:S217–24.
- Turner AJ, Moliner V, et al. Transition-state structural refinement with GRACE and CHARMM: flexible QM/MM modelling for lactate dehydrogenase. *Phys Chem Chem Phys.* 1999;1(6):1323–31.
- Wilkie J, Williams IH. Transition-state structural variation in a model for carbonyl reduction by lactate dehydrogenase: computational validation of empirical predictions based upon Albery-More O’Ferrall-Jencks diagrams. *J Am Chem Soc.* 1992;114(13):5423–5.
- Yadav A, Jackson RM, et al. Role of solvent reorganization energies in the catalytic activity of enzymes. *J Am Chem Soc.* 1991;113(13):4800–5.

Lactose Permease

► [H⁺-Lactose Membrane Transport Protein, LacY](#)

Laser Capture Microdissection

► [Laser Processing of Biomaterials and Cells](#)

Laser Doppler Electrophoresis (LDE)

► [Electrophoretic Light Scattering](#)

Laser Processing of Biomaterials and Cells

Shelby Skoog and Roger Narayan
Joint Department of Biomedical Engineering,
University of North Carolina and North Carolina State
University, Raleigh, NC, USA

List of Abbreviations

Alq3	tris(8-hydroxyquinolinato) aluminium
ArF	argon fluoride
DNA	deoxyribonucleic acid
IR	infrared
KrF	krypton fluoride
MEH-PPV	poly[2-methoxy-5-(2'-ethylhexyloxy)-p-phenylene vinylene]
PEG	poly(ethylene glycol)
PGA	poly(glycolic acid)
PLA	poly(lactic acid)
PLGA	poly(lactic-co-glycolic acid)
PMMA	poly(methyl methacrylate)
RNA	ribonucleic acid
Mn12-acetate	Mn ₁₂ O ₁₂ (CH ₃ COO) ₁₆ (H ₂ O) ₄ ·2CH ₃ COOH·4H ₂ O
NPP	N-(4-nitrophenyl)-(l)-prolinol
UV	ultraviolet

Synonyms

[Fabrication of biomaterials](#); [Laser capture microdissection](#); [Laser-based materials engineering of medically relevant materials](#)

Definition

Laser processing of biomaterials is the application of laser-based techniques for fabrication and/or analysis of medically-relevant materials and biological systems.



Introduction

Light amplification by stimulated emission of radiation (laser) has been used for materials processing since the early 1960s. Lasers are employed for a variety of materials processing techniques, including coating, machining, polymerizing, melting, sintering, and welding (Narayan and Goering 2011). Through these unique capabilities, lasers may be used to form intricate geometries, alter material properties, and surface engineer complex materials. Laser-based surface engineering involves melting, heating, or modifying the surface of a given material; it may be used to prepare surfaces with micro- and nanoscale features (Prodanov et al. 2011). Lasers are highly advantageous instruments for materials engineering as they may be used for processing of a broad range of materials, including metals, ceramics, polymers, and biomaterials. Since these processes do not involve laser-material contact, contamination and substrate damage are minimized (Stratakis et al. 2009).

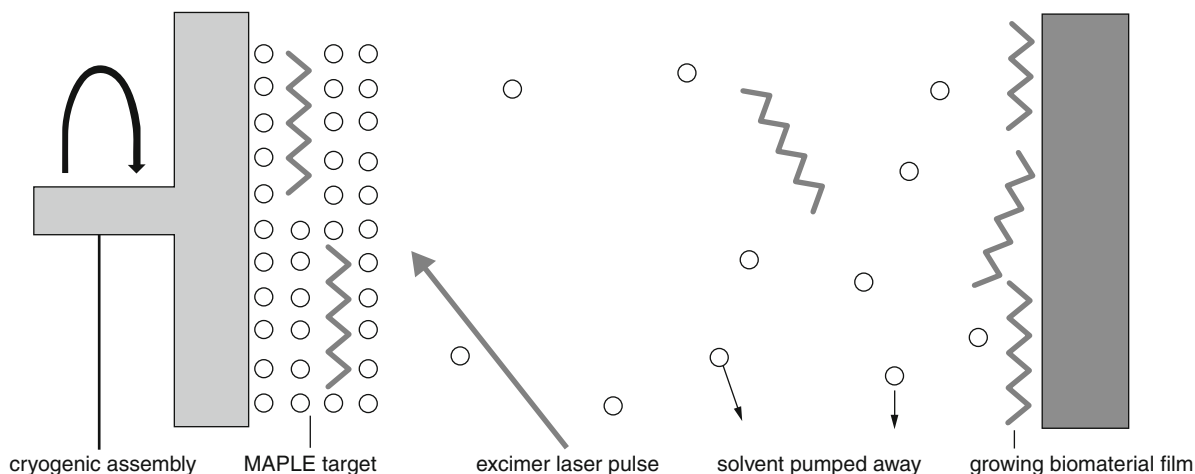
Due to the unique capabilities offered by laser processing, laser-based methods have been widely used in clinical medicine for diagnosis and treatment of diseases as well as for fabrication of medical devices. The earliest efforts utilizing laser-material interactions for development of biomedical devices involved laser welding of dental biomaterials. For example, lasers have been used to join together components of dental appliances such as dental brackets, crown units, and partial dental prostheses (Narayan and Goering 2011). Since this early research involving laser-based biomaterials, laser technology has rapidly evolved. Novel fabrication methods have been introduced, which provide a variety of laser processing capabilities. These laser-based techniques have become widely used for biomaterials fabrication as well as for analytical evaluation of biological structures and processes.

In this entry, three laser-based techniques for processing of biomaterials are described, including matrix-assisted pulsed laser evaporation, laser capture microdissection, and optical tweezers. Each of these processes provides unique capabilities for manipulation of biomaterials and tissues. The advantages and limitations of these processes are discussed as well as future prospects.

Matrix-Assisted Pulsed Laser Evaporation

Matrix-assisted pulsed laser evaporation (MAPLE) is a physical vapor deposition process that was created in the late 1990s at the US Naval Research Laboratory (Pique 2011). This process was originally developed to overcome the decomposition of polymeric target materials associated with traditional pulsed laser deposition (PLD) (Caricato and Luches 2011). In MAPLE, the material to be deposited is diluted in a highly volatile solvent to form a matrix, which is flash frozen in liquid nitrogen. The frozen matrix is placed in a vacuum chamber and is used as a target. When the frozen matrix is irradiated with a pulsed laser beam, the volatile solvent absorbs the laser energy. This energy is converted into thermal energy, causing the solvent to vaporize. Kinetic energy from the collisions between the solvent and solute molecules causes the solute material to transfer into the gaseous phase. When both material species are expelled from the target, the volatile solvent is pumped away and the solute material is transferred onto the substrate, forming a thin film (Caricato and Luches 2011; Patz et al. 2007). A schematic of the MAPLE process is shown in Fig. 1.

The primary goals of MAPLE are to preserve the structural and functional integrity of the materials, to control the thickness and uniformity of the film, to obtain desirable surface features, and to obtain adequate adhesion between the substrate and the deposited film (Caricato and Luches 2011). Control over the MAPLE processing parameters permits excellent control over multiple film characteristics, including thickness, surface morphology, and homogeneity. An excimer laser (KrF: 248 nm or ArF: 193 nm) with a pulse width of 10–30 ns and a repetition rate between 1 and 10 Hz is generally utilized for MAPLE processing. The laser is typically focused to a 1–10 mm² area, providing a laser fluence of 0.01–1.0 J/cm². MAPLE is capable of depositing uniform thin films over a broad range of thicknesses (10 nm to 1 μm) and over areas greater than 1 cm² (Pique 2011). Operating conditions are dependent on the solute and solvent materials; numerous processing parameters may be optimized to obtain the desired thin film properties. Studies have demonstrated that the material properties of the deposited film are strongly dependent on matrix composition (e.g., solute



Laser Processing of Biomaterials and Cells, Fig. 1 Schematic of the matrix assisted pulsed laser evaporation (MAPLE) process (With permission from Elsevier (Patz et al. 2007))

concentration and solvent properties), laser wavelength, laser energy density, laser pulse duration, and laser firing rate (Pique 2011).

MAPLE is a versatile technique which presents numerous advantages over conventional physical or chemical vapor deposition methods. In traditional PLD, polymeric and organic materials may be damaged due to photochemical and/or photothermal processes; the resulting thin film may exhibit properties different than those of the starting material (e.g., lower molecular weight) (Pique 2011). By operating at relatively low fluences, MAPLE provides an appropriate process for deposition of polymer, organic material, or biomaterial thin films. Several other physical and chemical vapor deposition techniques decompose the target material and therefore cannot be used for such materials (Caricato and Luches 2011). Various types of polymers, organic substances, and biomaterials have been successfully deposited using MAPLE. For example, films containing biologically-relevant polymers (PEG, PGA, PLA, PLGA, PMMA, chitosan), electrically conductive polymers (polypyrrole), electroluminescent and photoluminescent polymers (MEH-PPV), as well as functionalized copolymers have been deposited using MAPLE (Pique 2011; Patz et al. 2007). In addition, films containing organic molecules such as carbohydrates (glucose, sucrose, dextran, pullulan), organic magnetic materials (Mn12-acetate), and other organic materials (NPP polypyrrole and Alq3) have been grown using MAPLE (Caricato and

Luches 2011; Pique 2011). Films containing biomolecules and active proteins have also been deposited using MAPLE; films containing horseradish peroxidase, collagen, bovine serum albumin, phospholipids, fibrinogen, and mussel adhesive proteins have been grown using this process (Caricato and Luches 2011; Patz et al. 2007; Pique 2011).

MAPLE has recently been applied for fabrication of nanoparticle/polymer film composites in which a colloidal nanoparticle solution is used as the target. MAPLE-deposited nanoparticle thin films provide better control over the film thickness and uniformity than those deposited by spin coating or drop casting. For example, tin dioxide and titanium dioxide nanoparticle/polymer film composites have been produced using MAPLE; it is expected that nanomaterials fabrication will become a more common application of MAPLE technology in the future (Caricato and Luches 2011).

Although conventional MAPLE provides several advantages over other thin film fabrication methods, there are a few limitations. The low concentration of solute molecules in the matrix solution results in a low deposition rate (Pique 2011). In addition, some solvent materials, such as chloroform, have been shown to release highly reactive Cl radicals, which may cause chemical degradation of the deposited films (Caricato and Luches 2011; Pique 2011). The most significant shortcoming of MAPLE technology is the difficulty in controlling surface morphology. While optimization of processing parameters has been shown to produce very

smooth and uniform coatings for some materials, many films exhibit rough surfaces with well-defined aggregates or clusters (Pique 2011).

Since the introduction of MAPLE, several variations of the technology have been developed in order to reduce the limitations associated with conventional MAPLE technology. Resonant infrared MAPLE (RIR-MAPLE) is one variation that has shown great promise in providing increased deposition rates and decreased surface roughness values. RIR-MAPLE utilizes an IR laser rather than a UV laser to vaporize the target matrix. RIR-MAPLE may be carried out at larger laser fluences (3–5 J/cm²) and with higher solute matrix concentrations (15–20%) than traditional UV-MAPLE, enabling higher deposition rates (Pique 2011). Off-axis MAPLE is another variation, which places the substrate parallel to the deposition axis rather than perpendicular to the deposition axis. This process has been shown to eliminate the presence of droplets that are associated with the aggregates in conventional MAPLE-deposited films (Pique 2011). A laser process known as MAPLE-direct write has the ability to fabricate free-standing patterns and structures of living cells. For example, Harris et al. created microscale patterns of MG 63 osteoblast-like cells, hydroxyapatite, an extracellular matrix using MAPLE-direct write (Harris et al. 2008). The cells within these patterns were viable and proliferated after MAPLE-direct write processing. MAPLE-direct write may be used for patterning biomaterials for a variety of applications, including use in drug delivery devices, artificial, medical implants, wound-healing adhesives, as well as chemical and biological sensors (Caricato and Luches 2011; Riggs et al. 2011). The progression of MAPLE and its variants has enabled further control over thin film attributes and has become a standard technique for laser processing of polymeric, organic, and biological materials. It is expected that MAPLE will become a valuable tool for fabricating thin films of biological materials.

Laser Capture Microdissection

Laser capture microdissection (LCM), shown in Fig. 2, has become an essential instrument in the preparation of homogeneous cell populations for advanced cellular and molecular analysis of tissue microenvironments. LCM provides a fast, reliable method for capturing and

isolating specific cells from heterogeneous tissues while maintaining the molecular attributes of the cells (Espina et al. 2007). This unique preservation of the tissue environment is accomplished by combining direct microscopic imaging of the cells and activation of a thermoplastic membrane using pulsed laser energy.

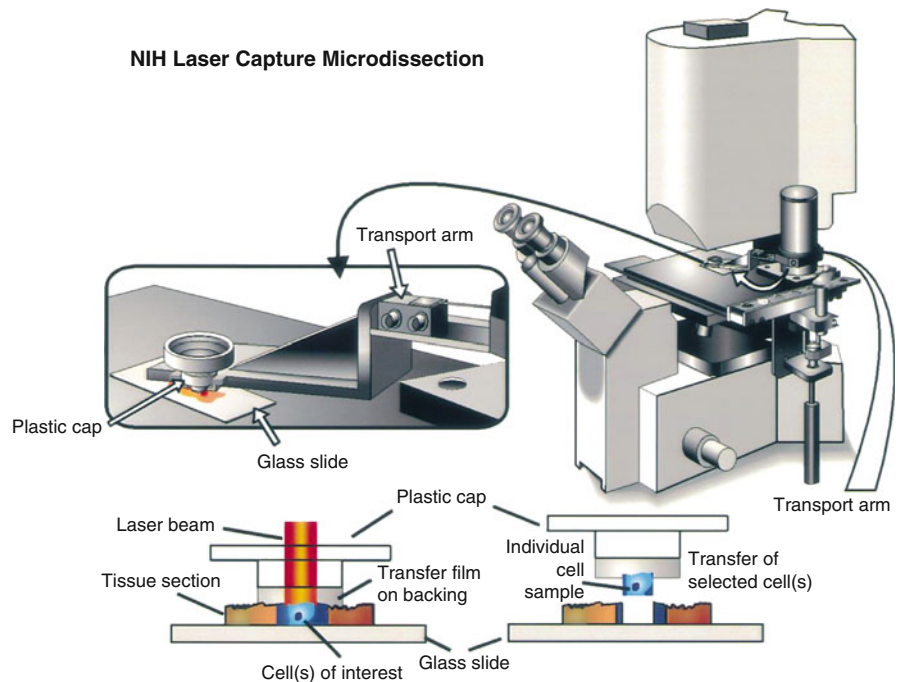
During LCM, a slide of sectioned tissue is placed onto a microscopic stage, where the cells of interest are identified. Near infrared (IR) laser pulses are then precisely applied to activate a thermoplastic polymer film adjacent to the tissue. The activated film embeds the cells of interest that are being targeted (Simone et al. 1998). The resulting polymer-cell composite is removed from the heterogeneous tissue, capturing only the targeted cells and leaving the remaining tissue intact (Espina et al. 2007). In many systems, the polymer film is on the bottom surface of a plastic cap, which is directly transferred to an extraction vial (Simone et al. 1998). The specimen may then be coupled with cell, DNA, RNA, or protein analyses.

The LCM process is compatible with a variety of tissue types, tissue preservation methods, and cellular staining techniques. LCM has been applied to numerous sample types, including formalin-fixed or paraffin-embedded tissue sections, flash frozen samples, cell smears, and chromosome separations (Ladanyi et al. 2006). Standard staining protocols have been utilized for enhanced identification of cells during microdissection. For example, immuno-LCM applies immunohistochemical staining for more accurate identification of cells. This technique permits cells that exhibit different immunologic phenotypes to be distinguished despite morphological similarities (Espina et al. 2007). Once the cells of interest have been targeted, the laser pulse may be applied. LCM uses short laser pulse durations, low laser power values, and long delays between laser pulses to reduce heat deposition at the tissue surface (Espina et al. 2007). This approach enables isolation of subpopulations of cells and individual cells without photochemical damage or degradation. By protecting the microenvironment of the tissue, LCM provides specimens that closely mimic the *in vivo* interactions of the native tissue (Espina et al. 2007).

Preservation of the tissue specimen permits coupling of the samples with multiplex analysis of cellular and molecular interactions. Sensitive amplification methods based on polymerase chain reaction (PCR),

Laser Processing of Biomaterials and Cells,

Fig. 2 Laser-capture microdissection (LCM) system. Through the use of a laser beam, tissue is embedded in a thermal polymer. The tissue is easily accessible to molecular analysis of any kind (With permission from Elsevier (Simone et al. 1998))



reverse transcriptase PCR, or enzymatic function are used to analyze the tissues (Emmert-Buck et al. 1996). By contributing to the understanding and identification of genes, proteins, and cellular pathways associated with complex tissues, LCM may be used for various applications, including discovery of drug targets; analysis of tumor microenvironment interactions; profiling of signaling pathways; real-time PCR; proteomic and genomic molecular profiling; forensic analysis; plant and cell biology analysis; biomarker discovery; and identifying molecular signatures of specific pathologies (Espina et al. 2007).

LCM has significantly progressed since its commercial introduction by researchers at the National Institute of Health in 1997 (Ladanyi et al. 2006). The primary limitation of LCM lies in the need for visual inspection of the cells. This step requires an individual trained in cell identification and can be time consuming. Cell recognition software and automated cell microdissection systems have gained significant attention as approaches for overcoming the manual aspects of LCM technologies. Novel processes have been developed such as manual and automated platforms; in addition, systems containing combined IR- and UV-lasers may be used to provide additional UV laser cutting and laser catapulting features (Espina et al. 2007). Future LCM technologies will likely permit

microdissection of subcellular structures, such as organelles, and microdissection of viable cells. Advancements in tissue preservation and staining will contribute to improved downstream analysis of LCM specimens.

Optical Tweezers

Optical tweezers have been applied as quantitative tools to exert calibrated forces on molecules and structures of interest as well as to measure forces and displacements generated by these systems. Nonbiological applications such as microrheology, particle sorting, microfabrication, colloidal hydrodynamics, and nonequilibrium thermodynamics have been investigated using optical tweezers (Moffitt et al. 2008); it should be noted that optical tweezers are most commonly applied for investigations of biological systems. Optical tweezers have been used to manipulate individual cells, cellular systems, and biological macromolecules, providing valuable insight into the mechanical properties of biological polymers and cells, the deformability of cellular vesicles and cells, and the dynamics of molecular motors (Moffitt et al. 2008; Zhang and Liu 2008). Investigations using optical tweezers have been invaluable in



comprehending the basic mechanisms of complex biological structures and processes.

Optical tweezers employ a highly focused laser beam to produce a field gradient trap for physically holding and manipulating microscopic particles. The laser beam is tightly focused using a high-numerical aperture microscope objective to form a stable optical trap (Moffitt et al. 2008). In conventional optical tweezers, a laser beam that exhibits a Gaussian profile is utilized (Zhang and Liu 2008). When the laser beam interacts with the particle, the particle experiences two kinds of forces: scattering forces and gradient forces. The scattering forces push the particle along the direction of propagation of the laser and the gradient forces pull the particle along the spatial gradient of light intensity from the laser profile. The gradient force is a restoring force, which pulls the particle to the center of the beam. A balance of these forces will hold a particle at the focal point in a stable manner, forming an optical trap (Moffitt et al. 2008; Zhang and Liu 2008). The two main trapping geometries include single-beam traps and dual-beam traps. In single-beam traps, only one single tightly focused laser beam is applied. Dual-beam traps enable trapping via two counterpropagating beams. Trapped particles may be translated in all directions by moving the laser or changing the focus of the laser (Nilsson et al. 2009)

The force of the optical trap applied to the particle is proportional to the displacement of the particle from the center of the trap. The force generated by the optical trap (F) may be expressed as $F = kx$, where k is the trap stiffness and x is the distance between the center of the particle and the center of the trap (Collard et al. 2007). It is difficult to directly measure the trapping forces applied in optical tweezers; however, numerous methods have been developed for calibrated measurement of the displacement and the force. Calibration generally involves measuring the response of the trapped particle to a known force, such as a viscous force (Collard et al. 2007). Furthermore, the Brownian motion of the trapped particle may be detected to experimentally determine the trap stiffness (Zhang and Liu 2008). The trap stiffness may vary depending on the power of the laser source, the aperture of the microscope objective, and the size of the particle. The trap stiffness and the measured displacement of the particle with respect to the focal point of the laser may then be used to calculate the applied force. With standard commercial optical tweezer instruments,

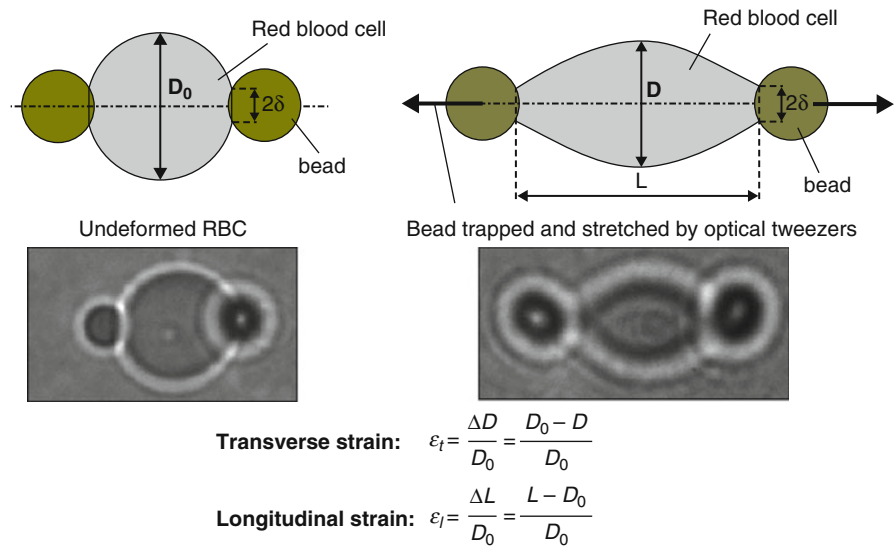
forces of up to 100 pN may be generated (Collard et al. 2007). The force exerted on the trapped particle is limited by the size and refractive index of the particle (Dienerowitz et al. 2008).

In many optical tweezer applications, the magnitude of the optical forces generated is inadequate to trap the molecules or particles of interest; therefore, dielectric particles, such as micrometer-sized polystyrene beads, are applied as handles or probes (Moffitt et al. 2008). These beads may be biochemically linked with molecules of interest to facilitate characterization. To exert the necessary forces on these molecules for analytical evaluation, the other end of the molecule is typically bound. This end may be attached to the surface of the sample chamber or another bead may be linked and held via another optical trap or with a micropipette (Collard et al. 2007). The beads are then manipulated using the optical tweezers, which indirectly control the molecules of interest. As shown in Fig. 3, a common use of this technology for studying the deformation of red blood cells (Li and Liu 2008). By applying these concepts, optical tweezers have become an essential tool for examining the chemical, physical, and mechanical properties of molecular systems.

Optical tweezers are a noncontact, low perturbation technology with high spatial and temporal resolution that enables researchers to quantitatively study the molecular kinetics of various molecules and structures (Long et al. 2011). Since the initial report of optic traps by Ashkin in 1970, there have been many major advances in the resolution and accuracy of optical tweezer technology (Moffitt et al. 2008). The spatial resolution has been reduced to the Angstrom length scale while the temporal resolution has been reduced to the microsecond time scale. Despite these achievements, experimental noise remains a problem and becomes more limiting at longer time scales (>1 s) (Moffitt et al. 2008). Other significant limitations of optical tweezers include concerns over photodamage to biological samples and low throughput (Zhang and Liu 2008). Nonconventional optical tweezer procedures have been developed using non-Gaussian laser beams (e.g., Bessel mode or Laguerre-Gaussian mode), dual beams, and multiple optical traps (Zhang and Liu 2008). One popular method for producing multiple optical traps involves the use of holographic optical tweezers. Holographic optical tweezers utilize spatial light modulators to produce precise patterns of multiple optical traps; this approach provides

Laser Processing of Biomaterials and Cells,

Fig. 3 Schematic drawings and microscopic images for the deformation of silica-bead-attached RBC stretched by laser tweezers (Li and Liu 2008)



versatility in terms of the size, geometry, three-dimensional orientation, and number of optical traps that are produced (Moffitt et al. 2008). Holographic optical tweezer technology is expected to have significant biomedical applications as it may be used to spatially organize one or multiple cell types in a well-defined pattern; potential applications include use in tissue engineering and regenerative medicine (DaneshPanah et al. 2010). Several recent research efforts have involved expanding the capabilities of traditional optical tweezers by identifying methods to control rotation and to measure torque (Moffitt et al. 2008). In addition to the advancements in conventional optical tweezer technology and the development of multi-trap processes, novel hybrid instruments have been developed. These systems combine optical tweezers with other techniques such as rapid detection and position devices, Raman spectroscopy, confocal microscopy, and rapid imaging techniques (Zhang and Liu 2008). Optical tweezers have also been used in microfluidic platforms to analyze the response of cells to other cells and/or biomaterials. It is anticipated that further advancements in hybrid devices will expand the capabilities of optical tweezers and will permit manipulation of more complex biological systems.

Summary

Laser processing of biomaterials and cells has enabled fabrication of complex materials for biomedical

applications. The extension of laser-based processes for polymeric, organic, and biological materials has facilitated use in tissue engineering, medical implant design, as well as biochemical and cellular analysis. MAPLE has demonstrated numerous advantages as a thin film deposition technique for complex materials. LCM and optical tweezers have become commonly used analytical tools. LCM has significantly contributed to our understanding and identification of genes, proteins, and cellular pathways associated with tissues. Optical tweezers have also become important instruments for manipulation and quantitative analysis of complex biological systems. These laser-based techniques are relatively new and have rapidly evolved in recent years. It is expected that these laser processing methods will continue to be instrumental for future biomaterials fabrication as well as for cellular as well as biomolecular evaluation.

Cross-References

► [Optical Tweezers](#)

References

Caricato AP, Luches A. Applications of the matrix-assisted pulsed laser evaporation method for the deposition of organic, biological, and nanoparticle thin films: a review. *Appl Phys A*. 2011;105:565–82.



- Collard D, et al. Towards mechanical characterization of bio-molecules by MNEMS tools. *Trans Electr Electron Eng.* 2007;2:262–71.
- DaneshPanah M, et al. 3D Holographic imaging and trapping for non-invasive cell identification and tracking. *J Disp Technol.* 2010;6(10):490–9.
- Dienerowitz M, Maziulu M, Dholakia K. Optical manipulation of nanoparticles: A review. *J Nanophoton.* 2008;2:1–31.
- Emmert-Buck MR, et al. Laser capture microdissection. *Science.* 1996;274:998–1001.
- Espina V, et al. Laser capture microdissection technology. *Expert Rev Mol Diagn.* 2007;7(5):647–57.
- Harris ML, et al. Recent progress in CAD/CAM laser direct-writing of biomaterials. *Mater Sci Eng C.* 2008;28:359–65.
- Ladanyi A, et al. Laser microdissection in translational and clinical research. *Cytometry A.* 2006;69:947–60.
- Li C, Liu KK. Nanomechanical characterization of red blood cells using optical tweezers. *J Mater Sci Mater Med.* 2008;19(4):1529–35.
- Long M, et al. Advances in experiments and modeling in micro- and nano-biomechanics: A mini review. *Cell Mol Bioeng.* 2011;4(3):327–39.
- Moffitt JR, et al. Recent advances in optical tweezers. *Ann Rev Biochem.* 2008;77:205–28.
- Narayan RJ, Goering P. Laser micro- and nanofabrication of biomaterials. *MRS Bull.* 2011;36(12):973–82.
- Nilsson J, et al. Review of cell and particle trapping in microfluidic systems. *Anal Chim Acta.* 2009;649:141–57.
- Patz TM, et al. Matrix assisted pulsed laser evaporation of biomaterial thin films. *Mater Sci Eng C.* 2007;27:514–22.
- Pique A. The matrix-assisted pulsed laser evaporation (MAPLE) process: Origins and future directions. *Appl Phys A.* 2011;105:517–28.
- Prodanov L, et al. Initial cellular response to laser surface engineered biomaterials. *MRS Bull.* 2011;36(12):1034–42.
- Riggs BC, et al. Matrix assisted pulsed laser methods for biofabrication. *MRS Bull.* 2011;36(12):1043–50.
- Simone NL, et al. Laser-capture microdissection: opening the microscopic frontier to molecular analysis. *Trends Genet.* 1998;14(7):272–6.
- Stratakis E, et al. Laser-based micro/nanoengineering for biological applications. *Prog Quantum Electron.* 2009;33:127–63.
- Zhang H, Liu K. Optical tweezers for single cells. *J R Soc Interface.* 2008;6:671–90.

Laser Trap

- ▶ [Optical Tweezers](#)

Laser-Based Materials Engineering of Medically Relevant Materials

- ▶ [Laser Processing of Biomaterials and Cells](#)

Lateral Modulated Excitation Microscopy (LMEM)

- ▶ [Structured Illumination Microscopy \(SIM\)](#)

Lateral Phase Separation

- ▶ [Lipid Lateral Diffusion](#)
- ▶ [Phase Transitions and Phase Behavior of Lipids](#)

Lateral Stress Profile

- ▶ [Lipid Bilayer Lateral Pressure Profile](#)

Law of Mass Action

Clive R. Bagshaw

Department of Biochemistry, University of Leicester, Leicester, UK

Department of Chemistry and Biochemistry, University of California Santa Cruz, Santa Cruz, CA, USA

Synonyms

[Chemical kinetics](#); [Mass action](#)

Definition

The Law of Mass Action is the foundation of chemical kinetics and states that the rate of an elementary reaction (i.e., one that effectively occurs as a single step) is proportional to the product of the concentration of the reactants. For a unimolecular reaction (i.e., one involving a single species) the reaction rate increases linearly with the concentration of the reactant because each reactant molecule has the same probability of reacting within a fixed time interval. Therefore, the observed rate for the population of reactant molecules will be proportional to the number of molecules in the reaction vessel. For a bimolecular reaction, the rate is proportional to the product of the concentrations of the two reactants because the collision frequency increases

with concentration. The Law of Mass Action was originally developed to describe an equilibrium system, $A + B \leftrightarrow C + D$, where the quotient $[A].[B]/[C].[D]$ is a constant, K_{eq} , but this reflects the balance of the rates in the forward and backward direction. In physical chemistry a distinction is often made between *concentration* and *activity* owing to nonideal behavior. However, in biological contexts this difference is usually ignored as the discrepancy is within experimental error and reactants are usually at very low concentrations relative to the solvent molecules. However in an intracellular context, effective concentrations may be modulated by “molecular crowding” which limits the diffusible space available to reactants.

Cross-References

► [Kinetics: Overview](#)

LC-NMR

► [Flow NMR](#)

LC-NMR/MS

► [Flow NMR](#)

LDH

► [Lactate Dehydrogenase – Computational Studies](#)

Lectins

Albert M. Wu
Glyco-Immunochemistry Research Lab, Institute of
Molecular and Cellular Biology, College of Medicine,
Chang-Gung University Kwei-San, Tao-Yuan, Taiwan

Synonyms

[Adhesin](#); [Agglutinin](#); [Carbohydrate binding proteins](#); [Oligosaccharide-protein interactions](#)

Definition

Lectins are carbohydrate binding proteins or glycoproteins, differing from (1) antibodies, (2) enzymes acting on glycans/glyco-ligands, and (3) sugar sensor/transport proteins. The term “lectin” was coined by W. C. Boyd in 1954. Lectins are also termed: hemagglutinins; adhesins; galectins; siglecs, . . .etc. The first alternative name was originated from the ability of proteins or glycoproteins to agglutinate the blood group ABO (H) glycotopes (epitopes) and sialic acid on red blood cells. On cell surfaces, they mediate cell–cell interactions by combining with complementary carbohydrates on opposing cells. Most lectin reagents were obtained from plants in the early 1970s and animal soluble tissue lectins became a wide attention in the life sciences in 1980s. The animal lectins were classified in to C-type lectins (selectins), S-type lectins (galectins) and other folds based on their amino acid sequences or Carbohydrate-Recognition Domain (CRD). Then, I-type lectins (siglecs) and more lectins were defined subsequently as detailed below.

Basic Characteristics

Lectins are found ubiquitously in plants, animals, and microbes. They play key roles in the control of various physiological and pathological processes in living organisms, such as fertilization, embryogenesis, cell migration, organ formation, inflammation, immune defense, and microbial infection (Sharon and Lis 1989; Barondes 2003; Gabius 2009; Wu et al. 2009). Before the roles of carbohydrate–protein interactions had been explored, many plant lectins were identified, characterized and applied to glycobiology for the detection, isolation, and characterization of glycoconjugates and the examination of cell surface transitions during some living processes including cell differentiation to cancer as a crucial (Sharon and Lis 2003). These plant lectins made valuable contributions to modern glycomics (Kamerling et al. 2007).

The functions of the lectins vary from each other and defects in them are linked to many diseases (Gabius 2009; Varki et al. 2009). Studies on pathogenic lectin–glycan interactions, especially the viral agglutinins, can provide scientists clues toward therapeutic strategies to prevent the infectious processes.



Lectins, Table 1 Expression of binding properties of Gal/GalNAc reactive lectins by decreasing order of carbohydrate structural units

Codes ^a	Lectins	Carbohydrate specificity ^a
F/A	<i>Dolichos biflorus</i> (DBA)	F_{penta} > A_n^b > A > Tn ≫ P
	<i>Helix pomatia</i> (HPA)	F_{penta} > A (>A_n^c) ≥ Tn, T ≫ P
A	Soybean (SBA, <i>Glycine max</i>)	A (>A_n^c), Tn and I/II
Tn	<i>Vicia villosa</i> B ₄ (VVA-B ₄)	Two Tn ≫ one Tn ≫ one or two T
	<i>Salvia sclarea</i> (SSA)	Two Tn > single or three sequential Tn structures
T	Peanut (PNA, <i>Arachis hypogaea</i>)	T ≫ I/II ≫ Tn
	<i>Amaranthus caudatus</i> (ACL)	T ≫ Tn ≫ I/II
T/Tn	<i>Agaricus bisporus</i> (ABA)	T_α and Tn > I ≫ GalNAc ≫ II, L
	<i>Maclura pomifera</i> (MPA)	T > Tn > > I/II and L
	<i>Artocarpus integrifolia</i>	T_α > P_α > T, Tn, II > I ≫ T_β
T/II	<i>Ricinus communis</i> toxin (ricin, RCA ₂)	T > I/II and Tn
	<i>Abrus precatorius</i> (APA)	T > I/II > E > B > Tn
I/II	<i>Ricinus communis</i> (RCA ₁)	Tri- II > II ≥ I > E, B > T
	<i>Erythrina cristagalli</i> (coral tree, ECA)	Tri- II > II > L, I
B	<i>Griffonia</i> (<i>Bandeiraea</i>) <i>simplicifolia</i> -B ₄ (GSI-B ₄)	B > E > A
E	<i>Abrus precatorius</i> toxin-a (Abrin-a)	E, B > T, L, I/II
	Mistletoe lectin-1 (ML-1)	E > II, L > T and I

^aThe symbols in bold indicate the human blood group activity and/or lectin determinants, which are: **F**(GalNAcα1→3GalNAc); **F_{penta}**(GalNAcα1→3GalNAcβ1→3Galα1→4Galβ1→4Glc); **A**(GalNAcα1→3Gal); **A_n**(GalNAcα1→3[Lfucα1→2]Gal); **Tn**(GalNAc→Ser/Thr of protein core); **T**(Galβ1→3GalNAc); **T_α**(Galβ1→3GalNAcα1→Ser/Thr of protein core); **T_β**(Galβ1→3GalNAcβ1→...ceramide); **I**(Galβ1→3GlcNAc); **II**(Galβ1→4GlcNAc); Tri-**II**(Triantennary Galβ1→4GlcNAc); **B**(Galα1→3Gal); **E**(Galα1→4Gal); **L**(Galβ1→4Glc); **P**(GalNAcβ1→3Gal); **P_α**(GalNAcβ1→3Galα1→)

^bSubstitution of Lfucα1→2 to subterminal Gal is important for binding

^cSubstitution of Lfucα1→2 to subterminal Gal blocks binding

C-type lectins expressed by dendritic cells have many functions – The Dendritic-Cell-Specific ICAM-3 Grabbing Non-integrin (DC-SIGN) binds to HIV-1 gp120 in the viral attachments; Siglecs are distinct lectins with the immunoglobulin-fold that specifically bind to sialic acids. Their importance for disease has been revealed and deserves further exploration (Figdor et al. 2002).

To provide a more valid and satisfactory depiction of the carbohydrate specificity of lectins in order to elucidate their functional roles and to optimize their biomedical applications, the following criteria should be taken into consideration: (1) the affinity for each monosaccharide and its derivatives; (2) expression of reactivities toward mammalian disaccharide structural units or their derivatives and finding the most active ligand; (3) simple oligovalent or cluster effect (e.g., multi-antennary oligosaccharides or **Tn** glycopeptides); and (4) complex multivalent or cluster effects present in macromolecules with multiple known glycotopes and organized in microdomains on cell surfaces (Gabijs et al. 2011). Example of item

(2) is Table 1, in which the lectins and their carbohydrate binding specificities are expressed by decreasing order of mammalian structural units. Most lectins are apparently specific for a monosaccharide but react with various oligosaccharide chains terminating with or containing this sugar with different affinities because the types of linkage and underlying sugar residues (glycotopes) also play significant roles in binding. For many lectins, e.g., *Agaricus bisporus* agglutinin (ABA), polyvalency of weak glycotopes (Gal_β1 → 3GalNAc_α (**T_α**) and Gal_β1 → 3/4GlcNAc_β (**I_β/II_β**)) are essential for lectin–glycan recognition and interaction. This phenomenon has a great biological importance because polyvalent interactions between lectins and ligands on the cell surfaces are presumed to play critical roles in a wide variety of biochemical recognition processes (Brewer et al. 2002; Wu 2011). Since the effect of polyvalency can be used to design polyvalent drugs with stronger therapeutic efficacy, it becomes pivotal to understand the polyvalent effects while establishing the binding profile of a lectin (Vance et al. 2008).

References

- Barondes SH. Lectins: their multiple endogenous cellular functions. *Annu Rev Biochem.* 1981;50:207–31. Review.
- Barondes SH, Cooper DN, Gitt MA, Leffler H. Galectins. Structure and function of a large family of animal lectins. *J Biol Chem.* 1994;269(33):20807–10. Review.
- Brewer CF, Miceli MC, Baum LG. Clusters, bundles, arrays and lattices: novel mechanisms for lectin–saccharide-mediated cellular interactions. *Curr Opin Struct Biol.* 2002;12:616–23.
- Cooper DN, Barondes SH. God must love galectin: He made so many of them. *Glycobiology.* 1999;10:979–84. Review.
- Figdor CG, van Kooyk Y, Adema GJ. C-type lectin receptors on dendritic cells and langerhans cells. *Nat Rev Immunol.* 2002;2:77–84.
- Gabius HJ, editor. *The sugar code: fundamentals of glycosciences.* Hoboken: Wiley; 2009. p. 1–597.
- Gabius H-J, André S, Jiménez-Barbero J, Romero A, Solís D. From lectin structure to functional glycomics: principles of the sugar code. *Trends Biochem Sci.* 2011;36:298–313.
- Kamerling JP, Boons GJ, Lee Y, Suzuki A, Taniguchi N, Voragen AGJ, editors. *Comprehensive glycoscience.* Four-Volume Set ed. Amsterdam: Elsevier; 2007. p. 1–3600. http://www.elsevier.com/wps/find/homepage.cws_home.
- Sharon N, Lis H. Lectins as cell recognition molecules. *Science.* 1989;246:227–34.
- Sharon N, Lis H. *Lectins.* Dordrecht/Boston/London: Kluwer; 2003.
- Vance D, Shah M, Joshi A, Kane RS. Polyvalency: a promising strategy for drug design. *Biotechnol Bioeng.* 2008; 101:429–34.
- Varki A, Cummings RD, Esko JD, Freeze HH, Stanley P, Bertozzi CR, Hart GW, Etzler ME. *Essentials of glycobiology.* 2nd ed. New York: Cold Spring Harbor; 2009. p. 380–1.
- Wu AM, Lisowska E, Duk M, Yang Z. Lectins as tools in glycoconjugate research. *Glycoconj J.* 2009;26:899–913.
- Wu AM (editors) *The molecular immunology of complex carbohydrates-3.* Adv Exp Med Biol, Springer/Plenum Publishers, New York, pp. 1–813.

L-fucose:Proton Symporter

- ▶ [FucP, the L-Fucose-H⁺ Membrane Transport Protein and Related Transporters](#)

Ligand Motions Relevant for Protein Binding

- ▶ [Protein–Ligand Dynamics](#)

Ligand-Binding Interactions

- ▶ [Absorption Spectroscopy to Probe Ligand Binding](#)
- ▶ [Mass Spectrometry: Application to Protein-Ligand Interactions](#)
- ▶ [NMR in Drug Discovery – Introduction](#)
- ▶ [NMR Studies of Macromolecular Interactions – Introduction](#)

Ligand–Ligand Interactions

- ▶ [DNA-Ligand Circular Dichroism](#)

Light Scattering

- ▶ [Absorbance Spectroscopy: Spectral Artifacts and Other Sources of Error](#)
- ▶ [Dynamic Light Scattering](#)
- ▶ [Dynamics of Colloids and Macromolecules](#)
- ▶ [Electrophoretic Light Scattering](#)
- ▶ [Multiangle Light Scattering from Separated Samples \(MALS with SEC or FFF\)](#)

Light, Oxygen, or Voltage Domains (LOV)

- ▶ [Flavin Mononucleotide-Binding Fluorescent Proteins](#)
- ▶ [LOV Proteins: Photobiophysics](#)

Light-Activated Conformation of Rhodopsin

- ▶ [Rhodopsin – Stability and Characterization of Unfolded Structures](#)

Light-Harvesting Complexes

- ▶ [Chlorophylls and Light-Harvesting Complexes](#)

Light-Induced Electron Transport

- ▶ [Photosynthetic Electron Transport](#)

Light-Signal Transduction

- ▶ [Rhodopsins – Intramembrane Signaling by Hydrogen Bonding](#)

Limiting Viscosity Parameter

- ▶ [Intrinsic Viscosity](#)

Linear Dichroism

Alison Rodger
Department of Chemistry, University of Warwick,
Coventry, UK

Synonyms

[Differential absorption of linearly polarized light – anisotropic absorbance spectroscopy](#)

Definition

Linear dichroism (LD) is the difference in absorption, A , of light linearly polarized parallel ($//$) and perpendicular (\perp) to an orientation axis (Michl and Thulstrup 1986; Rodger and Nordén 1997; Nordén et al. 2010).

$$LD = A_{//} - A_{\perp} \quad (1)$$

LD is used with systems that are either intrinsically oriented or are oriented during the experiment. The signal that is measured contains information about the orientation of subunits of the system relative to the orientation axis.

The reduced linear dichroism of an electronic transition that makes an angle α with the molecular orientation axis, z , (Fig. 1) is given by the equation (Nordén 1978; Nordén et al. 1991, 2010)

$$LD^r = \frac{LD}{A_{iso}} = \frac{3}{2}S(3\cos^2\alpha - 1) \quad (2)$$

where A_{iso} is the isotropic absorbance, S is referred to as the orientation parameter ($S = 1$ for a perfectly oriented sample and 0 for an unoriented one). The molecular orientation axis, z , is the most oriented direction of the molecule. If Z is the laboratory orientation axis it is the parallel direction of Eq. 1. $z = Z$ when $S = 1$. Strictly, Eq. 2 holds only for uniaxial orientation, but in practice most molecules and orientation methods approximate to this case.

A number of samples have the molecular orientation axis perpendicular to the long axis of the sample. These include carbon nanotubes (Rajendra et al. 2004), flow distorted liposomes (Ardhammar et al. 1998; Rodger et al. 2002), and peptidoglycan sacculi. In these cases, there is an extra element of rotational averaging resulting in (Ardhammar et al. 1998; Rodger et al. 2002) the following equation:

$$LD^r = \frac{LD}{A_{iso}} = \frac{3S}{4}(1 - 3\cos^2\beta) \quad (3)$$

where β is the angle between the liposome (or other structure) normal to the surface and the transition moment polarization as illustrated in Fig. 2.

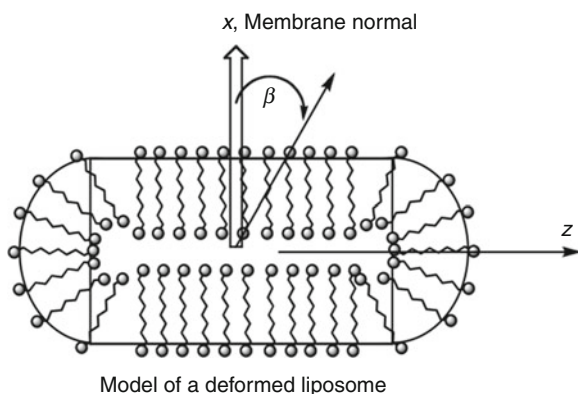
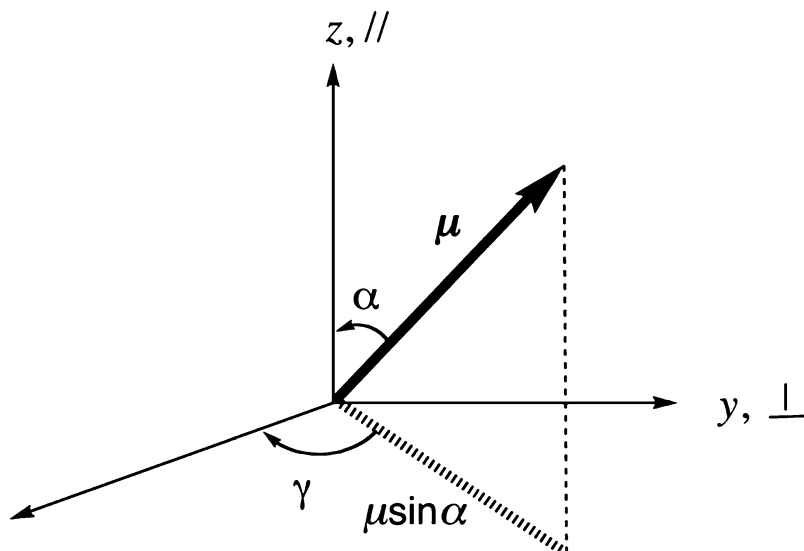
Basic Characteristics

LD is related to the more commonly used technique of circular dichroism (CD), in that both require the difference between the absorbances of different polarized light beams to be measured and CD spectropolarimeters can be adapted to produce the required alternating beams of polarized light for LD.

The LD experiment can be understood in the following way. If one places one polarizer, such as a polaroid film, on top of another and rotates it in front of a light source, the light coming through the polarizers goes from maximum to minimum every 90° of rotation. This is an LD experiment if one considers one polarizer to be the sample. In other words, the

Linear Dichroism,

Fig. 1 The orientations of an electric dipole transition moment, μ (whose length/magnitude is μ). The magnitude of the projection of μ onto the z axis is $\mu \cos\alpha$ and onto the x/y plane is $\mu \sin\alpha$. The y component of this projection is $\mu \sin\alpha \sin\gamma$. For a perfectly oriented molecular system $Z = z$ and $S = 1$



Linear Dichroism, Fig. 2 Schematic diagram of the geometric parameters relevant for liposomes distorted in shear flow

oriented sample in an LD experiment has the properties of a wavelength-dependent polarizer. Malus' law (Kahr and Claborn 2008) states that the intensity of the light between crossed polarizers scales as the cosine square of the angle between their polarization directions – hence the form of Eq. 1. If the polarizers are perfect, no light would pass at the 90° angle between the polarizers, while maximum light intensity would be let through when they are set in parallel orientation. In practice, in an LD experiment, while we hope that the polarizer used in the manufacture of our spectrometer is perfect, the second “polarizer” – the sample – only absorbs a fraction of the incident photons and is

seldom perfectly oriented, so even at wavelengths where it absorbs and thus operates as a polarizer, it is not a perfect polarizer.

The main practical differences between CD and LD (apart from the polarizations of light used) are that LD signals tend to be orders of magnitude larger than CD signals, so the data are easier to collect, however, LD measurements are performed on systems that are either intrinsically oriented or are oriented during the experiment, so the samples are harder to prepare.

Interpretations of LD data are based on Eqs. 1 and 2 above. From Eq. 1, if $\alpha = 0^\circ$ (i.e., the transition of interest is oriented parallel to the orientation direction) then $LD > 0$; conversely, if $\alpha = 90^\circ$ (i.e., the transition of interest is oriented perpendicular to the orientation direction) then $LD < 0$; and $LD = 0$ when $\alpha = 54.7^\circ$, the so-called magic angle. Orientations intermediate between these limits require Eq. 1 to be solved. With biomacromolecules, we often know the details of the spectroscopy of the chromophores (such as nucleic acid bases or amino acids) so the LD immediately gives us qualitative orientation information.

Quantitative analysis of LD spectra requires knowledge of the orientation parameter S . In some situations it is relatively straightforward to determine S . One can often proceed by assuming that the largest positive peak is pure z -polarized (with $\alpha = 0$) or the largest negative peak is pure x/y polarized (with $\alpha = 90^\circ$). For



example, if the 278 nm peak of tetracene in a stretched film has $LD = 0.174$ and $A_{iso} = 0.13$ from Eq. 1, we may deduce

$$S = \frac{LD}{A_{iso} \cdot 3} \approx \frac{0.174}{3 \times 0.13} = 0.45 \quad (4)$$

Thus, the orientation process for this long molecule is very efficient. S for flow-oriented DNA systems is typically 0.05–0.1 in magnitude.

Cross-References

- ▶ [Circular Dichroism and Chirality](#)
- ▶ [Circular Dichroism Spectroscopy of Biomacromolecules](#)
- ▶ [Circular Dichroism Spectroscopy: Units](#)
- ▶ [DNA-Ligand Circular Dichroism](#)
- ▶ [DNA-Ligand Flow Linear Dichroism](#)
- ▶ [Far UV Protein Circular Dichroism](#)
- ▶ [Linear Dichroism Spectra - Measurement](#)
- ▶ [Linear Dichroism Spectroscopy: Theory](#)
- ▶ [Near UV Protein CD](#)
- ▶ [Nucleic Acid Linear Dichroism](#)
- ▶ [Oriented Circular Dichroism Spectroscopy](#)
- ▶ [Polarized Light, Linear Dichroism, and Circular Dichroism](#)
- ▶ [Protein Circular Dichroism Analysis](#)
- ▶ [Synchrotron Radiation Circular Dichroism Spectroscopy](#)

References

- Ardhammar M, Mikati N, Nordén B. Chromophore orientation in liposome membranes probed with flow linear dichroism. *J. Am. Chem. Soc.* 1998;120:9957–8.
- Kahr B, Claborn K. The lives of Malus and his bicentennial law. *Chemphyschem.* 2008;9:43–58.
- Michl J, Thulstrup EW. *Spectroscopy with polarized light.* New York: VCH; 1986.
- Nordén B. Applications of linear dichroism spectroscopy. *Appl. Spectroscopy Rev.* 1978;14:157–248.
- Nordén B, Elvingson C, Jonsson M, Åkerman B. Microscopic behaviour of DNA during electrophoresis: electrophoretic orientation. *Quart. Rev. Biophys.* 1991;24:103–64.
- Nordén B, Rodger A, Dafforn TR. *Linear dichroism and circular dichroism: a textbook on polarized spectroscopy.* Cambridge: Royal Society of Chemistry; 2010.
- Rajendra J, Baxendale M, Dit Rap LG, Rodger A. Flow linear dichroism to probe binding of aromatic molecules and DNA

to single walled carbon nanotubes. *J. Am. Chem. Soc.* 2004;126:11182–8.

- Rodger A, Nordén B. *Circular dichroism and linear dichroism.* Oxford: Oxford University Press; 1997.
- Rodger A, Rajendra J, Marrington R, Ardhammar M, Nordén B, Hirst JD, Gilbert ATB, Dafforn TR, Halsall DJ, Woolhead CA, Robinson C, Pinheiro TJ, Kazlauskaitė J, Seymour M, Perez N, Hannon MJ. Flow oriented linear dichroism to probe protein orientation in membrane environments. *Phys. Chem. Chem. Phys.* 2002;4:4051–7.

Linear Dichroism Spectroscopy

- ▶ [Linear Dichroism Spectroscopy: Theory](#)

Linear Dichroism Spectra - Measurement

Alison Rodger
Department of Chemistry, University of Warwick,
Coventry, UK

Definition

Linear dichroism (LD) is the difference in absorption of light polarized parallel and perpendicular to an orientation axis. The component parts of an LD experiment are:

- A source of linearly polarized light
- A means of detecting how much light is absorbed
- A way to change the relative orientations of sample and light beam polarization
- A method of orienting the sample

Basic Characteristics

This section outlines what is needed for collecting LD data.

The Instrumentation

There are two main methods for measuring LD spectra. The one requiring less specialized equipment is the two-spectra method. In this case, one inserts a polarizer into a normal absorbance spectrometer, measures a spectrum, and then rotates either the polarizer or the sample. If the sample is rotated, care



must be taken to have the same light intensity through the same part of the sample for both polarizations. If the polarizer is rotated care must be taken to ensure the same light intensity is present in both beams.

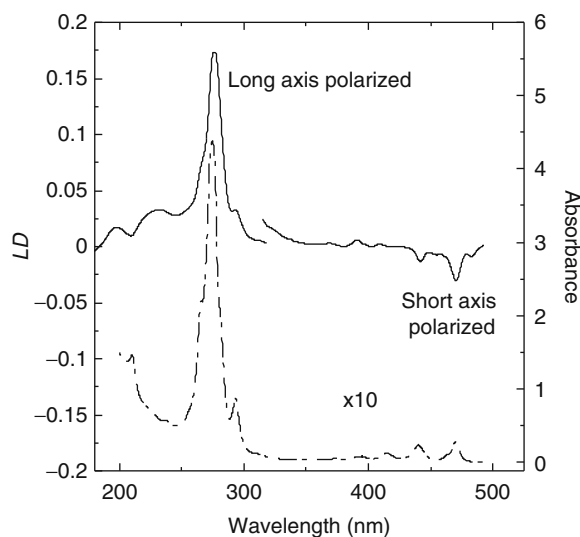
The second method, the differential method, where the instrument produces alternating beams of the two polarizations, is easier for the user to implement and a wide range of sample orientation techniques may be used. However, much more sophisticated instrumentation is required with the differential method. The differential method usually involves using a circular dichroism spectropolarimeter either with a quarter-wave plate to convert the circularly polarized light to linearly polarized light or alternatively a doubling of the voltage across the photoelastic modulator that produces the required oscillating linear polarizations directly. Both options for collecting LD data provide the required polarized light beams and detector (see definition above). The differential method also automatically deals with the need to change the relative orientation of sample and light beam – as long as one knows which direction the instrument defines as parallel.

Sample Orientation for LD Spectroscopy

Once the instrumentation has been established, the continuing challenge for the user of LD spectroscopy is to produce macroscopically well-oriented samples appropriate for determining the information required. Which orientation method one should use depends on the sample and the question being asked. For example, long and relatively rigid polymers, such as double-stranded DNA or RNA, or molecular assemblies of micrometer dimension, may be oriented in a fluid by shear flow whereas small molecules require a stronger orienting force. Some molecules which cannot themselves be oriented may be oriented when they bind to another molecule that is oriented. The rest of this entry summarizes various methods that may be implemented. More details of the underlying principles of molecular alignment and its significance for LD are given references (Nordén 1978; Nordén and Seth 1985; Nordén et al. 1991, 2010; Rodger 1993; Rodger and Nordén 1997; Rodger et al. 2006).

Stretched Polymers as Matrices in Which to Orientate Small Molecules

Small molecules can often be absorbed into polymer films. In 1934, A. Jablonski (1934) was the first to propose a method for orienting molecules by adsorption



Linear Dichroism Spectra - Measurement, Fig. 1 An LD spectrum of tetracene collected by the differential method. The base line was the stretched PE film to which dichloromethane had been added drop-wise and allowed to evaporate between additions. The sample was dissolved in dichloromethane and added drop-wise to a 5 \times stretched polyethylene film. Note in this case that the short-axis polarized transition has a positive LD signal in its shorter wavelength vibronic components due to coupling with the much stronger, higher-energy long-axis polarized transition

in anisotropic matrices. When the film is mechanically stretched, either before or after the small molecules are added, the analytes may align their long axes preferentially along the stretch direction. For a molecule to be aligned in a stretched polymer film it must be either an integral part of the film material or associated sufficiently strongly with the polymer chains that when the film is stretched the molecule follows the alignment of the polymer. The best baseline for such an experiment is either that collected for a piece of the same film that has been stretched but does not contain the molecule of interest, or the same film before adding the analyte or after washing it out. A typical film LD spectrum for tetracene is illustrated in Fig. 1. The two most popular films for LD are polyethylene for nonpolar molecules and polyvinyl alcohol for polar molecules. Polyvinyl chloride is also valuable in some applications. A film stretcher is illustrated in Fig. 2. Details of how to prepare films may be found in (Rodger and Nordén 1997; Ismail et al. 1998; Nordén et al. 2010).

Flow Orientation of Macromolecules

If a rigid or semi-flexible polymer, such as DNA, is dissolved in a solvent, such as water, and then flowed



Linear Dichroism Spectra - Measurement, Fig. 2 A mechanical film stretcher showing oppositely threaded screws to ensure even stretching of the film

past a stationary surface at about 1 m/s, then the molecules experience sufficient shear forces to give a net orientation of the long axis of the polymer along the flow direction. If light is incident on the sample perpendicular to the flow direction, then the absorbance parallel to the flow, A_{\parallel} , and the absorbance perpendicular to the flow direction, A_{\perp} , are different so an LD signal may be measured. If the cell components are quartz then data in the visible and UV regions may be collected. Other geometries for a flow LD experiment are also possible including measuring LD at $\pm 45^\circ$ to the flow direction (Rizzo and Schellman 1981).

One method to produce the required flow rate is to use a linear flow-through system such as provided by an HPLC pump or a pair of syringes. However, such an open system has an inherently large sample requirement and tends not to be completely stable. Wada (1964, 1972) solved these problems with the invention of a Couette flow cell for LD where the sample is endlessly flowed between two cylinders one of which rotates and one of which is stationary. This is schematically illustrated in Fig. 3 and some cells are illustrated in Fig. 4.

With a Couette flow system a number of possible baselines may be used. The simplest option is to stop the flow and measure the spectrum. The validity of such a baseline relies on the non-rotating spectrum being independent of the position of the rotor. A baseline of the same cell rotating slowly, causing no measurable orientation of the sample, may be used if the motor is stable at low rotation speeds and the scan speed is slow compared with the rotation speed. Alternatively, a spectrum of only the solvent/buffer with higher rotation speed may be measured as the baseline.

It is relatively easy to understand how a polymer such as DNA (Rodger et al. 2002) or a protein fiber

such as tubulin (Marrington et al. 2006) can be oriented in flow. More surprising is the fact that spherical membrane bilayers called liposomes can be oriented. In this case the orientation arises because the forces of the flow distort the liposome shape as schematically illustrated in Fig. 5. This means that membrane peptides and proteins can also be studied by LD (Rodger et al. 2002).

One of the key experimental parameters for flow LD is how fast the Couette cell spins. For an outer rotating Couette cell this is directly related to shear rate, G , by

$$G/s^{-1} = \frac{dv_z}{dx} = \frac{2\pi R_o \Omega}{60(R_o - R_i)} \quad (1)$$

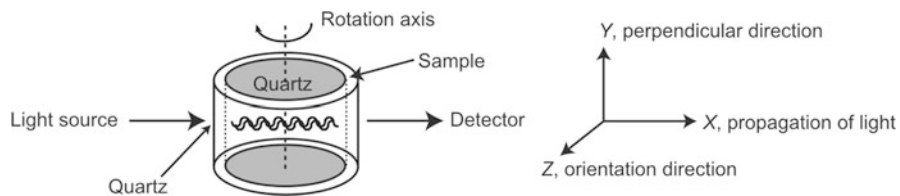
where the rate of rotation Ω is in revolutions per minute (rpm), R_o is the outer cylinder radius, and R_i is the inner cylinder radius. It should be noted that flow LD magnitudes are also dependent on solution viscosity, η , and temperature, T , as illustrated in Fig. 6. Small LD signals can be enhanced by adding glycerol to the solution to increase its viscosity (Dafforn et al. 2001; Hiort et al. 1990). It must be noted that viscosity itself is a function of both temperature and shear rate: viscosity of water at 60° is half that at 20° . Further, viscosity of water at $1,000 \text{ s}^{-1}$ is one third that at 0 s^{-1} ; higher shear rates have less effect (Rittman et al. 2009).

Electric Field Orientation

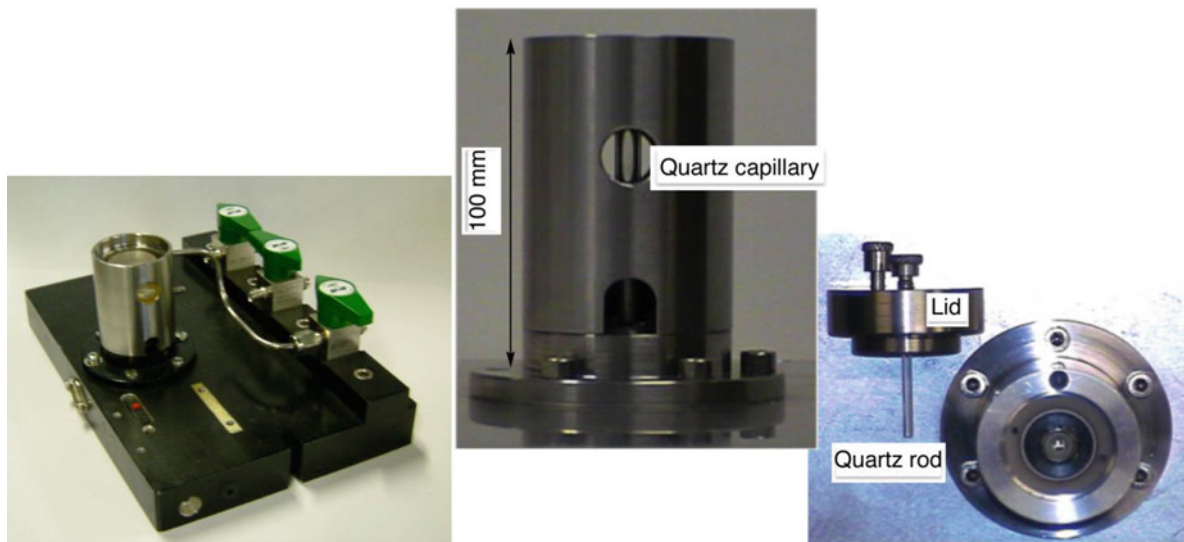
Effective orientation for polar or polarizable molecules may be achieved by setting up an electric field between two parallel plates. This produces uniaxial orientation of the molecules. Electric field orientation is conceptually simpler than flow orientation, and, when performed in nonconducting solvents, is an equilibrium orientation methodology whose effect can be predicted theoretically.

Crystalline Samples

Crystalline samples can provide perfect orientation if the sample is aligned so that the parallel direction is a unique axis in the crystal. However, for transmission spectroscopy, very thin slices are usually required because of high absorptivity. If the light is incidence along an axis about which the sample has threefold or higher symmetry, it will give $LD = 0$. Thus, to collect data for such a sample, the sample may be tilted from the perpendicular orientation and the equation for the magnitude modified accordingly (Nordén 1978).

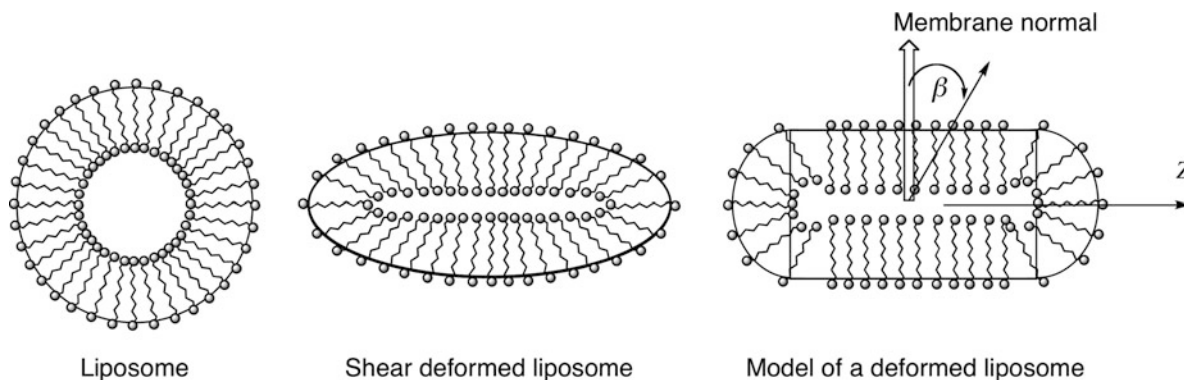


Linear Dichroism Spectra - Measurement, Fig. 3 Schematic of a Couette flow cell showing flow orientation in a coaxial flow cell with radial incident light. $\{X, Y, Z\}$ denotes the laboratory fixed axis system

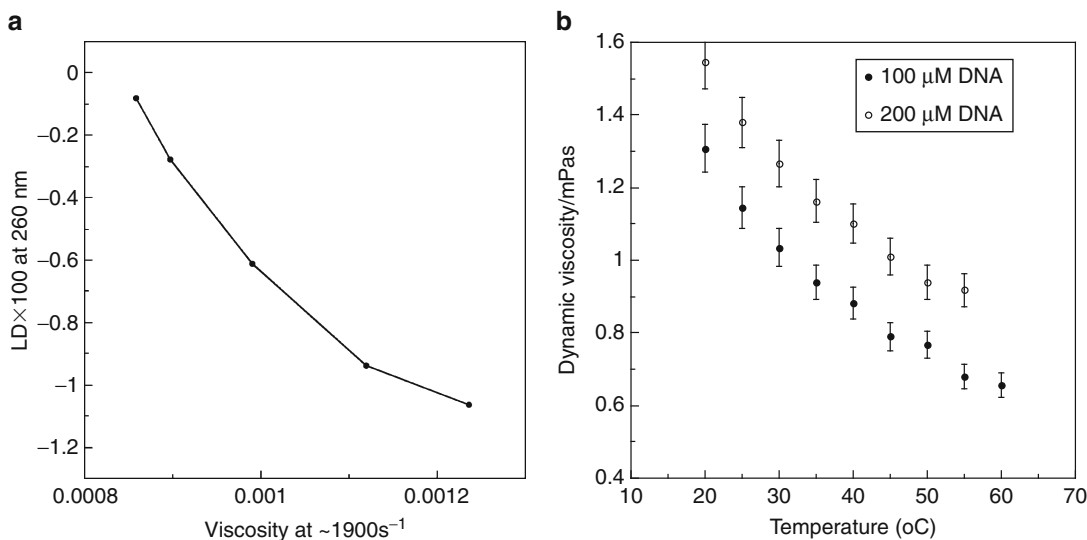


Linear Dichroism Spectra - Measurement, Fig. 4 Large volume (2 mL) inner rotating cylinder Couette flow cell with 500 μm annular gap (Rodger 1993) and microvolume (25–60 μL) outer rotating (Marrington et al. 2004, 2005) Couette flow

cell showing the outer quartz capillary (3 mm inner diameter) and inner quartz rod (2.4 mm outer diameter) which when assembled results in an annular gap of 250 μm



Linear Dichroism Spectra - Measurement, Fig. 5 Schematic diagram of liposomes distorted in shear flow



Linear Dichroism Spectra - Measurement, Fig. 6 (a) Viscosity dependence of Couette flow *LD* (measured on a Jasco J-815 spectropolarimeter) at 260 nm for a solution of DNA (200 μM calf thymus DNA in water). The viscosity was determined on the same solution as the *LD* using an Advanced Rheometer AR100. The viscosity was varied by changing the

temperature from 20°C to 60°C. The shear rate for both *LD* and rheometry was 1,900 s^{-1} . (b) Temperature dependence of the dynamic viscosity of DNA (200 μM calf thymus DNA in water). Viscosities were determined using a Cannon-Manning 25 E50 semi-micro viscometer (Gilroy et al. 2011)

Orientation by Evaporation or Assembly

Many molecules may be oriented simply by evaporating them onto a surface that is transparent to the radiation. This method works particularly well for planar aromatic molecules or samples embedded in lipid bilayers. However, the plate may need to be tilted for *LD* measurements (as discussed above for crystalline samples) since the molecules usually orient preferentially parallel to the surface of the quartz resulting in the unique axis being perpendicular to the plate and all in-plane directions having the same distribution of molecular orientations. The extent to which the solvent needs to be removed depends on the sample. Most work with lipids usually proceeds by drying the sample and then adding a salt solution chosen to give the required humidity (O'Brien 1948). Some molecules such as Alzheimer's fibers are sufficiently large and rigid that simply pipetting them onto a surface from solution may produce a significant degree of orientation (Marshall et al. 2010).

Summary

In this entry, some options for instrument configuration and sample orientation methodologies have been

discussed. Further information is available in the references.

Cross-References

- ▶ [Absorbance Spectroscopy: Overview](#)
- ▶ [Circular Dichroism Spectroscopy of Biomacromolecules](#)
- ▶ [DNA-Ligand Circular Dichroism](#)
- ▶ [DNA-Ligand Flow Linear Dichroism](#)
- ▶ [Linear Dichroism](#)
- ▶ [Linear Dichroism Spectra - Measurement](#)
- ▶ [Linear Dichroism Spectroscopy: Theory](#)
- ▶ [Nucleic Acid Linear Dichroism](#)
- ▶ [Polarized Light, Linear Dichroism, and Circular Dichroism](#)

References

- Dafforn TR, Halsall DJ, Rodger A. The detection of single base pair mutations using a novel spectroscopic technique. *Chem Commun.* 2001;2410–11.
- Gilroy E, Hicks MR, Smith DJ, Rodger A. Viscosity of aqueous DNA solutions determined using dynamic light scattering. *Analyst.* 2011;136(20):4159–63.

- Hiort C, Nordén B, Rodger A. Enantioselective DNA binding of $[\text{Ru}(1,10\text{-phenanthroline})_3]^{2+}$ studied with linear dichroism. *J Am Chem Soc.* 1990;112:1971–82.
- Ismail MA, Sanders KJ, Fennel GC, Latham HC, Wormell P, Rodger A. Spectroscopic studies of 9-hydroxyellipticine binding to DNA. *Biopolymers.* 1998;46:127–43.
- Jablonski A. Polarized photoluminescence of adsorbed molecules of dyes. *Nature.* 1934;133:140.
- Marrington R, Dafforn TR, Halsall DJ, Hicks MR, Rodger A. Validation of new microvolume Couette flow linear dichroism cells. *Analyst.* 2005;130:1608–16.
- Marrington R, Dafforn TR, Halsall DJ, Rodger A. Micro volume Couette flow sample orientation for absorbance and fluorescence linear dichroism. *Biophys J.* 2004;87:2002–12.
- Marrington R, Seymour M, Rodger A. A new method for fibrous protein analysis illustrated by application to tubulin microtubule polymerisation and depolymerisation. *Chirality.* 2006;18:680–90.
- Marshall KE, Hicks MR, Williams TL, Hoffmann SV, Rodger A, Dafforn TR, Serpell LC. Characterising the assembly of the Sup35 yeast prion fragment, GNNQQNY: structural changes accompany a fibre to crystal switch. *Biophys J.* 2010;98:330–8.
- Nordén B, Seth S. Critical aspects on measurement of circular and linear dichroism. A device for absolute calibration. *Appl Spectr.* 1985;39:647–55.
- Nordén B, Rodger A, Dafforn TR. *Linear dichroism and circular dichroism: a textbook on polarized spectroscopy.* Cambridge: Royal Society of Chemistry; 2010.
- Nordén B. Applications of linear dichroism spectroscopy. *Appl Spectr Rev.* 1978;14:157–248.
- Nordén B, Elvingson C, Jonsson M, Åkerman B. Microscopic behaviour of DNA during electrophoresis: electrophoretic orientation. *Q Rev Biophys.* 1991;24:103–64.
- O'Brien FEM. The control of humidity by saturated salt solutions. *J Sci Instrum.* 1948;25:73–6.
- Rittman M, Gilroy EL, Koohy H, Rodger A, Richards A. Is DNA a worm-like chain in Couette flow? In search of persistence length, a critical review. *Sci Prog.* 2009;92:163–204.
- Rizzo V, Schellman J. Matrix-method calculation of linear and circular dichroism spectra of nucleic acids and polynucleotides. *Biopolymers.* 1981;20:2143–63.
- Rodger A. Linear dichroism. *Meth Enzymol.* 1993;226:232–58.
- Rodger A, Nordén B. *Circular dichroism and linear dichroism.* Oxford: Oxford University Press; 1997.
- Rodger A, Marrington R, Geeves MA, Hicks MR, de Alwis L, Halsall DJ, Dafforn TR. Looking at long molecules in solution: what happens when they are subjected to Couette flow? *Phys Chem Chem Phys.* 2006;8:3131–71.
- Rodger A, Rajendra J, Marrington R, Ardhammar M, Nordén B, Hirst JD, Gilbert ATB, Dafforn TR, Halsall DJ, Woolhead CA, Robinson C, Pinheiro TJ, Kazlauskaitė J, Seymour M, Perez N, Hannon MJ. Flow oriented linear dichroism to probe protein orientation in membrane environments. *Phys Chem Chem Phys.* 2002;4:4051–7.
- Wada A. Chain regularity and flow dichroism of deoxyribonucleic acids in solution. *Biopolymers.* 1964;2:361–80.
- Wada A. Dichroic spectra of biopolymers oriented by flow. *App Spectr Rev.* 1972;6:1–30.

Linear Dichroism Spectroscopy: Theory

Alison Rodger
Department of Chemistry, University of Warwick,
Coventry, UK

Synonyms

[Linear dichroism spectroscopy](#)

Definition

LD is defined as the difference in absorption of two linearly polarized light beams that are polarized at right angles to one another and to the direction of propagation:

$$\text{LD} = A_{//} - A_{\perp} \quad (1)$$

This notation is normally reserved for uniaxial samples with // denoting the direction of the unique axis. So, although most LD experiments have (or are assumed to have) effective uniaxial orientation, it is better when deriving equations to use the more general definition

$$\text{LD} = A_Z - A_Y \quad (2)$$

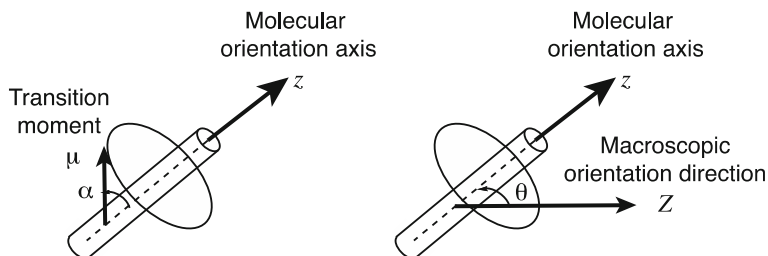
where A_Z is the absorbance of Z-polarized light, and similarly A_Y . $\{X, Y, Z\}$ form what is known as a laboratory-fixed axis system since they are used to identify macroscopic aspects of the experiment. We shall use $\{x, y, z\}$ for the molecule-fixed axis system where z is the molecular orientation axis. For any one molecule the two axis systems are related as illustrated in Fig. 1. Unfortunately, each molecule in a sample probably has different values of $\{\xi, \psi, \zeta\}$.



Linear Dichroism

Spectroscopy: Theory,

Fig. 1 Macroscopic $\{X, Y, Z\}$ and molecular axes $\{x, y, z\}$ systems and the angles relating them. For a uniaxial rod-like system we write $\theta = \zeta$



Basic Characteristics

The two key equations used in the analysis of biomacromolecules LD are derived below following the methodology of (Rodger and Nordén 1997; Nordén et al. 2010).

LD of Uniaxial Systems

Another key concept is that of the transition moment of a transition. It is a vectorial property having a well-defined direction (the transition polarization) within each molecule and a well-defined length (which is proportional to the square root of the absorbance). We denote the electric dipole transition moment by the vector μ . A_Z is then proportional to the square of the Z-component of μ , so the LD of a sample is:

$$LD = k \langle \mu_z^2 - \mu_y^2 \rangle \quad (3)$$

where $\langle \rangle$ denotes an average over the orientational distribution of the molecules in the sample, and k is a positive constant.

The main equation used to interpret LD spectra is

$$LD^r = \frac{LD}{A_{iso}} = \frac{3}{2} S (3 \cos^2 \alpha - 1) \quad (4)$$

where A_{iso} is the isotropic absorbance of the same sample in the same path length, S is the orientation parameter, and α is the angle between the molecular transition dipole moment and the molecular orientation axis. Its derivation proceeds from Eq. 3 as follows.

Assume first that the molecule of interest is perfectly oriented so that the molecular orientation axis lies along the macroscopic parallel direction, that is, $z = Z$, $S = 1$. Since the absorbance is proportional to

the square of the component of the electric dipole transition moment, μ , which lies along the direction of the electric field of the light, we may write

$$\begin{aligned} A_Z &= k \mu^2 \cos^2 \alpha \\ A_Y &= k \mu^2 \sin^2 \alpha \sin^2 \gamma \end{aligned} \quad (5)$$

where α is the angle between the transition dipole moment and z (Fig. 1), and γ is the angle the projection of this vector makes with the x axis. Thus

$$LD = A_Z - A_Y = k \mu^2 (\cos^2 \alpha - \sin^2 \alpha \sin^2 \gamma) \quad (6)$$

Similarly, the isotropic absorbance is the average of the absorbance in the X , Y , and Z directions, so

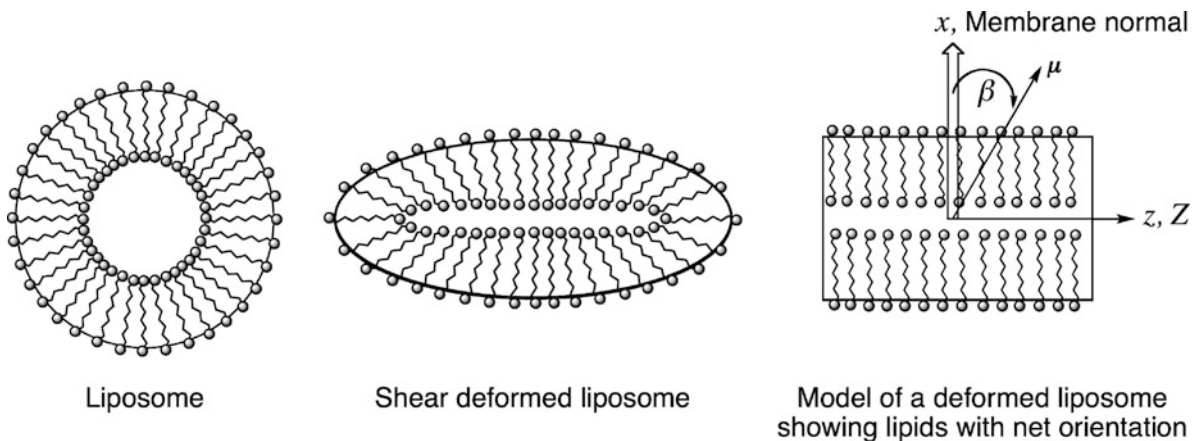
$$\begin{aligned} A_{iso} &= \frac{1}{3} (A_Z + A_Y + A_X) = \frac{1}{3} (A_Z + 2A_Y) \\ &= \frac{1}{3} k \mu^2 (\cos^2 \alpha + 2 \sin^2 \alpha \sin^2 \gamma) \end{aligned} \quad (7)$$

Since the experiment does not restrict the value of γ , we average over $\sin^2 \gamma$. As $\langle \sin^2 \gamma \rangle = 1/2$ we have

$$\begin{aligned} LD &= k \mu^2 \left(\cos^2 \alpha - \frac{1}{2} \sin^2 \alpha \right) \\ &= \frac{k \mu^2}{2} (2 \cos^2 \alpha - \sin^2 \alpha) \\ &= \frac{k \mu^2}{2} (3 \cos^2 \alpha - 1) \end{aligned} \quad (8)$$

and

$$A_{iso} = \frac{k \mu^2}{3} (\cos^2 \alpha + \sin^2 \alpha) = \frac{k \mu^2}{3} \quad (9)$$



Linear Dichroism Spectroscopy: Theory, Fig. 2 Schematic of liposomes distorted in shear flow

Equation 4 follows upon acknowledging that in reality the orientation is not perfect so we include S and get

$$\text{LD} = \frac{3}{2} A_{iso} S (3 \cos^2 \alpha - 1) \quad (10)$$

The form of S is derived in the final section of this article.

LD of Cylindrically Symmetric Systems

There are a number of systems where the axis about which the chromophores of interest are oriented are perpendicular to the surface of a cylinder. Such systems include flow distorted liposomes (as illustrated in Fig. 2), or ligands bound to the surface of carbon nanotubes. The equation analogous to Eq. 10 for such cylindrical systems is (Ardhammar et al. 1998; Rodger et al. 2002)

$$\text{LD}^r = \frac{\text{LD}}{A_{iso}} = \frac{3S}{4} (1 - 3 \cos^2 \beta) \quad (11)$$

where β is the angle between the lipid (or more generally cylinder surface) normal and the transition moment polarization as illustrated in Fig. 2. A derivation of this equation is outlined below.

We assume the orientation is locally uniaxial. Let z be along the long axis of the cylinder as in Fig. 2. z is uniformly distributed about Z , the macroscopic

orientation axis, to an extent accounted for by S . In this case, it is convenient to define the orientation of a transition moment, μ , of an analyte by sitting on the analyte and defining x to be the normal to the surface of the cylinder that goes through the analyte. Let β be the angle between x and μ (Fig. 2). The analyte orientation is not affected by the shear flow (the forces are too small), so on average any analyte transition moment, μ , will be uniformly distributed about the x axis. Let ψ be the angle between the projection of μ onto the y/z plane and z . Thus in the local cylinder coordinate system

$$\mu = \mu (\cos \beta, \sin \beta \sin \psi, \sin \beta \cos \psi)_{\{x,y,z\}} \quad (12)$$

where μ is the magnitude of μ . The reduced linear dichroism is by definition

$$\text{LD}^r = S \frac{A_Z - A_Y}{A_{iso}} = 3S \frac{(\mu_Z^2 - \mu_Y^2)}{\mu^2} \quad (13)$$

Now, $\mu_z = \mu_Z$ and μ_y may be written as the dot product of the transition moment vector and the vector for the Y axis in the $\{x, y, z\}$ coordinate system. Thus

$$\begin{aligned} \mu_y &= \mu \cdot Y \\ &= \mu (\cos \beta, \sin \beta \sin \psi, \sin \beta \cos \psi)_{\{x,y,z\}} \\ &\quad \cdot (\sin \gamma, \cos \gamma, 0)_{\{x,y,z\}} \\ &= \mu (\cos \beta \sin \gamma + \sin \beta \sin \psi \cos \gamma) \end{aligned} \quad (14)$$



where γ takes values from 0 to 2π . Thus,

$$LD^r = 3S \begin{pmatrix} \sin^2\beta\cos^2\psi - \cos^2\beta\sin^2\gamma - \sin^2\beta\sin^2\psi\cos^2\gamma \\ -2\cos\beta\sin\gamma\sin\beta\sin\psi\cos\gamma \end{pmatrix} \quad (15)$$

Both ψ and γ take values from 0 to 2π , so upon averaging over them:

$$LD^r = 3S \frac{2\sin^2\beta - 2\cos^2\beta - \sin^2\beta}{4} \quad (16)$$

$$= \frac{3}{4}S(1 - 3\cos^2\beta)$$

which is the required equation.

Two special cases of Eq. 16 are: (i) when a transition moment is parallel to the cylinder normal (e.g., the lipids), for which $\beta = 0$ and $LD^r/3S = -1/2$; and (ii) when it is perpendicular to the cylinder normal for which $\beta = 90^\circ$ and $LD^r/3S = +1/4$. The 210-nm transition of an α -helix inserted into the membrane is an example of case (i) – but this negative band usually only appears as a small dip between two larger positive signals. The same helix has $\beta = 90^\circ$ for its 222 nm and lower wavelength π - π^* transitions. Conversely it is the 210-nm transition of a helix lying on the surface that satisfies case (ii).

In general, for the case of molecules oriented perpendicular to the surface of a cylinder, the maximum positive LD^r signal ($3/4$) is half that of the maximum negative LD^r signal ($-3/2$). This is in contrast to the situation for the standard geometry of Eq. 4, such as flow-oriented DNA, where lower and upper limits are $-3/2$ and $+3$ respectively.

The Orientation Parameter for a Uniaxial System

The form of the orientation parameter for a uniaxial system can be derived as follows. Using the notation we developed above we may write the transition moment in the molecular coordinate system as

$$\mu = (\sin\gamma\sin\alpha, \cos\gamma\sin\alpha, \cos\alpha)_{xyz} \quad (17)$$

This vector can be transformed into the laboratory-fixed axis system using Euler's transformation where θ is the angle between z and Z , so

ϕ is the angle between x and a reference line defined to be perpendicular to both Z and z , and

ψ is the angle between X and the reference line.

Thus,

$$\mu_{\{XYZ\}} = \begin{pmatrix} \cos\phi\cos\psi - \sin\phi\sin\psi\cos\theta & \sin\phi\cos\psi + \cos\phi\sin\psi\cos\theta & \sin\psi\sin\theta \\ -\cos\phi\sin\psi - \sin\phi\cos\psi\cos\theta & -\sin\phi\sin\psi + \cos\phi\cos\psi\cos\theta & \cos\psi\sin\theta \\ \sin\phi\sin\theta & -\cos\phi\sin\theta & \cos\theta \end{pmatrix} \begin{pmatrix} \sin\gamma\sin\alpha \\ \cos\gamma\sin\alpha \\ \cos\alpha \end{pmatrix}_{\{xyz\}} \mu \quad (18)$$

Upon squaring the components and averaging over γ , ϕ , and ψ we get

$$\mu_Z^2 = \frac{1}{2}(\sin^2\theta\sin^2\alpha + 2\cos^2\theta\cos^2\alpha)\mu^2$$

$$= \frac{1}{2}((1 - \cos^2\theta)(1 - \cos^2\alpha) + 2\cos^2\theta\cos^2\alpha)\mu^2$$

$$= \frac{1}{2}(3\cos^2\theta\cos^2\alpha - \cos^2\alpha - \cos^2\theta + 1)\mu^2$$

$$= \left(\frac{1}{6}(3\cos^2\theta - 1)(3\cos^2\alpha - 1) + \frac{1}{3}\right)\mu^2 \quad (19)$$

and

$$\mu_Y^2 = \frac{1}{4}(\sin^2\alpha + \cos^2\theta\sin^2\alpha + 2\sin^2\theta\cos^2\alpha)\mu^2$$

$$= \frac{1}{4}((1 - \cos^2\alpha) + \cos^2\theta(1 - \cos^2\alpha) + 2(1 - \cos^2\theta)\cos^2\alpha)\mu^2$$

$$= \frac{1}{4}(-3\cos^2\theta\cos^2\alpha + \cos^2\alpha + \cos^2\theta + 1)\mu^2$$

$$= \left(-\frac{1}{12}(3\cos^2\theta - 1)(3\cos^2\alpha - 1) + \frac{1}{3}\right)\mu^2 \quad (20)$$

Thus,

$$LD = \mu_Z^2 - \mu_Y^2$$

$$= \frac{1}{2}(3\cos^2\theta - 1)\frac{1}{2}(3\cos^2\alpha - 1) \quad (21)$$

So

$$S = \frac{1}{2}(3\cos^2\theta - 1) \quad (22)$$

The main message to take from this is that molecules in most oriented systems adopt a distribution about Z .

Summary

In this entry, the derivation of the two key equations most frequently used to analyze biomacromolecules linear dichroism has been given. Further information is available in the references.

Cross-References

- ▶ [Circular Dichroism Spectroscopy of Biomacromolecules](#)
- ▶ [DNA-Ligand Circular Dichroism](#)
- ▶ [DNA-Ligand Flow Linear Dichroism](#)
- ▶ [Linear Dichroism](#)
- ▶ [Linear Dichroism Spectra - Measurement](#)
- ▶ [Linear Dichroism Spectroscopy: Theory](#)
- ▶ [Nucleic Acid Linear Dichroism](#)
- ▶ [Polarized Light, Linear Dichroism, and Circular Dichroism](#)

References

- Ardhammar M, Mikati N, Nordén B. Chromophore orientation in liposome membranes probed with flow linear dichroism. *J Am Chem Soc.* 1998;120:9957–8.
- Nordén B, Rodger A, Dafforn TR. *Linear dichroism and circular dichroism: a textbook on polarized spectroscopy.* Cambridge: Royal Society of Chemistry; 2010.
- Rodger A, Nordén B. *Circular dichroism and linear dichroism.* New York: Oxford; 1997.
- Rodger A, Rajendra J, Marrington R, Ardhammar M, Nordén B, Hirst JD, Gilbert ATB, Dafforn TR, Halsall DJ, Woolhead CA, Robinson C, Pinheiro TJ, Kazlauskaitė J, Seymour M, Perez N, Hannon MJ. *Phys Chem Chem Phys.* 2002;4:4051–7.

Linear Motifs in Protein-Protein Interactions

Robert B. Russell
Cell Networks, University of Heidelberg,
Heidelberg, Germany

Synonyms

[Protein complexes](#); [Protein–protein interactions](#);
[Peptide motifs](#)

Definition

Protein-protein interactions are highly diverse in terms of molecular mechanism. Perhaps, most typical are those where one large globular segment in one protein binds to another such segment in another. These kinds of interactions are seen everywhere in nature, particularly in large molecular machines such as RNA polymerases or the exosome. Another major class of mechanism includes those interactions mediated by a globular domain in one protein binding to a short linear stretch – typically between 3 and 10 amino acids in length – in another. The peptide stretches seen to bind the same or similar globular domains are frequently observed to contain a repeating pattern of residues or *motif*. Short linear motifs (or SLiMs) play major roles in interactions, being involved in binding, modification, cleavages, or targeting events in a wide range of cellular processes, particularly signaling, transcription, and intracellular transport. For example, one of the best known motifs is the canonical SH3 PxxP binding motif, where the prolines indicate the core residues common to the majority of SH3 protein binding sites.

Linear motifs stand apart from protein domains in a number of fundamental ways. First, their short length makes them virtually impossible to detect significantly by traditional sequence comparison methods. Second, they show a weaker pattern of conservation across orthologous proteins than protein domains and can, in contrast to domains, readily arise by convergent evolution. There are only a few hundred linear motifs currently known (in the ELM database as of early 2012) compared to more than 10,000 globular protein domains. This suggests that there are perhaps dozens

or even hundreds of new linear motifs to be discovered, and indeed, a number of computational methods have been developed to uncover them.

Significantly, the vast majority of linear motifs occur outside the globular parts of the proteome. At least 90% of known motifs occur within stretches of sequences that do not fold into tight compact units and are often intrinsically disordered, thus providing clues as to why so many eukaryotic proteins contain such regions. For example, the transcription factor p53 is largely disordered, and several known linear motifs lie within the disordered parts of its sequence. Given the roles of linear motifs in protein-protein interactions, this tallies well with the fact that p53 is one of the most promiscuous proteins in the cell with regard to interactions.

Cross-References

- ▶ [Coupled Folding and Binding](#)
- ▶ [Post-Translational Modifications](#)
- ▶ [Structurally Disordered Proteins](#)

References

- Davey NE, Edwards RJ, Shields DC. Computational identification and analysis of protein short linear motifs. *Front Biosci.* 2010;15:801–25.
- Diella F, Haslam N, Chica C, Budd A, Michael S, Brown NP, Trave G, Gibson TJ. Understanding eukaryotic linear motifs and their role in cell signaling and regulation. *Front Biosci.* 2008;13:6580–603.
- Neduva V, Russell RB. Linear motifs: evolutionary interaction switches. *FEBS Lett.* 2005;579:3342–5.
- Neduva V, Linding R, Su-Angrand I, Stark A, de Masi F, Gibson TJ, Lewis J, Serrano L, Russell RB. Systematic discovery of new recognition peptides mediating protein interaction networks. *PLoS Biol.* 2005;3:e405.

Linear Prediction in NMR Spectroscopy

Frank Delaglio
Software Science Consultant, North Potomac,
MD, USA

Synonyms

[Autoregressive analysis](#); [LPSVD](#)

Linear Prediction (LP) refers to methods which use autoregressive analysis to model one-dimensional time-domain NMR data. LP can be used to estimate signal frequencies, exponential decays, and amplitudes. More commonly, LP is used to extrapolate time-domain data, so that the corresponding Fourier transform spectrum has greater apparent resolution and smaller truncation artifacts. The same approach can be used to replace missing or distorted points in time-domain data.

LP methods determine a set of coefficients $c_1 \dots c_K$ which model the points $x_1 \dots x_N$ in a uniformly spaced time-domain data series. Depending on the specific LP method, the coefficients are adjusted and applied in different ways. In the LP model, a time-domain data point is expressed as a linear combination of the K points it follows (forward LP) or the K points which come after it (backward LP). The LP model has special significance for NMR, since in the absence of noise it is exact for exponentially decaying sinusoids, the usual ideal form of NMR signals.

The LP model leads to a series of linear equations in terms of the K LP coefficients and the N data points. If the number of coefficients is chosen so that $K \leq N/2$, the coefficients can be estimated by conventional least squares methods, usually Singular Value Decomposition (SVD). Each LP coefficient encodes a frequency and decay, which can be extracted by finding the roots of a complex polynomial whose coefficients are the $c_1 \dots c_N$ values. Once the frequencies and damping factors are determined, amplitudes can be extracted by fitting the original data to a corresponding sum of K damped sinusoids, again using conventional least squares methods. In practice, these parameter estimates are often of little direct use, since they encode combinations of true signal and noise. So, rather than using such parametric information directly, the LP coefficients are instead used to extend the time-domain data.

In this extrapolation procedure, the LP coefficients are used to append a new synthetic point using a linear combination of the last K points in the original data. The new point can then be used along with the previous $K-1$ points to append yet another synthetic point. This process can be continued indefinitely, but in practice it becomes more unstable as additional points are predicted from previous synthetic ones. Therefore, LP is often limited to extrapolating data to about twice its original size, so that the synthetic data does not outweigh the original data.

Various refinements are used to improve LP performance in the presence of noise. In root-fixing approaches, decays encoded in the LP coefficients are adjusted so that they always correspond to decreasing signals. In forward-backward approaches, forward and backward coefficients are determined separately, and averaged in an attempt to generate a single improved set of coefficients. In mirror-image approaches, which require non-decaying signals, time-domain data is temporarily appended to its mirror image before LP, increasing the effective data size so that more linear prediction coefficients can be extracted.

Cross-References

- ▶ [Absorbance Spectroscopy: Spectral Artifacts and Other Sources of Error](#)
- ▶ [Maximum Entropy Reconstruction](#)
- ▶ [NMR](#)
- ▶ [Sparse Sampling in NMR](#)
- ▶ [Triple Resonance NMR](#)

Lipid Bilayer

- ▶ [Alkanols – Effects on Lipid Bilayers](#)
- ▶ [Differential Scanning Calorimetry \(DSC\), Pressure Perturbation Calorimetry \(PPC\), and Isothermal Titration Calorimetry \(ITC\) of Lipid Bilayers](#)
- ▶ [Diffraction Methods for Studying Transmembrane Pore Formation and Membrane Fusion](#)
- ▶ [Fluorescence and FRET in Membranes](#)
- ▶ [Fluorescence Correlation Spectroscopy of Lipids](#)
- ▶ [Lipid Domains](#)
- ▶ [Lipid Flip-Flop](#)
- ▶ [Lipid Lateral Diffusion](#)
- ▶ [Lipid Organization, Aggregation, and Self-assembly](#)
- ▶ [Membrane Fluidity](#)
- ▶ [Micropipette Manipulation of Lipid Bilayer Membranes](#)
- ▶ [Neutron Scattering of Membranes](#)
- ▶ [Pressure Effects on Lipid Membranes](#)
- ▶ [Spin-Labeling EPR of Lipid Membranes](#)

- ▶ [Sum Frequency Generation Vibrational Spectroscopy](#)
- ▶ [Supported Lipid Bilayers](#)
- ▶ [Thermodynamics of Lipid Interactions](#)

Lipid Bilayer Asymmetry

Salvatore Chiantia and Erwin London
Dept. of Biochemistry and Cell Biology,
Stony Brook University, Stony Brook, NY, USA

Synonyms

[Bilayer asymmetry](#); [Membrane asymmetry](#)

Definition

Lipid bilayer asymmetry refers to the difference between the lipid composition and/or physical properties of the two lipid monolayers that make up a lipid bilayer.

Basic Characteristics

Lipid bilayer asymmetry refers in general to the vectorial nature of biological membranes, structures constituted by a bilayer of lipids into which

- ▶ [membrane proteins](#) are embedded. Membrane lipids contain a hydrophilic/polar *headgroup* that contacts the aqueous environment as well as (in general) two hydrophobic, long hydrocarbon chains, each of which most commonly contain 16–24 carbon atoms (Gennis 1989; Heimburg 2007). The membrane bilayer is composed of two lipid monolayers (leaflets). In each monolayer, the lipids are oriented so that their polar headgroups interact with water, while the hydrocarbon chains from each monolayer form the core of the membrane. The hydrocarbon chains from each monolayer contact each other at the bilayer midplane. For the plasma membrane that surrounds the cell, the two monolayers are often referred to as the inner leaflet, which faces the cytoplasm of the cell, and the outer leaflet, which faces the external environment. However, because the cell has many internal membranes for which

the cytoplasm-facing leaflet is on the outside, it is less ambiguous to distinguish the lipid monolayers by the terms cytofacial/cytoplasmic (i.e., the leaflet in direct contact with the cytoplasm) and exofacial/exoplasmic (i.e., the leaflet opposite the cytofacial leaflet).

While membrane proteins are also asymmetrically oriented across the bilayer, the expression bilayer asymmetry mainly refers to the difference in lipid composition of the two leaflets. There are in fact many different types of membrane lipids, which can vary in terms of both the chemical structure of the polar headgroups and/or that of the hydrocarbon chains, so that there can be asymmetry both of lipid headgroup type and hydrocarbon chain structure in the two monolayers. This implies that the two sides of the membrane might have different physical properties and that thermodynamic forces can act across the bilayer due to gradients in electrostatic, elastic, or, in general, chemical potential (Heimburg 2007). As an example, transverse lipid asymmetry has been quantitatively clearly demonstrated for the plasma membrane of erythrocytes. In these simple membrane systems, sphingomyelin (SM) and phosphatidylcholine (PC) are enriched in the outer leaflet, while aminophospholipids like phosphatidylethanolamine (PE) and phosphatidylserine (PS) are found mostly in the inner leaflet (Rothman and Lenard 1977; Gennis 1989). Similarly, lipid asymmetry has been characterized in the outer membrane of gram-negative bacteria, viruses, fibroblast phagosomes, platelets, and other membranes of eukaryotic cells (Rothman and Lenard 1977; Gennis 1989; Fadeel and Xue 2009). The extent to which there is asymmetry of cholesterol, which can undergo rapid transverse diffusion between the inner and outer leaflet, has proven difficult to measure and remains controversial.

Although the presence of a compositional difference between the leaflets seems to be a general feature of many natural membranes, the exact details of the lipid distribution across the bilayers vary from case to case. The amount of available unambiguous data is rather limited, due mainly to the complexity of the methods used to determine membrane asymmetry and to the inherent artifacts (e.g., interleaflet contamination, difficult isolation of a single specific cellular membrane, perturbation of the bilayer by asymmetry measurement methods, and lipid pools inaccessible to detection (Rothman and Lenard 1977)). Nevertheless, several approaches have been proven useful for

the determination of the lipid distribution across the bilayer, namely, selective chemical labeling, phospholipid transfer proteins, and digestion by phospholipases (Gennis 1989). The common basic feature of these methods is the presence of a water-soluble “probe” that cannot cross a closed bilayer and that can thus interact exclusively with the exposed leaflet.

Generation and Maintenance of Lipid Asymmetry

The origin of lipid asymmetry in biological membranes is based on the intrinsic asymmetric nature of lipid biosynthesis and metabolism. For biosynthesis, the needed enzymes, substrates, and energy sources are most frequently located in the cytoplasm of the cell and in the cytosolic side of its membranes. For example, PE, PC, and PS are synthesized on the cytofacial side of the endoplasmic reticulum (ER), with the aminophospholipids thus already on the side of the membrane where they will be finally enriched once transported in the plasma membrane. Similarly, SM and many glycosphingolipids are synthesized in the luminal surface (i.e., exoplasmic leaflet) of the ER or Golgi, although initial steps in their assembly occur in the cytoplasm (Daleke 2003). The presence of enzymes that degrade specific lipids on only side of a membrane can alter asymmetry by analogous principles.

Biosynthesis and degradation are not the only factors involved in asymmetry because lipids, under certain conditions, can undergo transverse translocation between leaflets. Spontaneous translocation of lipids across the bilayer is often extremely slow. The spontaneous transbilayer motion of lipids (flip-flop) has in fact been measured to happen at negligible rates, with half-times of several hours or days, in model membrane vesicles and certain natural membrane systems (e.g., influenza virus) (Gennis 1989). However, there are lipid transporters that specifically catalyze and direct the otherwise slow and random transbilayer dynamics. These transmembrane proteins can be generally divided into the following: (1) *flippases* (including *phospholipid translocases*), which catalyze the ATP-dependent transport into the cytoplasmic leaflet, (2) *floppases*, which catalyze the ATP-dependent transport towards the exoplasmic leaflet, and (3) *scramblases*, which catalyze bidirectional lipid movement in an energy-independent fashion (Daleke 2003). Several recent studies identified a group of P-type **ATPases**, the ATP-binding cassette transporter family, and a scramblase family of proteins,

as candidates for the these three categories of transporters, respectively (Fadeel and Xue 2009; Holzer et al. 2010).

Biological Function of Lipid Asymmetry

The considerable amount of energy invested by the cell in order to maintain and regulate the transbilayer lipid organization of its membranes is justified by the numerous normal and pathological processes connected to changes in membrane asymmetry. As already mentioned, the uneven distribution of lipid species across the bilayer determines its physical properties, such as permeability, local curvature, membrane shape or the negative surface charge of the cytosolic leaflet (Rothman and Lenard 1977; Holzer et al. 2010). The latter factor in particular influences the electrostatic interactions between the cell membrane and charged membrane-associated molecules. Also, the enrichment of aminophospholipids in the cytoplasmic leaflet and the breakdown of this asymmetry are connected to cellular processes such as apoptosis, neuronal development, cell differentiation, engulfment by macrophages, and platelets activation (Balasubramanian and Schroit 2003). Perturbation of lipid asymmetry also appears in the context of several pathological conditions like tumors, thalassemia, and diabetes (Balasubramanian and Schroit 2003). As a further example, Scott syndrome, a congenital bleeding disorder, is clearly caused by a deficiency of Ca^{2+} -induced phospholipid scramblase activity. Of interest, the underlying alteration of bilayer asymmetry control in Scott syndrome is not restricted to platelets but is also evident in other cell types, like lymphocytes (Fadeel and Xue 2009). Finally, it is well known that several cell types display a voltage gradient across their plasma membrane, the resting potential of a nerve cell being for example around -70 mV (Heimburg 2007). Recent studies suggest that the asymmetric distribution of lipids across the membrane and the intrinsic membrane potential are coupled (Fadeel and Xue 2009).

Asymmetric Model Membrane Systems

In order to understand the structure and function of complex biological membranes, artificial bilayers composed of membrane lipids have been used as simpler and more well-defined physical models. Biophysical investigation of such model membrane

systems can be used to derive fundamental information regarding transbilayer dynamics, lipid domain formation, membrane fusion, and the energetic interaction (coupling) between the two leaflets. They have proven invaluable for such studies, but it has been difficult to prepare asymmetric model membranes until recently. Important progress has been made in preparing asymmetric supported bilayers using different approaches: vesicle fusion (Lin et al. 2006), sequential depositing of monolayers, or a combination of the two (Kießling et al. 2009). Furthermore, methods have been developed to prepare asymmetric (free-standing) membranes based on redistribution of charged lipids via a pH gradient (Eastman et al. 1991), leaflet-by-leaflet assembly through an oil–water interface (Pautot et al. 2003; Hamada et al. 2008), Montal-Mueller assembly (Collins and Keller 2008), or outer leaflet exchange (Pagano et al. 1981). The latter approach is based on the transfer of certain lipids between the outer leaflets of two distinct vesicle populations. This process can be optimized using transporter molecules that facilitate the intermembrane dynamics, like phospholipid transfer proteins (Bloj and Zilversmit 1981) or cyclodextrins (Cheng et al. 2009), a family of cyclic oligosaccharides. The use of cyclodextrin has proven very useful in preparing stable asymmetric vesicles with different dimensions (from 10^{1-2} nm to 10^2 μm) and a large variety of lipid species (Cheng et al. 2009, 2011; Chiantia et al. 2011).

Acknowledgments This work was supported by NSF grant DMR 1104367 to E.L. S.C. is a HHMI fellow of the LSRF.

Cross-References

- ▶ [ATPase: Overview](#)
- ▶ [Chemical Diversity of Lipids](#)
- ▶ [Functional Roles of Lipids in Membranes](#)
- ▶ [Glycerolipids: Chemistry](#)
- ▶ [Glycosphingolipids](#)
- ▶ [Lipid Domains](#)
- ▶ [Lipid Flip-Flop](#)
- ▶ [Lipids: Isolation and Purification](#)
- ▶ [Membrane Lipid Electrostatics](#)
- ▶ [Membrane Proteins: Structure and Organization](#)
- ▶ [Sphingolipids and Gangliosides](#)

References

- Balasubramanian K, Schroit AJ. Aminophospholipid asymmetry: a matter of life and death. *Annu Rev Physiol.* 2003;65:701–34.
- Bloj B, Zilversmit DB. Lipid transfer proteins in the study of artificial and natural membranes. *Mol Cell Biochem.* 1981;40:163–72.
- Cheng HT, Megha, London E. Preparation and properties of asymmetric vesicles that mimic cell membranes effect upon lipid raft formation and transmembrane helix orientation. *J Biol Chem.* 2009;284:6079–92.
- Cheng HT, London E. Preparation and properties of asymmetric large unilamellar vesicles: interleaflet coupling in asymmetric vesicles is dependent on temperature but not curvature. *Biophys J.* 2011;100:2671–8.
- Chiantia S, Schwille P, Klymchenko AS, London E. Asymmetric GUVs prepared by MbetaCD-mediated lipid exchange: an FCS Study. *Biophys J.* 2011;100:L1–3.
- Collins MD, Keller SL. Tuning lipid mixtures to induce or suppress domain formation across leaflets of unsupported asymmetric bilayers. *Proc Natl Acad Sci USA.* 2008;105:124–8.
- Daleke DL. Regulation of transbilayer plasma membrane phospholipid asymmetry. *J Lipid Res.* 2003;44:233–42.
- Eastman SJ, Hope MJ, Cullis PR. Transbilayer transport of phosphatidic acid in response to transmembrane pH gradients. *Biochemistry.* 1991;30:1740–5.
- Fadell B, Xue D. The ins and outs of phospholipid asymmetry in the plasma membrane: roles in health and disease. *Crit Rev Biochem Mol Biol.* 2009;44:264–77.
- Gennis RB. *Biomembranes: molecular structure and function.* New York: Springer; 1989.
- Hamada T, Miura Y, Komatsu Y, Kishimoto Y, Vestergaard M, Takagi M. Construction of asymmetric cell-sized lipid vesicles from lipid-coated water-in-oil microdroplets. *J Phys Chem B.* 2008;112:14678–81.
- Heimburg T. *Thermal biophysics of membranes.* Weinheim: Wiley-VCH; 2007.
- Holzer M, Momm J, Schubert R. Lipid transfer mediated by a recombinant pro-sterol carrier protein 2 for the accurate preparation of asymmetrical membrane vesicles requires a narrow vesicle size distribution: a free-flow electrophoresis study. *Langmuir.* 2010;26:4142–51.
- Kiessling V, Wan C, Tamm LK. Domain coupling in asymmetric lipid bilayers. *Biochim Biophys Acta Biomembr.* 2009;1788:64–71.
- Lin WC, Blanchette CD, Ratto TV, Longo ML. Lipid asymmetry in DLPC/DSPC-supported lipid bilayers: a combined AFM and fluorescence microscopy study. *Biophys J.* 2006;90:228–37.
- Pagano RE, Martin OC, Schroit AJ, Struck DK. Formation of asymmetric phospholipid membranes via spontaneous transfer of fluorescent lipid analogues between vesicle populations. *Biochemistry.* 1981;20:4920–7.
- Pautot S, Frisken BJ, Weitz DA. Engineering asymmetric vesicles. *Proc Natl Acad Sci USA.* 2003;100:10718–21.
- Rothman JE, Lenard J. Membrane asymmetry. *Science.* 1977;195:743–53.

Lipid Bilayer Lateral Pressure Profile

Derek Marsh

Max-Planck-Institut für biophysikalische Chemie,
Göttingen, Germany

Synonyms

[Lateral stress profile; \(negative\) Lateral tension profile](#)

Definition

The lateral pressure profile is the distribution of lateral stresses across the width of a lipid bilayer. It is composed of repulsive pressure components from interactions between the lipid molecules and a cohesive hydrophobic tension that favors segregation of the lipid chains from water. These components are distributed inhomogeneously across the bilayer.

Introduction

The bilayer analog of the well-known surface pressure of a lipid monolayer spread at the air-water, or oil-water, interface is a negative tension. Thus, the net lateral pressure is zero in a lipid bilayer that is not under tension. The bilayer does, however, possess an internal lateral pressure that balances the hydrophobic tension, which is the driving force for self-assembly of amphiphilic lipid molecules in water. These different stresses are not distributed uniformly across the bilayer, and the resulting lateral pressure profile can affect the conformation and stability of membrane-embedded proteins or drive transitions to nonlamellar lipid phases.

Lateral Pressure

The lateral pressure in a hydrated lipid assembly is defined by the derivative of the free energy with respect to the area:

$$\pi_{\text{tot}} = - \left(\frac{\partial \Delta g_{\text{tot}}}{\partial A_l} \right)_T \quad (1)$$

where Δg_{tot} is the total elastic free energy and A_l is the surface area per lipid molecule. For a lipid monolayer

at the air-water or oil-water interface, this is the conventional surface pressure, and for a bilayer vesicle, it corresponds to a negative membrane tension. Units are force per unit length (\equiv energy per unit area).

At mechanical equilibrium ($\partial\Delta g_{\text{tot}}/\partial A_l = 0$), in the absence of external forces, the lateral pressure in a bilayer vesicle is zero, i.e., the natural state of the membrane is tension-free. The free energy of the bilayer can be partitioned into a net-repulsive component, Δg_{int} , that arises from the lipid-lipid interactions (headgroups and chains) and headgroup-water interactions, and a cohesive component, $-\gamma_{\text{phob}}A_l$, that minimizes hydrophobic contact of the chains with water (see, e.g., Cevc and Marsh 1987). At equilibrium, the corresponding opposing forces balance giving:

$$\pi_{\text{int}} = \gamma_{\text{phob}} \quad (2)$$

where π_{int} ($= -\partial\Delta g_{\text{int}}/\partial A_l$) is the repulsive internal lateral pressure in the bilayer and γ_{phob} is the hydrophobic tension or free energy density. In terms of molecular surface, the surface density of the hydrophobic interaction is ≈ 10 – 20 kJ mol $^{-1}$ /nm 2 , depending on whether volume corrections are introduced (Cevc and Marsh 1987; Marsh 1996). Taking into account roughness of the molecular surface (a factor of two for a hemisphere, or of 1.2 for close-packed spheres), the hydrophobic free energy density at the planar polar-apolar interface corresponds to a hydrophobic tension of $\gamma_{\text{phob}} \approx 35$ – 39 mN m $^{-1}$ at 300 K (Marsh 1996). It thus might be expected that a monolayer is equivalent to a bilayer at surface pressures in the region of 35–39 mN m $^{-1}$; at this point of the monolayer π - A isotherm, the area per lipid A_l is indeed similar to that in the bilayer (Marsh 1996, 2006a).

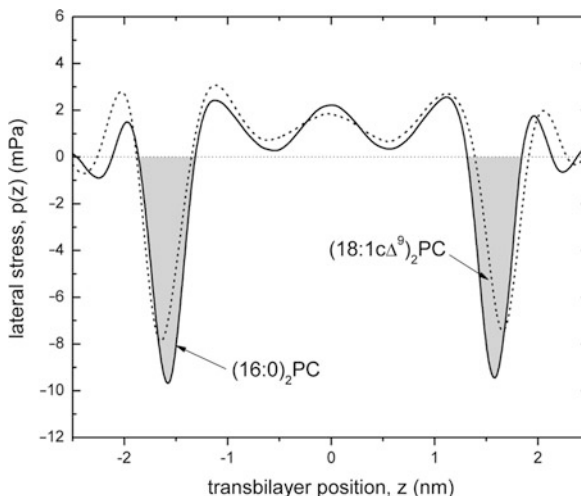
Because the net tension in a bilayer membrane is zero, the repulsive internal lateral pressure, π_{int} , cannot be measured directly and contributes only in second order to the elastic stretching energy via the lateral compressibility (Marsh 1997). The elastic modulus for area extension is given by:

$$K_A = A_l \left(\frac{\partial^2 \Delta g_{\text{tot}}}{\partial A_l^2} \right)_T = A_l \left(\frac{\partial \pi_{\text{int}}}{\partial A_l} \right)_T \quad (3)$$

Typical values obtained from unilamellar bilayer vesicles are $K_A \approx 70$ – 100 mN m $^{-1}$ per monolayer

Lipid Bilayer Lateral Pressure Profile, Table 1 Area extension modulus, K_A , of lipid monolayers and bilayers (Cevc and Marsh 1987; Marsh 2006a)

Lipid	Monolayer			Bilayer	
	T (°C)	π (mN m $^{-1}$)	$A(\partial\pi/\partial A)_T$ (mN m $^{-1}$)	T (°C)	$K_A/2$ (mN m $^{-1}$)
(18:1c Δ^9) $_2$ PC	21	35	78	21	118 \pm 8
(12:0) $_2$ PE	44.2	32	112		



Lipid Bilayer Lateral Pressure Profile, Fig. 1 Atomistic molecular dynamics simulations of the lateral pressure profiles in hydrated bilayers of dipalmitoyl phosphatidylcholine (solid line) or dioleoyl phosphatidylcholine (dashed line) at 50°C (Adapted from Ollila et al. 2007a, b)

(Marsh 2012), which is similar to values obtained from the slopes of monolayer π - A isotherms at a surface pressure of ~ 35 mN m $^{-1}$ (Cevc and Marsh 1987; Marsh 2006a) (see Table 1).

Lateral Stress Profile

The lateral pressure enters in first order to the bending elasticity, but this is via the transmembrane profile of lateral pressure:

$$p(z) = \frac{\partial \pi_{\text{tot}}}{\partial z} \quad (4)$$

where z lies along the bilayer normal, rather than by the lateral pressure directly. The lateral stress profile, $p(z)$, has the dimensions of a three-dimensional pressure, i.e., force per unit area. Representative simulations of the transmembrane profiles of lipid bilayers that are



Lipid Bilayer Lateral Pressure Profile, Table 2 Moments of the lateral pressure profile from coarse-grained MD simulations and experimental values of bending elasticity

Lipid	P_1 (pN)	$k_c c_o$ (pN)	$2\delta P_1 - P_2$ (J)	\bar{k}_c (J)	References
(18:1c Δ^9) ₂ PE	-10.5	-15.2 ± 0.9^a		$-(3.0 \pm 0.3) \times 10^{-20b}$	Marrink et al. (2007)
(14:0) ₂ PC	-0.8 ± 0.1	≈ 0	$-(2.3 \pm 0.1) \times 10^{-20}$	$-(2.3 \pm 0.2) \times 10^{-20b}$	Orsi et al. (2008)

^aExperimental value from H_{II} phases corrected to the neutral plane (Marsh 2012)

^bCalculated from the experimental monolayer value of k_c for (18:1c Δ^9)₂PE or (14:0)₂PC (Marsh 2012), together with the experimental ratio $\bar{k}_c/k_c = -0.75 \pm 0.08$ (Templer et al. 1998)

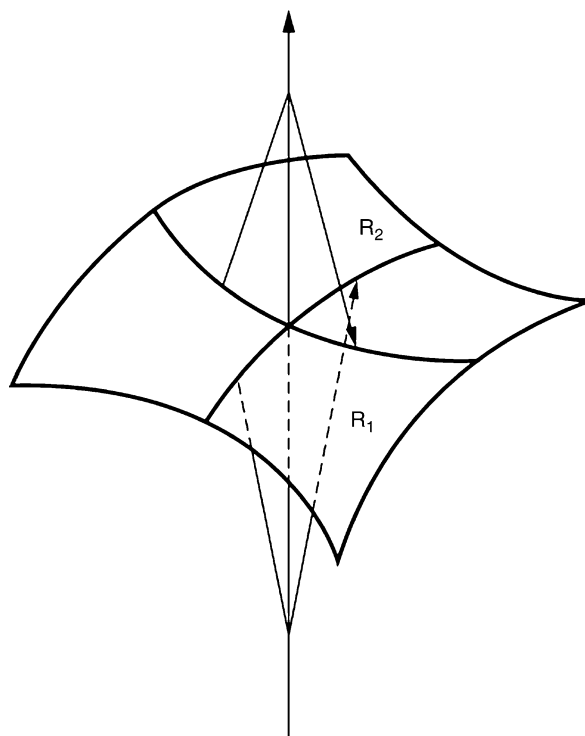
obtained from molecular dynamics (MD) calculations are shown in Fig. 1. These are characterized by a large negative (cohesive) component that is centered about the polar-apolar interface, and positive net repulsive components in the region of the lipid headgroups and lipid chains. The negative peak has an integrated area that is comparable to the hydrophobic tension (cf. above). The positive pressure in the headgroup region is the lateral hydration pressure (Cevc and Marsh 1985, 1987) plus possible electrostatic repulsion, and that in the chain region is an entropic pressure driven by rotational isomerism in the lipid chains (Fattal and Ben-Shaul 1993).

Moments of the Lateral Pressure Profile

The spontaneous bending moment per unit length of one monolayer of a lipid bilayer is given by the first moment, P_1 , of the lateral pressure profile (see, e.g., Marsh 2001; Marsh et al. 2003):

$$k_c c_o = \int_0^l z p(z) dz \equiv P_1 \quad (5)$$

where k_c is the elastic modulus of mean curvature and c_o is the spontaneous curvature (Marsh 2006b); l is the width of the lipid monolayer, and the origin of z is at the bilayer midplane. The first moment does not depend on the choice of the origin for z because $\int p(z) dz = 0$. Spontaneous curvature expresses the intrinsic propensity of a lipid monolayer to bend and is determined from the radius of the pivotal plane ($c_o = 1/R_{o,p}$) of inverted hexagonal (H_{II}) phases of the lipid in question (Marsh 2011). Evaluation of the first moment of the lateral pressure profile simulated by coarse-grained molecular dynamics produces values for the spontaneous bending moment in each monolayer that are of the same order as those found



Lipid Bilayer Lateral Pressure Profile, Fig. 2 Saddle-splay bending of a lipid bilayer, where the principal curvatures are $c_1 (=1/R_1) = -c_2 (=1/R_2)$, giving zero mean curvature and a Gaussian curvature of $c_G^2 = c_1 c_2 = -1/R_1^2$

experimentally (see Table 2). For a symmetrical lipid bilayer membrane, the net spontaneous curvature is zero because the spontaneous bending moments in the two apposing monolayers cancel. Both monolayers are then in a state of curvature frustration that is imposed upon them by being forced into a lamellar configuration. The resulting inhomogeneity in lateral stress can control the folding, insertion, and activity of membrane-bound proteins (Marsh 2007; Pocanschi et al. 2006).

The second moment, P_2 , of the lateral pressure profile determines the Gaussian curvature modulus of the lipid monolayer (see Helfrich 1981; Marsh 2006b):

$$\bar{k}_c = - \int_0^l (z - \delta)^2 p(z) dz = 2\delta P_1 - P_2 \quad (6)$$

where $z = \delta$ is the position of the neutral plane (or plane of inextension). Bicontinuous inverse cubic lipid phases are based on infinite periodic minimal surfaces that have zero mean curvature ($c_1 + c_2 = 0$) everywhere, and only the Gaussian curvature is non-zero ($c_1 c_2 < 0$) – see Fig. 2.

The ratio of Gaussian to mean curvature moduli, based on the swelling behavior with increasing water content of inverse cubic phases that are formed from a mixture of monooleoylglycerol, dioleoyl phosphatidylcholine, and dioleoyl phosphatidylethanolamine (58:38:4 mol/mol/mol) at 25°C, is $\bar{k}_c/k_c = -0.75 \pm 0.08$ for a monolayer (Templer et al. 1998). Coarse-grained MD simulations produce moments of the transbilayer stress profile that are consistent with this ratio (see Table 2). The lateral pressure profile is, therefore, one of the crucial controlling factors in the formation of nonlamellar lipid phases.

Summary

The net lateral pressure in a tension-free lipid bilayer is zero, but the compensating lateral stresses are distributed nonuniformly across the bilayer width. The area derivative of the repulsive component of the internal lateral pressure (which is equivalent to a monolayer surface pressure) is proportional to the area elastic modulus. The first moment of the lateral pressure profile for one monolayer leaflet is equal to the product of the monolayer mean curvature modulus and spontaneous curvature. The second moment of the leaflet lateral pressure profile determines the Gaussian curvature modulus. Bilayer lateral pressure profiles are important for bending elasticity, nonlamellar phases, and conformational stability of embedded proteins.

References

- Cevc G, Marsh D. Hydration of non-charged lipid bilayer membranes. Theory and experiments with phosphatidylethanolamines. *Biophys J.* 1985;47:21–31.
- Cevc G, Marsh D. Phospholipid bilayers. Physical principles and models. New York: Wiley-Interscience; 1987.
- Fattal DR, Ben-Shaul A. A molecular model for lipid-protein interaction in membranes: the role of hydrophobic mismatch. *Biophys J.* 1993;65:1795–809.
- Helfrich W. Amphiphilic mesophases made of defects. In: Balian R, Kléman M, Poirier JP, editors. *Physics of defects*, Les Houches, Session XXXV, 1980. Amsterdam: North-Holland; 1981. p. 716–55.
- Marrink SJ, Risselada HJ, Yefimov S, Tieleman DP, de Vries AH. The MARTINI force field: coarse grained model for biomolecular simulations. *J Phys Chem B.* 2007;111:7812–24.
- Marsh D. Lateral pressure in membranes. *Biochim Biophys Acta.* 1996;1286:183–223.
- Marsh D. Renormalization of the tension and area expansion modulus in fluid membranes. *Biophys J.* 1997;73:865–9.
- Marsh D. Elastic constants of polymer-grafted lipid membranes. *Biophys J.* 2001;81:2154–62.
- Marsh D. Comment on interpretation of mechanochemical properties of lipid bilayer vesicles from the equation of state or pressure-area measurement of the monolayer at the air-water or oil-water interface. *Langmuir.* 2006a;22:2916–9.
- Marsh D. Elastic curvature constants of lipid monolayers and bilayers. *Chem Phys Lipids.* 2006b;144:146–59.
- Marsh D. Lateral pressure profile, spontaneous curvature frustration, and the incorporation and conformation of proteins in membranes. *Biophys J.* 2007;93:3884–99.
- Marsh D. Pivotal surfaces in inverted hexagonal and cubic phases of phospholipids and glycolipids. *Chem Phys Lipids* 2011;164:177–83.
- Marsh D. *Handbook of lipid bilayers*. 2nd ed. New York: CRC Press; 2012.
- Marsh D, Bartucci R, Sportelli L. Lipid membranes with grafted polymers: physicochemical aspects. *Biochim Biophys Acta.* 2003;1615:33–59.
- Ollila S, Róg T, Karttunen M, Vattulainen I. Role of sterol type on lateral pressure profiles of lipid membranes affecting membrane protein functionality: comparison between cholesterol, desmosterol, 7-dehydrocholesterol and ketosterol. *J Struct Biol.* 2007a;159:311–23.
- Ollila S, Hyvönen M, Vattulainen I. Polyunsaturation in lipid membranes: dynamic properties and lateral pressure profiles. *J Phys Chem B.* 2007b;111:3139–50.
- Orsi M, Haubertin DY, Sanderson WE, Essex JW. A quantitative coarse-grain model for lipid bilayers. *J Phys Chem B.* 2008;112:802–15.
- Pocanschi CL, Patel GJ, Marsh D, Kleinschmidt JH. Curvature elasticity and refolding of OmpA in large unilamellar vesicles. *Biophys J.* 2006;91:L75–7.
- Templer RH, Khoo BJ, Seddon JM. Gaussian curvature modulus of an amphiphilic monolayer. *Langmuir.* 1998;14:7427–34.

Lipid Domains

Richard M. Epand

Department of Biochemistry and Biomedical Sciences,
McMaster University Health Sciences Centre,
Hamilton, ON, Canada

Synonyms

Lipid bilayer

Introduction

Biological membranes are not homogeneous along the plane of the membrane, but rather form clusters of molecules resulting in the formation of membrane domains. In eukaryotes, sterols, such as cholesterol, play a major role in driving the formation of lateral inhomogeneities in the membrane. However, domains also are present in bacterial membranes that are devoid of cholesterol. We will review some of the interactions resulting in the formation of domains and indicate how they can affect the biological properties of the membrane.

Membrane Domains

It is now appreciated that biological membranes and many model membranes are inhomogeneous in the plane of the bilayer. This is a more recent conceptual advance over the fluid mosaic model of membranes. As a consequence of this lateral heterogeneity, some molecular components will be enriched in certain regions of the membrane that are referred to as domains.

Biological membranes are composed principally of phospholipids and proteins. ► [Membrane proteins](#) can also be reconstituted into a lipid membrane to study the properties of a membrane with a more limited number of components than biological membranes. Domains can be enriched in either lipid and/or in protein components in both biological and model membranes. If the system is at equilibrium, the molecular components of the membrane will rearrange themselves to achieve a state of minimum energy. The line

tension that develops as a result of the formation of a boundary between a domain and the bulk lipid makes an important contribution to the thermodynamics of domain formation (Garcia-Saez et al. 2007) (► [Thermodynamics of Lipid Interactions](#)). Molecules that partition into the boundary interface can strongly affect lateral heterogeneity (Schafer and Marrink 2010).

The most common arrangement of lipids in biological membranes is the bilayer. Model membranes can undergo morphological rearrangements to form other phases including cubic phases and the inverted hexagonal phase (► [Lipid Shape and Curvature Stress](#)). This may also occur, particularly the formation of cubic phases, in biological membranes, but it is not a common situation. In this chapter on domains, we will only consider domains in bilayer membranes.

Bilayers can form crystalline, subgel, gel, ripple, or liquid crystalline phases (► [Phase Transitions and Phase Behavior of Lipids](#)). Biological membranes are generally in the liquid crystalline phase. Organisms have homeostatic mechanisms to maintain their membranes in this physical state and avoid the formation of gel phases that may be too rigid to carry out certain biological functions, or inverted hexagonal phases that would destroy the permeability barrier of the membrane bilayer. The liquid crystalline phase can exist in two different states, the liquid-ordered or L_o phase and the liquid-disordered or L_d phase. These are both liquid crystalline phases in which the lipid components undergo rapid lateral diffusion, more rapid than is found with gel state lipid. However, the acyl chain geometry in the L_o phase is extended, resembling that of a gel phase, with saturated $\text{CH}_2\text{-CH}_2$ groups forming *trans* rotomers. In contrast, the acyl chain geometry of the L_d phase has both *trans* and *gauche* rotomers and is less extended. Phase diagrams can represent transitions between phases. At a particular point in the phase diagram, defined as the critical point, the system becomes very sensitive to large fluctuations as a result of small changes in concentrations or in the environment (Honerkamp-Smith et al. 2009).

Model Raft Domains

The increased interest in membrane domain formation among biologists is a consequence of the growing

awareness of the existence of such structures in biological membranes. One type of domain has been termed the membrane “raft.” Raft domains in biological membranes are enriched with cholesterol and sphingomyelin (► [Sphingolipids and Gangliosides](#)) and are believed to be in the liquid-ordered (L_o) phase. Interestingly, model membranes composed of equimolar quantities of palmitoyl-sphingomyelin, dioleoyl-phosphatidylcholine, and cholesterol will spontaneously form sphingomyelin-enriched domains over a wide range of temperatures (Feigenson 2009).

Raft Domains in Biological Membranes

There has been an ongoing discussion about the extent of the relationship between model raft domains and cholesterol-dependent domains in biological membranes. There is a general agreement that the domains found in biological membranes are smaller in size and have a shorter lifetime. The most recent evidence (Bramshuber et al. 2011) indicates that there are mobile long-lived cholesterol-dependent domains in the plasma membrane of living CHO and Jurkat T cells in the resting state with a lifetime longer than several seconds, the upper limit of detection by this method (► [Single Fluorophore Photobleaching](#)). The size of these domains is estimated to be ~ 45 nm. Raft domains are associated with the actin cytoskeleton that is required to maintain the structural and functional (► [Functional Roles of Lipids in Membranes](#)) properties of rafts (Chichili and Rodgers 2009).

Proteins and Cholesterol-Rich Domains

One of the major differences between model phospholipid membranes and biological membranes is the presence of a large fraction of proteins in the biological membrane. It is known that certain proteins spontaneously partition into raft domains and these proteins can stabilize rafts. However, not only proteins that partition into cholesterol-rich domains will favor the formation of these domains but also proteins that preferentially bind to phospholipids rather than cholesterol will also favor the clustering of cholesterol but in other regions of the membrane. This is a thermodynamic requirement, as long as the system is in equilibrium.

There is particular interest in understanding which proteins partition into raft domains (Poveda et al. 2008). This is because there is evidence that these domains play an important role in signal transduction (Zech et al. 2009). Some of the features resulting in the partitioning of proteins in cholesterol-rich domains include the presence of certain types of lipidation, a segment of the protein with the amino acid pattern called the CRAC domain or a cluster of transmembrane helices with a particular structure termed the sterol-sensing domain (Epand et al. 2010). The CRAC domain is a protein segment with the sequence $-L/V-X_{1-5}-Y-X_{1-5}-R/K-$. The first residue can be either L or V and the last residue, either of the two basic amino acids, R or K. There are also two variable segments, X_{1-5} , each of which can have any length between 1 and 5 residues, as well as any kind of sequence (Li and Papadopoulos 1998). In contrast to the short CRAC domain, the sterol-sensing domain is comprised of a cluster of five transmembrane helices and is found in several proteins that are involved in cholesterol homeostasis. There also appears to be a pattern of particular amino acids within transmembrane segments of G-protein-coupled receptors (Paila et al. 2009) that results in the interaction of these proteins with clusters of cholesterol molecules (Cherezov et al. 2007), apparently modulating the function (► [Functional Roles of Lipids in Membranes](#)) of G-protein-coupled receptors.

Caveolae

Although there is some uncertainty in the exact size and lifetime of biological rafts, there is much more certainty about the raft-like domains, the caveolae, that are abundant in certain types of cells (Parat 2009). Both caveolae and rafts are believed to be in the L_o phase and have similar lipid compositions. However, unlike rafts, caveolae are morphologically distinct 50–80 nm diameter, flask-shaped invaginations in the plasma membrane. The protein caveolin is highly enriched in this domain and plays an important function in maintaining the integrity of this domain (Parton and Simons 2007). Caveolae are believed to function in signal transduction but are also involved in a separate pathway for endocytosis, including the uptake of certain pathogens (Harris et al. 2002; Parton and Simons 2007; Razani et al. 2002).

Another group of proteins, the cavins, are involved in regulation of caveolae by promoting membrane remodeling and trafficking (Chidlow and Sessa 2010). Caveolae have been implicated in chronic inflammatory conditions and other pathologies including atherosclerosis, inflammatory bowel disease, muscular dystrophy, and generalized dyslipidemia.

Bacterial Domains

There are several examples indicating that bacterial membranes have lipid domains (Matsumoto et al. 2006). There is increasing interest in these domains because they can also be formed with the addition of certain antimicrobial agents. This phenomenon is correlated with the toxicity of these agents toward different species of bacteria (Epanand and Epanand 2010).

There are bacterial domains that develop at the time of bacterial cell division (Mazor et al. 2008); however, there are also domains detected in anucleated bacteria that are apparently independent of cell division (Muchova et al. 2010). A feature of bacterial membranes that has allowed more facile imaging of lipid domains in these biological membranes is that most bacterial strains have a significant amount of cardiolipin in their membranes and clusters of cardiolipin will preferentially bind to 10-N-nonyl acridine orange (Mileykovskaya et al. 2001).

Membrane Domains in Mitochondria

Mitochondria, like Gram-negative bacteria, are enclosed by a double membrane. Furthermore, the inner membrane of mitochondria, like most bacterial membranes, is the only membrane of eukaryotic cells that contains a high concentration of cardiolipin. The inner mitochondrial membrane also has a particular folded morphology that results in the formation of the mitochondrial cristae. An important role of mitochondria is the production of ATP by oxidative phosphorylation (► [Mitochondrial Electron Transport](#)). This ATP is produced on the inner monolayer of the inner membrane of mitochondria, but the utilization of ATP occurs principally in the cytosol. There thus has to be a system for transporting this energy across two membranes. In many cells, this is accomplished indirectly through the phosphocreatine

circuit (Wallimann et al. 2007). ATP is transported across the inner mitochondrial membrane by the ADP/ATP carrier protein that exchanges ATP in the mitochondrial matrix for ADP in the mitochondrial interstitial space. Most of the ADP formed in the interstitial space is a consequence of the transfer of the γ phosphate of ATP to creatine, catalyzed by the enzyme mitochondrial creatine kinase, producing ADP and phosphocreatine. The ADP is shuttled into the mitochondrial matrix where it serves as a substrate for oxidative phosphorylation, while the phosphocreatine is exported across the mitochondrial outer membrane to be used as an energy source for the production of ATP in the cytosol, catalyzed by other isoforms of creatine kinase. This system requires a high degree of organization and interactions between lipids and proteins. It is also likely that in some cases these protein-lipid interactions lead to the formation of lipid domains. There is direct evidence that oligomers of the ubiquitous isoform of mitochondrial creatine kinase clusters cardiolipin (Epanand et al. 2007).

Mitochondria also play an important role in a major pathway of apoptosis as a result of the movement of cardiolipin from the mitochondrial inner membrane to the outer membrane where it participates in the activation of the proapoptotic protein Bid. It is suggested that in the outer membrane, cardiolipin forms a membrane domain where apoptotic proteins can bind and be activated (Sorice et al. 2009).

Summary

Lipid domains are found in both model and biological membrane. There are at least two driving forces for the formation of these domains. One is the preferential interaction of one component for another. The other is more specifically based on electrostatic interactions between a polycationic molecule and anionic lipids.

In many cases, cholesterol is an important component in the formation of domains by the mechanism of preferential interactions. This is likely the case because the chemical structure and physical properties of cholesterol are very different from those of phospholipids and, therefore, there is frequently a preferential interaction of other lipid components or of peptides or proteins with cholesterol or with phospholipids. The phase behavior of lipid mixtures containing cholesterol that segregate into domains has been well studied and

is reasonably well understood. There is much evidence that domains with some relationship to those of cholesterol-rich domains of model membranes are also present in biological membranes. However, the biological membranes are more complex with many more molecular components as well as interactions with an underlying cytoskeleton that has also been shown to affect domain formation. Nevertheless, it is clear that there are domains in biological membranes, but a complete understanding of their composition, physical properties, and heterogeneity is still evolving. In biological membranes, raft domains play an important role in signal transduction by sequestering different proteins that can interact with one another or with the lipid components of these rafts. Despite the lack of complete knowledge about the rafts of biological membranes, there is a related domain, the caveolae that appears to have similar lipid composition to those of rafts. However, caveolae are larger structures with a long lifetime. Their morphology, size, and chemical composition are well established. Caveolae also play important biological roles both in signal transduction as well as in the movement of substances into and out of cells.

The other mechanism for domain formation is the clustering of anionic lipids by polycationic molecules. This mechanism is particularly effective for the sequestering of the lipid phosphatidylinositol-(4,5)-bisphosphate that has several negative charges (McLaughlin and Murray 2005). Anionic lipid clustering also plays a role in the action of certain antimicrobial agents and in the formation of cardiolipin-rich domains in mitochondria.

Cross-References

- ▶ [Lipid Lateral Diffusion](#)
- ▶ [Thermodynamics of Lipid Interactions](#)

References

- Bramshuber M, Weghuber J, Ruprecht V, Gombos I, Horvath I, Vigh L, Eckerstorfer P, Kiss E, Stockinger H, Schuetz GJ. Imaging of mobile long-lived nanoplateforms in the live cell plasma membrane. *J Biol Chem*. 2011;285:41765–71.
- Cherezov V, Rosenbaum DM, Hanson MA, Rasmussen SG, Thian FS, Kobilka TS, Choi HJ, Kuhn P, Weis WI, Kobilka BK, Stevens RC. High-resolution crystal structure of an engineered human beta2-adrenergic G protein-coupled receptor. *Science*. 2007;318:1258–65.
- Chichili GR, Rodgers W. Cytoskeleton-membrane interactions in membrane raft structure. *Cell Mol Life Sci*. 2009;66:2319–28.
- Chidlow Jr JH, Sessa WC. Caveolae, caveolins, and cavins: complex control of cellular signalling and inflammation. *Cardiovasc Res*. 2010;86:219–25.
- Epand RF, Tokarska-Schlattner M, Schlattner U, Wallimann T, Epand RM. Cardiolipin clusters and membrane domain formation induced by mitochondrial proteins. *J Mol Biol*. 2007;365:968–80.
- Epand RM, Epand RF. Biophysical analysis of membrane-targeting antimicrobial peptides: membrane properties and the design of peptides specifically targeting gram-negative bacteria. In: Wang G, editor. *Antimicrobial peptides: discovery, design and novel therapeutic strategies*, Chapter 7. Henderson B, Wilson M, editors. *Advances in molecular and cellular microbiology*, vol. 18. Wallingford, UK: CABI; 2010. p. 116–27.
- Epand RM, Thomas A, Brasseur R, Epand RF. Cholesterol interaction with proteins that partition into membrane domains: an overview. In: Harris JR, editor. *Cholesterol binding and cholesterol transport proteins*, Chapter 9. *Subcellular biochemistry*, vol. 51. Harris JR, Quinn PJ, editors. Heidelberg: Springer; 2010. p. 253–78.
- Feigenson GW. Phase diagrams and lipid domains in multicomponent lipid bilayer mixtures. *Biochim Biophys Acta*. 2009;1788:47–52.
- Garcia-Saez AJ, Chiantia S, Schwille P. Effect of line tension on the lateral organization of lipid membranes. *J Biol Chem*. 2007;282:33537–44.
- Harris J, Werling D, Hope JC, Taylor G, Howard CJ. Caveolae and caveolin in immune cells: distribution and functions. *Trends Immunol*. 2002;23:158–64.
- Honerkamp-Smith AR, Veatch SL, Keller SL. An introduction to critical points for biophysicists; observations of compositional heterogeneity in lipid membranes. *Biochim Biophys Acta*. 2009;1788:53–63.
- Li H, Papadopoulos V. Peripheral-type benzodiazepine receptor function in cholesterol transport. Identification of a putative cholesterol recognition/interaction amino acid sequence and consensus pattern. *Endocrinology*. 1998;139:4991–7.
- Matsumoto K, Kusaka J, Nishibori A, Hara H. Lipid domains in bacterial membranes. *Mol Microbiol*. 2006;61:1110–7.
- Mazor S, Regev T, Mileykovskaya E, Margolin W, Dowhan W, Fishov I. Mutual effects of MinD-membrane interaction: II. Domain structure of the membrane enhances MinD binding. *Biochim. Biophys. Acta*. 2008;1778:2505–11.
- McLaughlin S, Murray D. Plasma membrane phosphoinositide organization by protein electrostatics. *Nature*. 2005;438:605–11.
- Mileykovskaya E, Dowhan W, Birke RL, Zheng D, Lutterodt L, Haines TH. Cardiolipin binds nonyl acridine orange by aggregating the dye at exposed hydrophobic domains on bilayer surfaces. *FEBS Lett*. 2001;507:187–90.
- Muchova K, Jamroskovic J, Bara'k I. Lipid domains in *Bacillus subtilis* anucleate cells. *Res Microbiol*. 2010;161:783–90.
- Paila YD, Tiwari S, Chattopadhyay A. Are specific nonannular cholesterol binding sites present in G-protein coupled receptors? *Biochim Biophys Acta*. 2009;1788:295–302.

- Parat M. Chapter 4 The biology of caveolae. Achievements and perspectives. Vol. 273. (2009), pp. 117–162
- Parton RG, Simons K. The multiple faces of caveolae. *Nat Rev Mol Cell Biol.* 2007;8:185–94.
- Poveda JA, Fernandez AM, Encinar JA, Gonzalez-Ros JM. Protein-promoted membrane domains. *Biochim Biophys Acta.* 2008;1778:1583–90.
- Razani B, Woodman SE, Lisanti MP. Caveolae: from cell biology to animal physiology. *Pharmacol Rev.* 2002;54:431–67.
- Schafer LV, Marrink SJ. Partitioning of lipids at domain boundaries in model membranes. *Biophys J.* 2010;99:L91–3.
- Sorice M, Manganelli V, Matarrese P, Tinari A, Misasi R, Malorni W, Garofalo T. Cardiolipin-enriched raft-like microdomains are essential activating platforms for apoptotic signals on mitochondria. *FEBS Lett.* 2009;583:2447–50.
- Wallimann T, Tokarska-Schlattner M, Neumann D, Epand RM, Epand RF, Andres RH, Widmer HR, Hornemann T, Saks V, Agarkova I, Schlattner U. The phosphocreatine circuit. In: Saks V, editor. *Molecular systems bioenergetics: energy for life*, Chapter 7. London: Wiley; 2007. p. 195–264.
- Zech T, Ejsing CS, Gaus K, De Wet B, Shevchenko A, Simons K, Harder T. Accumulation of raft lipids in T-cell plasma membrane domains engaged in TCR signalling. *EMBO J.* 2009;28:466–76.

Lipid Flip-Flop

Anant K. Menon¹ and Andreas Herrmann²

¹Department of Biochemistry, Weill Cornell Medical College, New York, NY, USA

²Molecular Biophysics, Humboldt-Universität zu Berlin, Berlin, Germany

Synonyms

Transbilayer movement; Lipid bilayer

Definitions

Biogenic membranes are “self-synthesizing” membranes, capable of synthesizing and integrating their lipid and protein components. Examples are the endoplasmic reticulum and the bacterial cytoplasmic membrane.

Flippases are membrane proteins that facilitate vectorial, ATP-dependent transport of lipids across membranes, or the ATP-independent bidirectional movement of lipids. ATP-dependent flippases are either P-type ATPases or ATP-binding cassette (ABC) transporters. The molecular identity of most ATP-independent flippases (also called scramblases) is not known.

Flipping describes the reorientation of a lipid from one leaflet of a membrane bilayer to the other. It is used interchangeably with “flip-flop,” “transbilayer translocation,” or “transbilayer movement.” Flip refers to transport of a lipid from the exoplasmic or luminal membrane leaflet to the cytoplasmic leaflet, that is, out → in, whereas flop designates in → out transport.

Membrane proteins are integral to the membrane and contain one or more transmembrane domains comprised of sequences rich in hydrophobic amino acids.

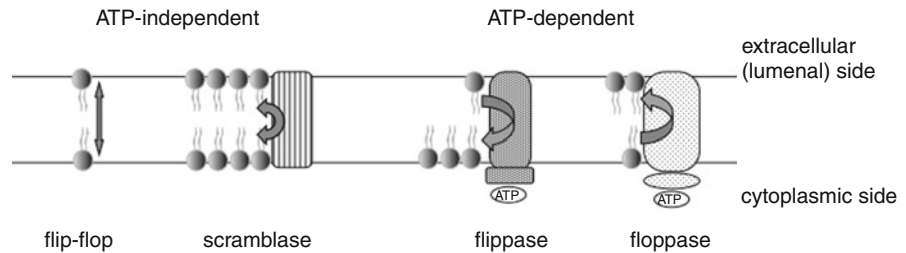
Polar lipids are amphipathic molecules, with a hydrophobic unit derived from fatty acids, sphingosine, or isoprenoids (such as dolichol and undecaprenol), and a zwitterionic or charged hydrophilic headgroup. Examples are phosphatidylcholine, sphingomyelin, dolichyl phosphate mannose, and bacterial Lipid II.

Introduction

Polar lipids diffuse rapidly in the plane of the membrane, but their transverse diffusion – movement from one side of the bilayer to the other, or flip-flop – is intrinsically very slow (Kornberg and McConnell 1971). This is because the hydrophobic interior of the membrane presents an energy barrier to the transit of the polar lipid headgroup. For common phospholipids such as phosphatidylcholine (PC), the barrier is estimated at ~20–50 kcal/mol. However, rapid flip-flop of polar lipids is essential for numerous physiological processes, and lipids move rapidly across many types of biological membranes as a result of the action of lipid transport proteins termed flippases. It is important to note that for lipids without a substantial polar headgroup, spontaneous flipping is rapid and does not require flippases. Examples of such lipids include cholesterol, ceramide, and diacylglycerol whose headgroup is a simple hydroxyl moiety.

Lipid flippases are membrane proteins that either use the energy of ATP hydrolysis to move lipids across the membrane against their concentration gradient, or facilitate bidirectional movement of lipids without metabolic energy input (Fig. 1). The former are sometimes referred to as flippases or floppases depending on whether they move lipids toward the cytoplasmic or exoplasmic (or luminal) leaflet of cellular membranes, respectively, whereas the latter are also termed “scramblases” because they dissipate transbilayer lipid asymmetry.

Lipid Flip-Flop, Fig. 1 Lipid flip-flop and the role of flippases



Lipid Transport Catalyzed by P-Type ATPases and ABC Transporters

Flippases in the eukaryotic plasma membrane (PM) are generally membrane proteins that belong to the family of type IV P-type ATPases (P4-ATPases) or the family of ABC (ATP-binding cassette) transporters. These proteins use the energy of ATP hydrolysis to catalyze transbilayer transport of a variety of polar lipids. The P4-ATPases transport glycerophospholipids from the exoplasmic to the cytoplasmic leaflet of the PM. In many instances, transport is specific for certain phospholipids. Indeed, the first of the PM lipid translocation activities to be described was shown to be highly specific for aminophospholipids, especially phosphatidylserine (Seigneuret and Devaux 1984). ABC transporters generally catalyze transport from the cytoplasmic to the exoplasmic leaflet. The principle function of PM lipid transporters is to maintain the biologically significant transbilayer lipid asymmetry of the PM, first reported in the early 1970s by Bretscher, in which phosphatidylcholine, sphingomyelin, and glycolipids are located in the exoplasmic leaflet whereas phosphatidylserine, phosphatidylethanolamine, and phosphoinositides are enriched on the cytoplasmic side. Loss of lipid asymmetry at the PM is a hallmark of programmed cell death where exposure of phosphatidylserine at the cell surface signals engulfment of the cell by macrophages.

P4-ATPases commonly associate with a member of the Cdc50 family of membrane proteins. Complex formation must occur before the P4-ATPase can exit the endoplasmic reticulum (ER). P4-ATPase complexes have been isolated from yeast and retina and shown to have flippase activity in reconstituted vesicles. However, it is unclear whether the Cdc50 subunit is essential for flippase activity or whether it provides a regulatory function. The specificity of P4-ATPases varies. Originally thought to be specific for aminophospholipids in general and phosphatidylserine in particular, members of this

transporter family can also transport other phospholipids. The activity of P4-ATPases is regulated. In *Saccharomyces cerevisiae*, one regulatory mechanism is phosphorylation triggered by changes in membrane composition.

The ability of ABC transporters to transport lipids was originally highlighted in studies of P-glycoprotein (also called MDR1). Studies in transgenic animals as well as in cultured cells showed that this protein could transport phospholipids from the cytoplasmic leaflet to the exoplasmic leaflet of the PM. ABC transporters also function in less obvious ways to transport lipids. For example, sterol movement across membranes is controlled in several physiologically important contexts by ABC transporters (such as ABCA1) even though sterols can flip-flop across membranes at a rapid spontaneous rate. The role of ABC transporters in these cases may be to increase the chemical activity of the sterol molecule, thus facilitating its hand-off to an acceptor particle or protein.

The PM of eukaryotes has an ATP-independent flippase activity that depends on an elevation in calcium ion concentration. This flippase, historically referred to as scramblase, is typically activated under conditions where the ATP-dependent flippase activities of the PM are inactivated. Thus, in apoptotic cells, the P4-ATPase and ABC transporter activities of the PM are silenced, scramblase is activated, and phosphatidylserine is exposed at the cell surface. The protein responsible for calcium-induced phospholipid scrambling has not been convincingly identified although candidates (PLSCR1, TMEM16F) (Suzuki et al. 2010) have been proposed.

ATP-Independent Lipid Flippases

Glycerophospholipids are synthesized on the cytoplasmic face of biogenic membranes such as the ER in



eukaryotes and cytoplasmic or inner membrane (CM) in bacteria. For normal expansion of the membrane during cell growth, half of the newly synthesized lipids must be flipped to the opposite leaflet of the bilayer. The rate of phospholipid synthesis and flipping must match the demand for new membrane as the cell grows. In a bacterial cell that doubles every ~30 min, at least ~5,000 phospholipids must flip across the CM every second. For Gram-negative cells where phospholipids are also needed for outer membrane biogenesis, the demand for lipid synthesis and flipping is greater. Biochemical reconstitution studies indicate that both the ER and CM have specific transport proteins that facilitate ATP-independent bidirectional movement of phospholipids across the membrane. The flippases are nonselective with respect to glycerophospholipid structure and are capable of flipping different stereoisomers. Although their activity has been studied for over 30 years, the molecular identity of these flippases is not known. It was recently shown that certain G-protein coupled receptors are ATP-independent phospholipid flippases (Menon et al. 2011).

The ER also supports the biosynthesis of complex glycolipids required for *N*-glycosylation and glycosylphosphatidylinositol (GPI)-anchoring of proteins. The assembly of these glycolipids occurs via a multistep pathway that starts in the cytoplasmic leaflet of the ER and continues in the luminal leaflet, necessitating flipping of lipid intermediates. For synthesis of the dolichol-linked oligosaccharide precursor of protein *N*-glycans, three different lipids must be flipped across the ER membrane. Biochemical reconstitution studies indicate that distinct ATP-independent flippases are required for these flipping events. Although the molecular identity of these flippases is not known, activity assays indicate that they are highly specific and capable of distinguishing between structural isomers.

Related flipping events occur in the CM. Thus, Lipid II, a glycopeptidolipid precursor of the bacterial cell wall, must move from the cytoplasmic side of the membrane to the periplasmic side to contribute building blocks for cell wall assembly. The membrane proteins, FtsW (Mohammadi et al. 2011) and MviN, have both been proposed as being responsible for flipping Lipid II flippase. Lipopolysaccharide (LPS), a major component of the cell surface of Gram-negative bacteria, is composed of lipid A, a core oligosaccharide and in some cases, a repeating oligosaccharide termed O-antigen. LPS biosynthesis is initiated on the

cytoplasmic side of the CM and requires flipping of both Lipid A (by the ABC transporter MsbA) and lipid-linked O-antigen oligosaccharide units (by the Wzx family of proteins) before LPS can be assembled and delivered to the cell surface.

A number of pathogenic bacteria repel cationic antimicrobial peptides by decreasing their cell surface negative charge. They do this by modifying phosphatidylglycerol with lysine on the cytoplasmic face of the CM, then moving the positively charged, lysinylated phospholipid across the membrane. Lysinylated phosphatidylglycerol is synthesized and flipped across the membrane by MprF, a CM membrane protein.

Cross-References

- ▶ [Bacterial Lipopolysaccharide, OPS, and Lipid A](#)
- ▶ [Chemical Diversity of Lipids](#)
- ▶ [Functional Roles of Lipids in Membranes](#)
- ▶ [Glycerolipids: Chemistry](#)
- ▶ [Glycoproteins](#)
- ▶ [Glycosphingolipids](#)
- ▶ [Glycosylphosphatidylinositol](#)
- ▶ [Lipid Bilayer Asymmetry](#)
- ▶ [Lipid Trafficking in Cells](#)
- ▶ [Lipids: Isolation and Purification](#)
- ▶ [Membrane Proteins: Structure and Organization](#)
- ▶ [Sum Frequency Generation Vibrational Spectroscopy](#)

References

- Devaux PF, Herrmann A. Transmembrane dynamics of lipids. Hoboken: Wiley; 2012.
- Komberg R, McConnell HM. Inside-outside transitions of phospholipids in vesicle membranes. *Biochemistry*. 1971; 10:1111–20.
- Menon I, Huber T, Sanyal S, Banerjee S, Barré P, Canis S, Warren JD, Hwa J, Sakmar TP, Menon AK. Opsin is a phospholipid flippase. *Curr Biol*. 2011;21:149–53.
- Mohammadi T, van Dam V, Sijbrandi R, Vernet T, Zapun A, Bouhss A, Diepeveen-de Bruin M, Nguyen-Distèche M, de Kruijff B, Breukink E. Identification of FtsW as a transporter of lipid-linked cell wall precursors across the membrane. *EMBO J*. 2011;30:1425–32.
- Sanyal S, Menon AK. Flipping lipids: why an' what's the reason for? *ACS Chem Biol*. 2009;4:895–909.
- Sebastian TT, Baldrige RD, Xu P, Graham TR. Phospholipid flippases: building asymmetric membranes and transport vesicles. *Biochim Biophys Acta*. 2012.

- Seigneuret M, Devaux PF. Proc Natl Acad Sci USA. 1984;81:3751–5.
- Sharom FJ. Flipping and flopping – lipids on the move. IUBMB Life. 2012. doi:10.1002/iub.515.
- Suzuki J, Umeda M, Sims PJ, Nagata S. Calcium-dependent phospholipid scrambling by TMEM16F. Nature. 2010;468:834–8.
- van Meer G, Halter D, Sprong H, Somerharju P, Egmond MR. ABC lipid transporters: extruders, flippases, or floppase activators? FEBS Lett. 2006;580:1171–7.

Lipid Lateral Diffusion

Göran Lindblom

Department of Chemistry, Biophysical Chemistry,
Umeå University, Umeå, Sweden

Synonyms

Bacterial lipids from *Acholeplasma laidlawii* and *Escherichia coli*; Cholesterol; Lateral phase separation; Lipid Bilayer; Lipid membrane; Lipid packing; Lipid phase equilibria; Lipid raft; Phospholipids; Sphingomyelin

Definition

Based on statistical thermodynamics, Einstein showed that Brownian motion, i.e., the stochastic motion of particles due to thermal collisions with the solvent molecules, is well described by an equation where the mean square of the translation distance of the particle, $\langle x^2 \rangle$, is proportional to Dt , where D is the diffusion coefficient and t is the time. *Lipid lateral diffusion* = the translational motion of lipids along the lipid bilayer or membrane characterized by a diffusion constant, D_L , and in two dimensions, the diffusion law assumes the form $\langle x^2 \rangle = 4D_L t$.

Introduction

The Singer and Nicholson model of the “fluid membrane” 1972 aroused a great interest in the dynamics and in particular the two-dimensional diffusion of molecular components in biological membranes. Both lipids and proteins undergo random walks within

the plane of the lipid bilayer. The theoretical and experimental aspects of lateral diffusion of lipids and proteins in lipid membranes have been reviewed by several authors, two of which can be mentioned here, namely, by Almeida and Vaz (1995) and by Saxton and Jacobson (1997). The former of these reviews discusses lipid lateral diffusion in both homogeneous and heterogeneous bilayers composed of both one and several different lipids. It appears that the most interesting turn that the field has taken in recent years, both theoretically and experimentally, has been the study of lipid lateral diffusion in heterogeneous membranes – in multicomponent lipid bilayers, where two or more laterally separated phases coexist over a large range of temperatures. Then, a new fundamental property may appear, namely, the lateral connectivity of each phase, the so-called percolation. This property of membranes is discussed in Saxton’s review (“diffusion in an archipelago”), and the reader is directed to that review to learn more about this matter. To study the organization of biological membranes remains a challenge, because it is inherently difficult to characterize fluctuating lipid assemblies in the membranes of living cells. Lipid bilayer membranes and isolated plasma membranes, on the other hand, are successfully studied. Moreover, large-scale phase separation can occur in these systems. In particular, ternary mixtures of saturated and unsaturated lipids plus cholesterol can segregate into two coexisting fluid lipid domains, liquid-ordered (l_o), and liquid-disordered (l_d) phases. Such domains have been widely studied because they may be closely linked to lipid nanodomains in cell membranes. Here, we briefly discuss the lateral diffusion of the lipid components in bilayers containing one or several different lipids and in particular systems with cholesterol, leading to the formation of domains, often referred to as “lipid rafts” (Orädd and Lindblom 2007). In recent years, a great number of publications on this subject has appeared, using various methods, as different fluorescence methods like fluorescence recovery after photobleaching (FRAP) or fluorescence correlation spectroscopy (FCS) and single particle tracking (SPT). These methods are treated at other places in this encyclopedia and will not be discussed any further. Here, results of lipid diffusion in model membranes measured by a powerful and recently improved technique of NMR spectroscopy will be discussed. This method is convenient, straightforward, and noninvasive; no probe molecule is necessary; and



the lipid lateral diffusion coefficients are directly obtained (for reviews see Lindblom and Orädd 1994, 2009).

NMR Measurements of Lipid Lateral Diffusion Coefficients

The translational diffusion coefficient is obtained by monitoring the NMR signal in the time domain, a so-called spin echo, for a sample located in a magnetic field gradient. This so-called pulsed field gradient (pfg) NMR spectroscopy provides one of the most attractive techniques for studies of molecular transport, and lipid lateral diffusion coefficients (D_L) are most conveniently measured on macroscopically aligned bilayers (Lindblom and Orädd 1994). Oriented samples with bilayer normals at an angle of 54.7° (the so-called magic angle) with respect to the external magnetic field are generally used in order to get well-resolved spectra. Nonoriented lipid crystalline samples usually show broad, featureless spectra in NMR spectroscopy and are difficult to use for diffusion measurements. Generally, the ^1H NMR spectra for aligned samples show linewidths that are reduced by several kilohertz.

For the diffusion measurements, the echo amplitude of each spectral component, A_i , is given by (see Lindblom and Orädd 1994 for details):

$$A_i = A_{0i} \exp\left(-\gamma^2 \delta^2 g^2 D_i \left(\Delta - \frac{\delta}{3}\right)\right) \quad (1)$$

where A_{0i} is a factor proportional to the content of the studied nucleus (usually proton) in the system, γ is the gyromagnetic ratio, Δ is the time interval between two identical gradient pulses, $(\Delta - \delta/3)$ is the diffusion time, δ and g are the duration and amplitude of the pulsed field gradients, respectively, and D_i is the self-diffusion coefficient of spectral component i . The observed spectrum will be a superposition of all spectral components present in the sample. Varying one or more of the variables δ , Δ or g results in a series of attenuated spectra, from which D_i can be extracted. A global analysis of the entire data set generally gives one fast component corresponding to the water and one or two lipid components, together with the corresponding spectral shapes (Orädd and Lindblom 2007).

Diffusion Models

As long as the lipid bilayer is laterally homogeneous, diffusion is described by one diffusion coefficient and $\langle x^2 \rangle = 4D_L t$, where $\langle x^2 \rangle$ is the mean-squared displacement and t is the diffusion time. The situation is more complicated when lateral heterogeneities are present, like if the lipid matrix contains diffusion obstacles. Here, we will only discuss fluid membranes, where domains or phase separation may occur on a length scale observed by the pfg method, i.e., the size of domains is of the order of micrometer, the time during which diffusion is observed is of the order of millisecond. Then, two or more diffusion coefficients may be detected, depending on the number of phases present in the lipid membrane. In principle, hindered diffusion, like in a smaller domain or cavity, may be observed as schematically shown in Fig. 1, where a time-dependent diffusion coefficient is observed upon a change in the length of the diffusion time $\Delta - \delta/3$.

Although a good number of quantitative studies of lateral diffusion in several lipid systems have been published, the mechanism by which lipids migrate along the bilayer has remained unknown. There are in principle two different models proposed on this matter, namely, a free volume theory, discussed by Almeida and Vaz (1995), and a recent model from computer simulation studies where it is proposed that diffusion of lipids in fluid bilayers takes place through concerted lipid motions and tens or possibly hundreds of lipids move in concert as loosely defined clusters (for a recent review, see Apajalahti et al. 2010). This is in contrast to the free volume or free area model, where it is assumed that the lipids diffuse via thermally activated, lateral displacements or jumps; these jumps occur as often as there is a large enough free volume pocket adjacent to the lipid. Further investigations, both experimentally and theoretically, are needed to finally settle this point, although the collective motion of lipids sounds like a very attractive mechanism judging from the many theoretical studies recently published.

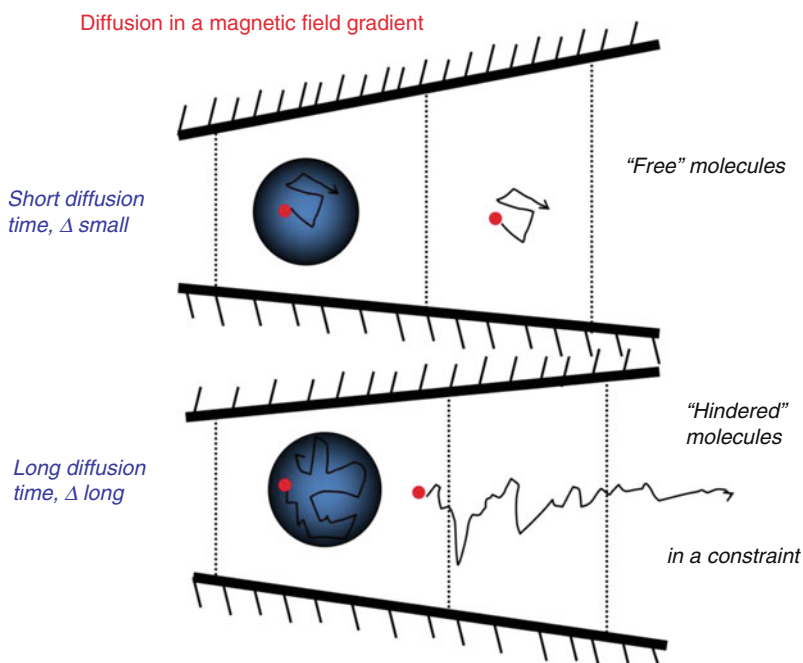
Lipid Packing: Influences of Lipid Head-Group Area on D_L

In general, a closer packing of the lipids in a bilayer results in a decrease in D_L (Lindblom and Orädd 2009). Table 1 shows D_{LS} for a number of lipid bilayer



Lipid Lateral Diffusion,

Fig. 1 A schematic drawing showing the effect of a change in the time during which diffusion occurs ($\Delta - \delta/3$) on a diffusing molecule inside or outside a cavity



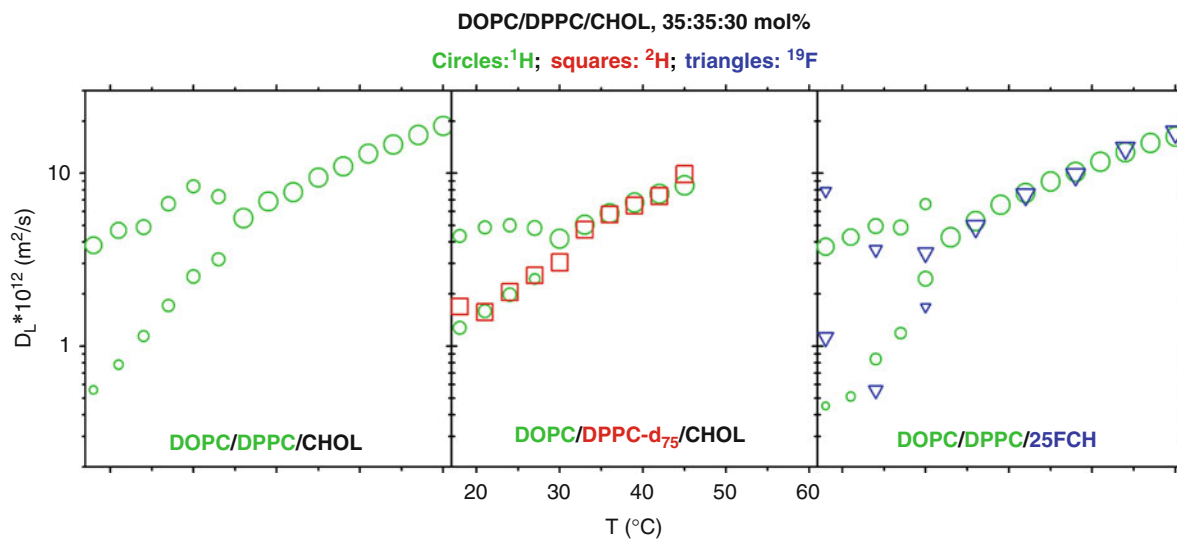
Lipid Lateral Diffusion, Table 1 Head-group areas and corresponding D_L for some lipids in bilayers

Lipid	Area (nm ²)	D_L ($\mu\text{m}^2\text{s}^{-1}$)	t (°C)
DOPC	0.72	8.25	25
POPC	0.68	7.79	25
DPPC	0.64	17.8	45
DMPC	0.61	5.82	25
SOPC	0.63	6.6	25
SLPC	0.66	8.2	25
SAPC	0.68	10.0	25
SDPC	0.70	11.2	25
eSM	0.53	4.5	50
DOPG	0.80	15	30
<i>A. laidlawii</i> lipid extract	ca. 0.6	2.7	30
CHOL/(CHOL + DMPC)			
0.0	0.61	9.0	30
0.1	0.53	4.9	30
0.2	0.48	2.6	30
0.3	0.44	2.0	30

DOPC dioleoylphosphatidylcholine, *POPC* palmitoyloleoylphosphatidylcholine, *DPPC* dipalmitoylphosphatidylcholine, *DMPC* dimyristoylphosphatidylcholine, *SOPC* stearylloleoylphosphatidylcholine, *SLPC* stearylloleoylphosphatidylcholine, *SAPC* stearylarachidonoylphosphatidylcholine, *SDPC* stearyl docosahexaenoylphosphatidylcholine, *eSM* egg sphingomyelin, *DOPG* dioleoylphosphatidylglycerol, *CHOL* cholesterol

systems and, in particular, an illustration of the effect of increased unsaturation in the *sn*-2 fatty acyl chain of phosphatidylcholines on the lipid lateral diffusion. D_L of phospholipids with an increasing number of double bonds from one (SOPC), two (SLPC), and four (SAPC) to six (SDPC), is shown. It can be seen that the lateral diffusion increases with increasing number of double bonds, as a consequence of the increased head-group area caused by the unsaturation. It can also be inferred from this table that D_L decreases in the order DOPC > POPC > DPPC > DMPC again in line with the decrease in the head-group area, mainly caused by the degree of saturation/unsaturation of the acyl chains. Moreover, egg sphingomyelin (eSM) has a lower D_L than DPPC, and dioleoylphosphatidylglycerol (DOPG) with its repulsive charged head group exhibits a larger diffusion coefficient than DOPC, once more in agreement with what can be expected from the head-group area.

Finally, the effect on D_L upon a change in lipid packing is shown by the classical systems of a mixture of phospholipids and cholesterol and the "condensing effect of cholesterol." In Table 1, this is illustrated by an increasing content of CHOL in DMPC bilayers. The flat, rigid ring system of cholesterol is effective in tightening the packing of the



Lipid Lateral Diffusion, Fig. 2 D_L in oriented bilayers of DOPC/DPPC- d_{75} /CHOL- f_7 . By using differently labeled lipids, it is possible to study the lateral diffusion of each lipid species individually. As the temperature goes below 30°C, the two-

phase area is entered and two separate diffusion coefficients are observed for DOPC and CHOL. DPPC, on the other hand, seems to partition only into the l_o phase (Adapted from Orådd et al. (2005))

hydrocarbon chains, resulting in a reduced lipid lateral diffusion.

The lateral diffusion has also been investigated for bacterial membranes, and it was found that for two different such species, the much more tightly packed lipid bilayers from the *Acholeplasma laidlawii* membrane has a much slower translational diffusion than membrane lipids from *Escherichia coli*. Thus, there is a striking difference in D_L for membranes from *A. laidlawii*, which consists of 70–80 mol% glucolipids, and *E. coli* that consists of only phospholipids; the diffusional motion of the latter kind of lipids is much faster. Another interesting observation is that D_L for *A. laidlawii* membranes is independent of the growth temperature of the bacteria, because the lipid composition is regulated and substantially varied with temperature, so that the packing of the lipids in the membrane is the same at the different growth temperatures (Lindblom et al. 2002).

Lateral Phase Separation and Domain Formation in Bilayers

The influence of domains on the lipid lateral diffusion enables pfg NMR to determine lateral phase separation in lipid bilayers. Lipids will diffuse either into or out

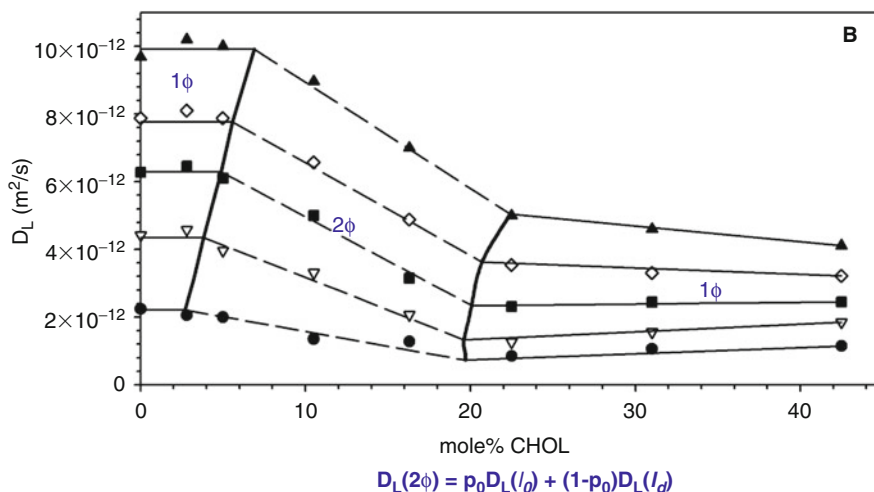
from the separated phases in the fluid bilayer by some exchange mechanism or, provided that the border between different domains presents an obstacle to lipid diffusion, the lipids will encounter restrictions in their translational motion.

Two illustrative examples will be given here: The ternary system DOPC/DPPC/CHOL, where large domains form, and the binary system eSM/CHOL, where smaller domains with lipid exchange is present.

In the ternary system, the three components were isotopically labeled; DOPC contained ^1H , DPPC contained ^2H labeled acyl chains, and CHOL has ^{19}F at the 25-position on the hydrocarbon chain. By observing ^1H , ^2H , or ^{19}F NMR on the labeled lipids, it is thus possible to separately study each individual lipid species as illustrated in Fig. 2. Lateral phase separation is observed for all the three different NMR active nuclei, and it is also found that the diffusion of the lipids is governed by the properties of the phase, in which they reside, rather than the properties of the molecules themselves. Thus, all lipid species, including CHOL, have the same diffusion coefficient as long as they are in the same phase! From the diffusion data, the partitioning of the lipids into the two phases could also be estimated. Note that at the phase separation temperature, the diffusion coefficient increases slightly in the disordered phase.

Lipid Lateral Diffusion,

Fig. 3 Lateral eSM diffusion coefficients at different CHOL concentrations for the eSM/CHOL system with 35 wt% $^2\text{H}_2\text{O}$ and at 313 K (circle), 318 K (triangle top down), 323 K (square), 328 K (diamond), and 333 K (triangle top up). The thick solid lines are estimations of the extension of the two-phase area (with l_o and l_d phases). The solid and dotted lines are linear estimations of D_L in the one-phase and two-phase areas, respectively (Adapted from Filippov et al. (2003))



The system of eSM/CHOL exhibits domain formation in the range of 6–22 mol% CHOL, and this is seen as a sudden break in the curve D_L versus CHOL (Fig. 3). Due to fast exchange between the separated phases, l_o and l_d , the observed diffusion coefficient, $D_L(2\phi)$, will be a weighted average of the diffusion coefficients in the separate phases:

$$D_L(2\phi) = p_o D_L(l_o) + (1 - p_o) D_L(l_d) \quad (2)$$

in which p_o is the relative amount of the l_o phase. As p_o increases, the diffusion will decrease as $D_L(l_o)$ becomes dominant (note: lower diffusion because of closer packing in the l_o phase). A fast exchange is an indication that the domains are smaller than the mean diffusion length (ca. 1 μm) calculated from $r^2 = 4D_L t$. In the one-phase regions on each side of the two-phase area, the diffusion coefficients are almost constant.

Cross-References

- ▶ [Fluorescence Correlation Spectroscopy](#)
- ▶ [Functional Roles of Lipids in Membranes](#)
- ▶ [Glycerolipids: Chemistry](#)
- ▶ [Lipid Bilayer Lateral Pressure Profile](#)
- ▶ [Lipid Domains](#)
- ▶ [Lipid Organization, Aggregation, and Self-assembly](#)
- ▶ [NMR](#)
- ▶ [NMR Methods for Kinetic Analysis](#)

- ▶ [Pulsed Field Gradient NMR](#)
- ▶ [Supported Lipid Bilayers](#)

References

- Almeida PFF, Vaz WLC. Lateral diffusion in membranes. In: Lipowsky R, Sackmann E, editors. Structure and dynamics of membranes. From cells to vesicles, Handbook of biological physics, vol. 1. Amsterdam: Elsevier; 1995. p. 305–57.
- Apajalahti T, Niemelä P, Govindan PN, Miettinen MS, Salonen E, Marrink SJ, Vattulainen I. Concerted diffusion of lipids in raft-like membranes. *Faraday Discuss.* 2010;144:411–30.
- Filippov A, Orädd G, Lindblom G. The effect of cholesterol on the lateral diffusion of phospholipids in oriented bilayers. *Biophys J.* 2003;84:3079–86.
- Lindblom G, Orädd G. NMR studies of translational diffusion in lyotropic liquid crystals and lipid membranes. *Prog Nucl Magn Reson Spectrosc.* 1994;26:483–516.
- Lindblom G, Orädd G. Lipid lateral diffusion and membrane heterogeneity. *Biochim Biophys Acta.* 2009;1788:234–44.
- Lindblom G, Orädd G, Rilfors L, Morein S. Regulation of lipid composition in *Acholeplasma laidlawii* and *Escherichia coli* membranes. NMR studies of lipid lateral diffusion at different growth temperatures. *Biochemistry.* 2002;41:11512–5.
- Orädd G, Lindblom G. Lateral diffusion coefficients of raft lipids from pulsed field gradient NMR. In: McIntosh TJ, editor. Methods in molecular biology, Lipid rafts, vol. 398. Totowa: Humana; 2007. p. 127–41.
- Orädd G, Westerman PW, Lindblom G. Lateral diffusion coefficients of separate lipid species in a ternary raft-forming bilayer: a pfg-NMR multinuclear study. *Biophys J.* 2005;89:315–20.
- Saxton M, Jacobson K. Single particle tracking: applications to membrane dynamics. *Annu Rev Biophys Biomol Struct.* 1997;26:373–99.



Lipid Membrane

► Lipid Lateral Diffusion

Lipid Mesophases for Crystallizing Membrane Proteins

Charlotte E. Conn
CSIRO Materials Science and Engineering, Clayton
South, VIC, Australia

Synonyms

In cubo crystallization; *In meso* crystallization

Definitions

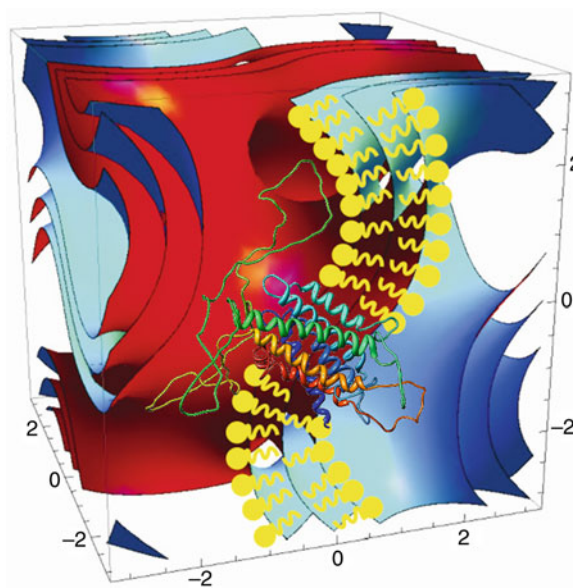
In meso crystallization uses nanostructured lipidic materials, in particular, bicontinuous cubic or sponge phases, as matrices for the growth of protein crystals, particularly membrane proteins.

Lipid mesophases self-assemble when amphiphilic lipid molecules are mixed with an aqueous solvent, typically water.

Bicontinuous cubic phases consist of a continuous lipid bilayer, which subdivides space into two interpenetrating, but not connected, water networks. The bilayer midplane may be closely described as a surface of constant zero mean curvature, known as a triply periodic minimal surface.

Introduction

Integral membrane proteins (MPs) are found embedded within the phospholipid bilayer of the cell membrane. More than 30% of the genome codes for MPs which are implicated in diseases ranging from cardiovascular disease to neurological diseases such as schizophrenia and Parkinson's disease. Determining the structures of MPs is important to determine their mode of action and for the rational design of drugs. However, the structures of many MPs remain elusive. This is reflected in the lack of specificity of current drugs; many commercially available drugs target

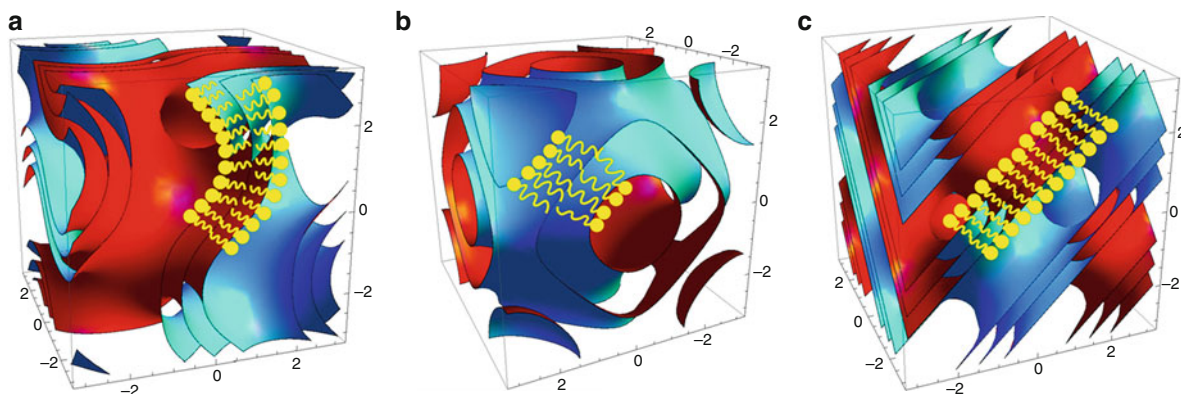


Lipid Mesophases for Crystallizing Membrane Proteins, Fig. 1 The dopamine D2 long (D2L) receptor, implicated in Parkinson's disease, is depicted within a cubic mesophase environment (Conn et al. (2010b) – Reproduced by permission of the Royal Society of Chemistry)

several homologous receptors within each receptor subtype. The main obstacle in structural determination of MPs is in high-quality crystal growth for X-ray diffraction (XRD) analysis (DeLucas 2009).

Just over 15 years ago, it was demonstrated that 3-D crystals of MP could grow within the matrix of a nanostructured lipidic cubic phase (Landau and Rosenbusch 1996). Bicontinuous cubic phases provide a unique environment for crystallization of MPs (Fig. 1) and fulfill two crucial roles. The first is that their fundamental bilayer structure mimics the protein's natural environment within the cell membrane, and secondly, the continuous nature of the bilayer and the water networks allows for lateral diffusion of the protein across the plane of the bilayer thus facilitating crystallization. MPs are more likely to retain their active conformation within a bilayer-based environment, and crystals grown in lipidic mesophases have generally been robust, of high quality, and often superior to detergent grown crystals. Human G-protein-coupled receptors recently solved using *in meso* crystallization include the adenosine A_{2A} receptor, the β_2 -adrenergic-receptor-Gs protein complex (Rasmussen et al. 2011), and the dopamine D3 receptor.





Lipid Mesophases for Crystallizing Membrane Proteins, Fig. 2 A schematic representation of the (a) Q_{II}^G , (b) Q_{II}^P , and (c) Q_{II}^D phases (Conn et al. (2010a) – Reproduced by permission of the Royal Society of chemistry)

Lipid Mesophases for In Meso Crystallization

Bicontinuous cubic phases, which are based around the fundamental structure of the lipid bilayer, are the primary type of lipid mesophase used for *in meso* crystallization. The bilayer midplane is considered to be draped across a periodic minimal surface of zero mean curvature and subdivides space into two interpenetrating but not connected water networks (Hyde et al. 1997). There are three main types (Fig. 2): the diamond, Q_{II}^D , phase (crystallographic space group Pn3m), the gyroid, Q_{II}^G , phase (crystallographic space group Ia3d), and the primitive, Q_{II}^P , phase (crystallographic space group Im3m). The lipidic cubic phase is highly viscous and incompatible with standard crystallization robotics which has limited its use. A Flexus Crystal IMP robotic system, which dispenses nano volumes of viscous cubic phase directly onto a 96-well crystallization plate using a microsyringe pump, was developed to overcome some of these limitations (Caffrey and Cherezov 2009). It offers reproducibility, a reduction in sample volume relative to manual setup and fast setup times (<10 min). However, the robot is expensive and specific to the technique of *in meso* crystallization. In addition, a microfluidic device, which mixes protein directly with preformed cubic phase, has recently been used for the growth of crystals of photosynthetic reaction center from *Rhodobacter sphaeroides* and *Blastochloris viridis* (Li et al. 2010).

There has been increasing interest in the use of lipidic sponge mesophases as a new generation of crystallization media for MPs (Cherezov et al. 2006).

The lipidic sponge mesophase may be visualized as a melted cubic phase with a less curved lipid bilayer and two to three times larger aqueous pores. Such phases may be simply obtained by mixing the dry lipid with a buffer solution and a crystallization agent such as PEG, MPD, or jeffamine M600. Due to their high fluidity, sponge phases are compatible with conventional crystallization robotics. In addition, the larger aqueous pore size makes such systems suitable for larger MPs containing large extra- and/or intracellular domains extending the range of proteins which may be investigated.

Novel Lipids

Virtually all crystallization trials to date have used the same lipid, monoolein (MO), or a very similar analog, despite recent research showing that physical parameters of the cubic phase can affect crystallization (Caffrey 2009). The MO molecule is susceptible to hydrolysis and transesterification and MO is unsuitable for crystallization of more labile proteins as it does not form a cubic phase below room temperature. Due to the scarcity of suitable cubic phase matrices, *in meso* crystallization is currently incompatible with the majority of MPs and their functional complexes, due to their large size. Recently, some research has begun to investigate new cubic phases suitable for *in meso* crystallization. The Caffrey research group has focused on the synthesis and characterization of a homologous series of monoacylglycerols (MAGs) (Caffrey 2009). By variation of the hydrocarbon chain length, it is possible to exert some control over the bilayer thickness and water channel diameter,



although these parameters are relatively tightly coupled and cannot be varied independently of each other. This research has indicated that a reduction in bilayer thickness may promote crystal growth, and crystals of bacteriorhodopsin, cytochrome *caa3* oxidase, and the cobalamin transporter BtuB were successfully grown within a shorter chain (C14) MAG (Caffrey 2009). However, the presence of the ester bond within MAGs increases their susceptibility to chemical degradation, which could potentially affect the cubic structure.

Therefore, recent efforts have focused on the design and characterization of alternative lipids which form the cubic phase but are more chemically robust, retain the cubic phase down to lower temperatures, and may provide a more “natural” environment for the MP. The LCP (lipidic cubic phase) resources website run by the Cherezov Lab at the Scripps Institute currently lists only eight non-MAG molecules, many of which are sugar surfactants, as suitable matrices for *in meso* crystallization. Recent research by the Drummond research group has focused on endogenous lipids and their analogs, including those based on the biologically relevant monoethanolamide headgroup (Conn et al. 2010a); many unsaturated monoethanolamides, including arachidonyl monoethanolamide (anandamide), are endogenous and have been shown in a number of studies to exhibit active biological and medicinal properties.

Addition of Membrane Additives

Most cubic phases consist of a binary lipid–water system. However, the native cell membrane consists of a range of lipids from three different classes: phospholipids, glycolipids, and cholesterol. The particular lipid composition is dependent on the cell type with hydrocarbon chain lengths typically between 16 and 20, saturated or unsaturated, and usually contain an even number of C atoms.

The cubic phase is fairly robust to addition of additives which may provide an environment more similar to the native cell membrane environment of the particular MP. Phospholipids (including phosphatidylcholine (PC), phosphatidylethanolamine (PE), and phosphatidylserine (PS)), cardiolipin, 2-MO, and cholesterol are all tolerated by the MO cubic phase to varying degrees (Caffrey 2009). In particular, addition of cholesterol has been extremely successful in crystal growth, particularly for human GPCRs (Caffrey 2009).

Lipid additives can affect both the local bilayer environment of the protein and the cubic nanostructure in a variety of ways.

Membrane fluidity – The fluidity of the lipid bilayer may affect crystal growth by influencing the diffusion rate of proteins. Cholesterol decreases membrane fluidity while unsaturated chain hydrocarbons increase membrane fluidity.

Lateral pressure within the bilayer – The lipid bilayer exerts a lateral pressure on embedded MPs thought to be crucial for retention of the active conformational state. The lateral pressure depends strongly on the lipid composition within the bilayer. In general, more than 50% of a typical cell membrane will consist of type 0 lipids, which have a cylindrical molecular architecture, and typically form a flat bilayer structure. Increasing the composition of type 0 lipids may therefore provide a more native environment for the incorporated MP.

Cubic nanostructure – The nanostructure of the lipid matrix strongly depends on the molecular architecture of all lipids within the bilayer. Both cholesterol and type 0 phospholipids will act to swell the cubic nanostructure suitable for crystallization of larger MP complexes. Incorporated lipids may, however, promote a transition to a noncubic architecture unsuitable for crystallization.

Mechanism of Crystallogensis

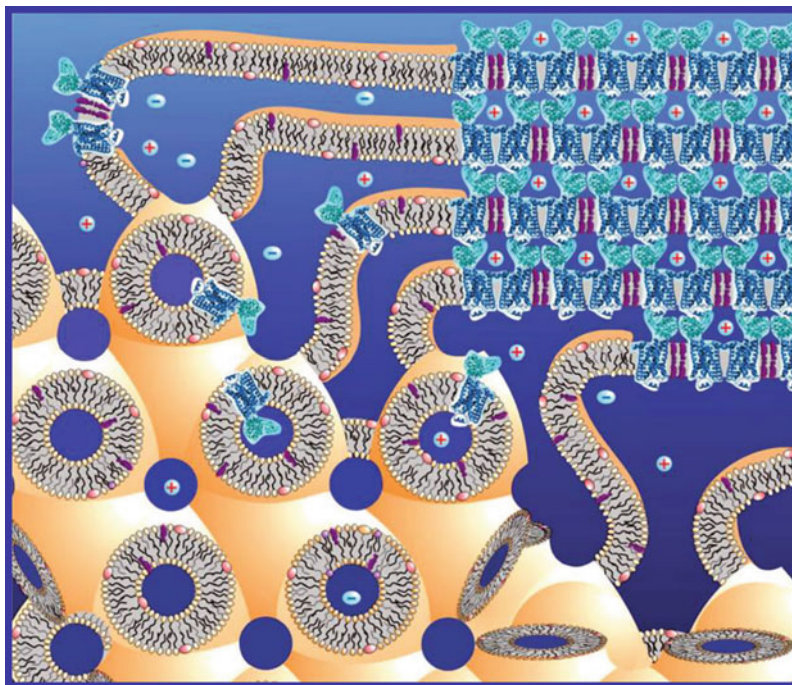
The process of *in meso* crystallization is deceptively simple. The bicontinuous cubic phase spontaneously self-assembles upon addition of protein solution at an appropriate ratio. Crystallogensis, or crystal growth, begins upon addition of a precipitant, known as a crystallization screen, normally a combination of polyethylene glycol (PEG), a salt, and buffer. It has been proposed that addition of the crystallization screen components triggers phase separation, with protein nucleation occurring in the protein-rich separated phase. A local lamellar phase is proposed to act as a conduit-moving protein from the bulk cubic phase to the growing crystal face (Fig. 3) (Caffrey 2008).

The proposed mechanism for *in meso* crystallization therefore depends, at least initially, on retention of the underlying cubic or sponge mesophase. However, a crystallization trial requires screening across a wide range of crystallization conditions, containing polymers, salts, buffers, and at varying pH, all of which are known to drive structural changes in lipid



Lipid Mesophases for Crystallizing Membrane Proteins, Fig. 3

A schematic representation of the proposed mechanism for membrane protein crystallization within a bicontinuous cubic phase. The protein is depicted embedded within the bilayer environment of the cubic phase. Addition of precipitants triggers phase separation. A local lamellar phase is shown acting as a conduit-moving protein from the bulk cubic phase to the growing crystal face (Reprinted with permission from Caffrey (2008). Copyright 2008 American Chemical Society)



mesophases. Each individual well within a crystallization trial will therefore contain a unique combination of lipid, MP and associated detergents and buffers, and the components of the crystallization screen. Any of these components could affect the structure of the underlying lipid mesophase, and this structure may evolve during the time period of crystal growth. Detergents and buffers associated with the MP, as well as the components of the crystallization screen, have been shown to destabilize the cubic phase matrix. In addition, incorporation of the MP itself can significantly impact the cubic phase. In particular, destruction of cubic phase was shown to occur when there was a large discrepancy in size between the hydrophobic and hydrophilic domain sizes of the MP and the bilayer thickness and water channel diameter of the cubic mesophase (Conn et al. 2010a).

Despite recent advances, in practice, the technique of *in meso* crystallization is poorly understood, and it remains an essentially empirical technique. In particular, virtually nothing is known about the factors that promote crystallization. Crystallization trials therefore require screening across a wide range of conditions; successful crystal growth invariably results from screening tens of thousands of conditions randomly. This situation is particularly unfavorable for crystallization of MPs which are typically available in

extremely small quantities; less than 1 mg of protein may result from months of expression and purification. The scarcity of MP has contributed to the dearth of knowledge in this area; available MP tends to be used directly in crystallization trials rather than in fundamental characterization studies.

Cross-References

- ▶ [Lipid Bilayer Lateral Pressure Profile](#)
- ▶ [Lipid Shape and Curvature Stress](#)
- ▶ [Macromolecular Crystallography: Overview](#)
- ▶ [Membrane Fluidity](#)
- ▶ [Phase Transitions and Phase Behavior of Lipids](#)
- ▶ [Wide and Small Angle X-Ray Scattering](#)
- ▶ [X-Ray Diffraction and Crystallography of Oligosaccharides and Polysaccharides](#)

References

- Caffrey M. On the mechanism of membrane protein crystallization in lipidic mesophases. *Crystal Growth Des.* 2008;8(12):4244–54.
- Caffrey M. Crystallizing membrane proteins for structure determination: use of lipidic mesophases. *Ann Rev Biophys.* 2009;38:29–51.

- Caffrey M, Cherezov V. Crystallizing membrane proteins using lipidic mesophases. *Nat Protoc.* 2009;4(5):706–31.
- Cherezov V, Clogston J, et al. Room to move: crystallizing membrane proteins in swollen lipidic mesophases. *J Mol Biol.* 2006;357(5):1605–18.
- Conn CE, Darmanin C, et al. Incorporation of the dopamine D2L receptor and bacteriorhodopsin within bicontinuous cubic lipid phases. 2. Relevance to in meso crystallization of integral membrane proteins in novel lipid systems. *RSC Soft Matter.* 2010a;6(19):4838–46.
- Conn CE, Darmanin C, et al. Incorporation of the dopamine D2 receptor and bacteriorhodopsin within bicontinuous cubic lipid phases. 1. Relevance to in meso crystallization of integral membrane proteins in monoolein. *RSC Soft Matter.* 2010b;6(19):4828–37.
- DeLucas L. *Current topics in membranes: membrane protein crystallization.* Amsterdam/Boston: Elsevier; 2009.
- Hyde ST, Andersson K, et al. *The language of shape.* Amsterdam: Elsevier Science B.V; 1997.
- Landau EM, Rosenbusch JP. Lipidic cubic phases: a novel concept for the crystallization of membrane proteins. *Proc Natl Acad Sci U S A.* 1996;93(25):14532–5.
- Li L, Fu Q, et al. A plug-based microfluidic system for dispensing lipidic cubic phase (LCP) material validated by crystallizing membrane proteins in lipidic mesophases. *Microfluid Nanofluid.* 2010;8(6):789–98.
- Rasmussen SGF, DeVree BT, et al. Crystal structure of the beta(2) adrenergic receptor-Gs protein complex. *Nature.* 2011;477(7366):549–55.

Lipid Organization, Aggregation, and Self-assembly

Himanshu Khandelia³ and Ilpo Vattulainen^{1,2,3}

¹Department of Physics, Tampere University of Technology, Tampere, Finland

²Aalto University School of Science, Espoo, Finland

³Center for Biomembrane Physics, University of Southern Denmark, Odense, Denmark

Synonyms

[Lipid bilayer](#); [Polymorphic and mesomorphic behavior of lipids](#); [Self-assembly](#)

Definition

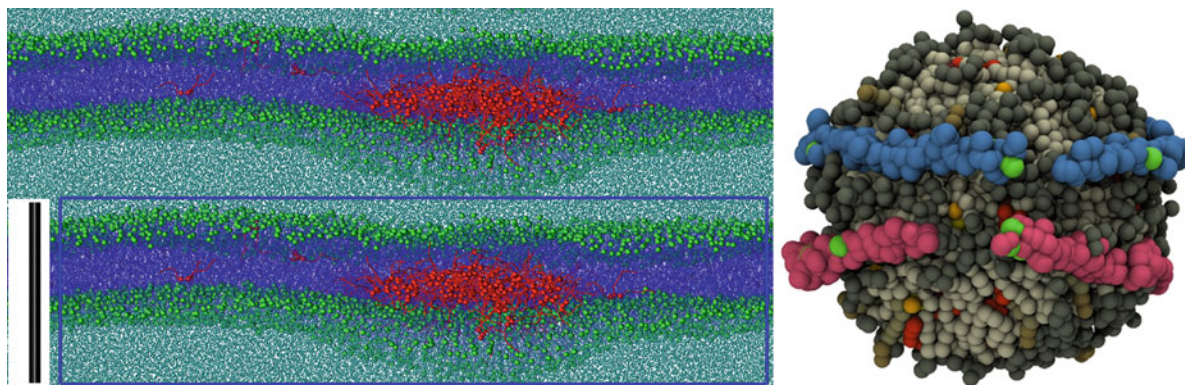
Lipids are a class of naturally occurring organic molecules that perform essential cellular functions in living systems. They have been defined as fatty acids, and

their derivatives and substances are related biosynthetically or functionally to these compounds (Larsson 1994). Lipids form the structural matrix of biological membranes, function as energy storing molecules in the form of fat, and are involved in signaling pathways. Self-assembly is a thermodynamically spontaneous process during which a disordered system composed of entities such as molecules comes together to form well-defined microstructures or macrophases as a result of local and long-range physicochemical interactions.

Introduction

Lipids (Mouritsen 2005) come in a large variety of sizes, shapes, and chemistry. The chemical classification of lipids categorizes them mainly into fatty acids, glycerolipids, glycerophospholipids, sphingolipids, sterols, and saccharolipids. Of these, glycerophospholipids, sphingolipids, sterols, and saccharolipids are the major components of biological membranes and the first three are commonly used in model membrane constructs. These four categories of lipids have a common underlying chemical property: amphipathicity, which enables them to inhabit oil-water interfaces. The lipids are composed of a hydrophilic head group that associates with water and one or more hydrophobic acyl tails which prefer to partition into an oily region. The chemical nature and size of the head group as well as the hydrophobic tails is very varied. On a molecular level, the richness of lipid phase behavior owes its existence to this chemical complexity of the individual heads and tails of the lipids as well as the balance between the sizes and shapes of the two. In living tissue, lipids are mainly organized into (1) 5-nm-thick lipid bilayers that form the cellular membrane and several intracellular structures such as the endoplasmic reticulum and the Golgi apparatus, (2) intracellular lipid droplets, and (3) lipoprotein particles which shuttle between cells.

Outside a living cell, individual lipids and lipid mixtures can be observed to undergo a rich variety of phase behavior depending on lipid composition and external conditions such as pH, temperature, pressure, hydration, and ionic strength. The structures include planar lipid bilayers, uni- and multilamellar vesicles, giant unilamellar vesicles, lipid droplets and



Lipid Organization, Aggregation, and Self-assembly,

Fig. 1 Snapshots of exemplary lipid structures. *Left:* Simulation snapshot of a self-assembled triglyceride lipid aggregate inside a phospholipid bilayer (Khandelia et al. 2010). Shown here is the side view, depicting two periodic images along the bilayer normal (the bar is 10 nm). POPC tails are shown in blue, POPC phosphate beads are shown as green spheres, triglyceride tails are shown in red, triglyceride glycerol backbone as red spheres, and water is depicted in cyan. The blue lines represent the central simulation cell boundaries. *Right:* Molecular

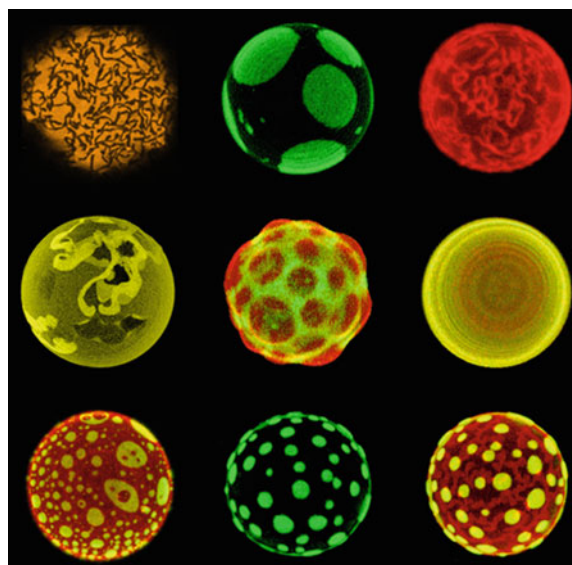
structure of high-density lipoprotein with two apoA-I proteins around the lipid droplet (Vuorela et al. 2010). Dark gray stands for POPC head group and dark brown for palmitoyl-PC (PPC) head groups, light gray for POPC hydrocarbon chains, light brown for PPC chains, light orange for cholesterol OH-groups, bright yellow for cholesterol body, dark orange for cholesteryl ester (CE) bond, orange for CE ester body and chain, dark green for triglyceride (TG) ester bonds, and bright green for TG chain. Proline residues in apoA-I sequences are shown in green

lipoproteins, and cubic, hexagonal, and inverted hexagonal phases (Hyde et al. 1997) to name a few. Figures 1 and 2 highlight some of them as typical examples.

In this entry, we will present an overview of the structures and phases that model lipid mixtures can adopt in mostly aqueous phases and the biophysical methods that are commonly used to analyze lipid systems. The physical and chemical principles that emerge from analysis of model lipid mixtures are often applicable to complex living systems and are of significant consequence to the science and art of the design of drug delivery vehicles, which increasingly exploit the rich environment-dependent phase behavior of lipid particles.

Methods

The structures of lipid systems and their dynamic properties can be determined and characterized by numerous techniques. Given that space is limited, here, we aim to provide some flavor for the techniques that are commonly used in the field, more extensive discussions being available elsewhere (Serdyuk et al. 2007; Feller 2008).



Lipid Organization, Aggregation, and Self-assembly,

Fig. 2 “Spheres” – liposomes of varying lipid and protein composition, the typical size being 40 μm . Courtesy of Luis Bagatolli and Jorge Bernardino de la Serna (Science in Your Eyes 2011)

Experimentally, large-scale phase behavior is most often elucidated by differential scanning calorimetry, which gauges changes in heat capacity to pinpoint the boundaries between different phases. Neutron and

small angle x-ray scattering are also commonly used for measuring phase behavior and lipid structures, as are also Langmuir pressure-area isotherms for lipid monolayers to consider different phases emerging for increasing surface pressure in the membrane plane. In fluorescence microscopy, one follows the partitioning of fluorescent probes into different membrane regions, and by knowing the preference of each probe for ordered versus disordered environments, one can get insight into the structures in a given lipid system. Meanwhile, nuclear magnetic resonance (NMR) is perhaps the most commonly used method to elucidate the ordering of lipid hydrocarbon chains, which correlates with the ordering of lipids in general. NMR also allows one to exploit lipids' dynamic properties to unravel different phases: as the pace of lipid diffusion largely depends on how densely the lipids are packed with respect to one another, NMR can differentiate between long-range gel and fluid phases and also detect nanodomains with different packing properties, reflecting their ordered nature.

For consideration of structures over smaller scales, the techniques mentioned above work quite well for nanodomains and can be complemented by, e.g., atomic force microscopy, which is an ideal technique to unravel nanometer-sized lipid structures, structural defects, and different lipid domains.

The dynamics of lipid systems overall is a very exciting topic to explore (Vattulainen and Mouritsen 2005), and NMR is just one of the many suitable techniques for this purpose. Considering again diffusion as an example, fluorescence recovery after photobleaching (FRAP) is a particularly often used technique, as is also fluorescence correlation spectroscopy (FCS) and single-particle tracking (SPT). The downside of all of these methods is the use of fluorescent probes, which affect the structural and dynamical properties of lipid systems in which they lie. Their use in studies of lipid systems and the interpretation of their results therefore warrant particular care.

On the computational side, the current methods of choice are either atomistic or coarse-grained (CG) simulations usually based on classical molecular dynamics. The present models allow simulations of essentially all lipid types with all possible structures that one can think of. The main limitation of lipid simulations is the performance of the simulation engines and computers. Atomistic simulations are

currently limited by system sizes of the order of 1 million atoms (roughly a system of size $20 \times 20 \times 20 \text{ nm}^3$) and time scales of the order of 1 millisecond. The speedup of coarse-grained models compared to atomistic ones varies quite a lot, but roughly, a speedup of 100–10,000 is typical in the field. That is, for the same system sizes as in atomistic simulations, CG models can go beyond the time scale of seconds. If coarse-graining is extended over molecules to design models based on fields instead of molecules, such as in the case of phase-field models, the possible time and length scales increase even further. With the ever increasing scales considered in simulations, we also face the challenge of hydrodynamic interactions. Those interactions emerge from the conservation of momentum in local particle-particle interactions and play an important role especially at large length and time scales. However, currently, too few simulation techniques take hydrodynamics properly into account. The use of hydrodynamic methods such as dissipative particle dynamics and stochastic rotational dynamics are therefore to be strongly encouraged in large-scale simulations of lipid systems. Altogether, the field of simulations has established itself as a remarkable means that not only complements experiments but also provides testable predictions. Examples below provide a taste of this fascinating novel field.

Physical Principles of Lipid Organization and Self-assembly

Self-assembly and organization of lipids are driven by forces that are surprisingly weak (Evans and Wennerström 1999). This is the essence of “soft matter” that lipid systems also are – in soft materials, the forces of interest are comparable to the thermal energy $k_B T$, where k_B is the Boltzmann constant and T is the temperature.

The soft nature of lipid systems and its relation to thermal fluctuations has two important consequences. First, what matters in lipid organization are the interactions that are somewhat larger than $k_B T$ but considerably smaller than the strength of covalent bonds, the latter being $\sim 200 k_B T$. In practice, the most central interactions are those due to dispersion (van der Waals, about $1\text{--}3 k_B T$), hydrogen bonds ($\sim 3\text{--}8 k_B T$), and electrostatics (with a wide range of interaction strengths depending on distance and solvent

properties). These give rise to the enthalpic component (E) of free energy (F), which the system aims to minimize. Second, in soft materials, one cannot neglect the entropic component of free energy, which aims to drive the system away from crystallization by keeping it fluid through thermal motion. The subtle competition of enthalpic forces with entropic ones in systems with amphiphilic molecules is often pictured as the so-called hydrophobic effect, which represents the tendency of water to exclude nonpolar molecules such as oil. The effect originates from the inability of water to interact favorably with oil-like molecules, for which reason water has to restructure its hydrogen bonding network around oil-like particles, which in turn decreases entropy (S) and therefore also the entropic component (TS) of the free energy $F = E - TS$. Given this, it is easy to figure out what happens when lipid molecules are solvated in water: to minimize the free energy, above the so-called critical micelle concentration, lipids spontaneously aggregate into spherical lipid structures known as micelles, where the contact between oil-like hydrocarbon chains of lipids and water is minimized and only the polar head groups of lipids face water molecules.

At larger lipid concentrations, essentially the same principle drives the formation of other lipid structures, such as lipid droplets, liposomes, planar bilayers, cylindrical micelles, and the so-called plumber's nightmare cubic phase (Hyde et al. 1997). What determines the shape and the morphology of an emerging lipid structure depends on, e.g., lipid-lipid interactions, pH, salt, and distribution of lipids in a membrane. Commonly, the structure is predicted by the surfactant packing parameter $p = v/l_c a_0$, where v is the volume of a single lipid, a_0 is the cross-sectional area of the head group region, and l_c is the critical (maximum) length of the hydrocarbon region. The parameter describes in a simplified manner conditions for, e.g., micelles ($p \leq 1/3$) and planar bilayers ($p \approx 1$). However, its predictions should be considered as suggestive only, since v , l_c , and a_0 are not only difficult to measure but also depend on thermodynamic conditions and interactions between lipids, ions, and the lipid composition overall. In simplified model systems, the parameter p works reasonably well, but should be applied with great care in native systems.

Lipid Structures with Varying Shapes

Lamellar Lipid Phases

At sufficiently high lipid concentration, an aqueous lipid dispersion forms unilamellar vesicles consisting of a single bilayer of lipids (packing parameter $p \approx 1$), or multilamellar vesicles comprised of concentric multiple bilayers separated by a layer of water (Science in Your Eyes 2011), see Fig. 2. The essential structure here is a lipid bilayer, which consists of lipids arranged in two lamellae with the hydrophobic lipid tails pointing toward each other and the hydrophilic headgroups guarding the hydrophobic core of the bilayer from water (Bloom et al. 1991). Above the so-called main phase transition temperature T_m , a single-component lipid bilayer with a thickness of ~ 5 nm is in the fluid (liquid-crystalline, L_c) phase, which is liquid in terms of allowing lipids to diffuse freely in the plane of the membrane. Meanwhile, the bilayer is also liquid-crystalline as there is orientational order due to the lipids being on average aligned along the bilayer normal. The L_c phase is also often denoted as liquid-disordered since the liquid-crystalline order in this phase is rather weak, the conformations of lipid hydrocarbon chains being largely disordered. For decreasing temperature, the diffusion of lipids slows down and, at T_m , eventually drops down by several orders of magnitude as the bilayer undergoes a phase transition from the fluid to the gel phase with a thickness of ~ 6 nm. The gel phase is broadly speaking quasicrystalline, characterized by tight packing of lipids, tilted lipid orientations with respect to membrane normal, strong conformational order in the hydrocarbon region, and quasi-long-range order in the membrane plane. In multilamellar vesicles, a "ripple" phase sometimes intervenes between the fluid and the solid-like gel phases, and the accompanying phase transition is referred to as the pretransition. Overall, the transitions are determined by soft interactions between adjoining lipids as briefly discussed in the previous section. Thus, the chemical nature of the lipid (size of head group, degree of unsaturation, length of the lipid tails, etc.) determines its T_m . For example, DPPC (dipalmitoylphosphatidylcholine), which is a lipid with fully saturated tails, has T_m above room temperature, while POPC (palmitoyl-oleoyl-PC), which is identical to DPPC

except for one slightly longer hydrocarbon chain that has a single double bond, melts well below room temperature. In native cell membranes comprised of hundreds or even thousands of different lipids, the main transition temperature is not well defined since T_m reflects the properties of a single-component bilayer (see below). Nonetheless, there is a considerable amount of data suggesting that cell membranes at physiological temperatures operate in the fluid phase. The consequent ability of lipids to freely diffuse in fluid membranes enables them to quickly seal membrane defects. Given that one of the central tasks of membranes is to compartmentalize cells, this is also essential for their biological function.

When several lipid types with different T_m are mixed together, the mixture's phase behavior becomes more complex with a range of phase transition temperatures, and several phases can simultaneously coexist at a given temperature. Even for a two-component system, the resulting phase diagram can be rather complex. The phase behavior of the lipid mixture can then be described as a typical two-axis binary liquid mixture diagram such as that of ethanol water. Particularly relevant to mammalian membranes is a mixture of PCs with cholesterol, both lipid types being abundant and the molar cholesterol concentration in some related membranes being even $\sim 50\%$. Cholesterol is in many ways fascinating, one of the reasons being that it induces a new liquid-ordered phase (L_o) to complement the fluid and gel phases (Bloom et al. 1991). In the L_o phase, a membrane is liquid as it allows rapid diffusion of lipids as in the fluid phase, but it is also ordered due to the high conformational order as in the gel phase. Interestingly, while cholesterol slows down lipid diffusion and hence decreases membrane fluidity in the fluid phase, it increases the fluidity in the gel phase.

One of the topics that have received substantial attention during the last 15–20 years is the relevance of lipids in biological functions. The lipid that has found its place in the spotlight is cholesterol. There is now a major body of evidence supporting the view that membrane proteins and lipids such as cholesterol form functional nanoscale complexes that work in unison (Lingwood and Simons 2010). Lipid rafts, as they are commonly called, are considered to be rich especially in cholesterol and sphingolipids, and the role of these

nano-sized membrane proteins in cellular functions is currently investigated very actively. Lipid rafts seem to be particularly important in signaling, and they likely also play an important role in membrane-associated phenomena such as receptor trafficking and regulation of neurotransmission.

At an air-water interface, lipids can also assemble into a monolayer, with the lipid tails pointing into the air. An appealing example of this structure is the lipid monolayer in the lung alveolae, which reduces the surface tension of the air-water interface and enables mammals to breathe without exerting otherwise overwhelmingly large forces that would be required to contract and expand the alveolar surface.

Nonlamellar Phases

Quite a few lipids are not characterized by an approximately constant cross-sectional area profile along their length. Instead, they can be cone-like and hence promote an inherent spontaneous curvature when inserted at water-lipid interfaces. Lipids in a bilayer containing two monolayers of finite spontaneous curvature are frustrated because of entropic reasons. If the curvature stress exceeds the noncovalent cohesive forces that keep a bilayer together, then the lipids form nonlamellar structures to release the stress, resulting in complex three-dimensional structures. Inverted hexagonal, cubic, and less common hexagonal phases are examples of these structures. The formation of these microstructures is not only driven by lipid composition but also by environmental conditions. For example, the inverted hexagonal phase can be promoted from a lamellar phase by increasing the temperature, or by incorporation of a variety of amphipathic molecules such as drugs, detergents, and acylglycerols. Meanwhile, mammalian cells are endowed with two important nonlamellar lipid structures: lipoproteins and lipid droplets (Vuorela et al. 2010; Hevonoja et al. 2000), see Fig. 1. Lipoproteins known as carriers of cholesterol and its esters consist of a hydrophobic core comprised of disordered triacylglycerols and cholesteryl esters, surrounded by a lipid monolayer containing phospholipids and cholesterol. In the low-density lipoprotein, a single protein wraps the ~ 25 -nm-sized lipid particle, while in the high-density lipoprotein, the number of proteins around the lipid droplet is greater. While the formation

mechanism of lipid droplet is currently not understood, lipoprotein particles possibly emerge as globular triglyceride droplets that pick up phospholipids when released from the membrane of a cell or a cell organelle.

Current State of the Art

What is amazing in both experiments and simulations is their ability to pinpoint how individual molecules move in space, cluster together, form ordered structures, and, by doing so, give rise to fascinating phenomena that describe the dynamics of a given system. In atomistic and CG simulations, these molecular-scale dynamic phenomena can be visualized more accurately than in experiments since, in quite a few experimental techniques, the low spatial resolution is a major limitation. However, as also in experiments the methodology has made substantial progress, characterization of molecular-scale processes is becoming more and more possible. Thus, below, we briefly present a couple of examples for the state of the art in the field, highlighting the progress in both experiments and simulations.

Experimental Means to Visualize Lipids in Motion

The most appropriate means to visualize molecular motion in lipid systems is to use fluorescence. As natural lipids do not fluoresce, they are merged with fluorescent labels such as pyrene and BODIPY. The labels are most often attached to the lipids' hydrophobic chains, as in this manner, the perturbations induced by the labels are the weakest. The fluorescent probes are then excited by photons (light), and after a typical waiting time of a few nanoseconds, the probe emits part of its excess energy as light. Obviously, this reveals the location of the probe just like in the systems shown in Fig. 2. This simple principle is the core of a number of techniques based on fluorescence imaging, such as FRAP, FCS, SPT, and confocal microscopy.

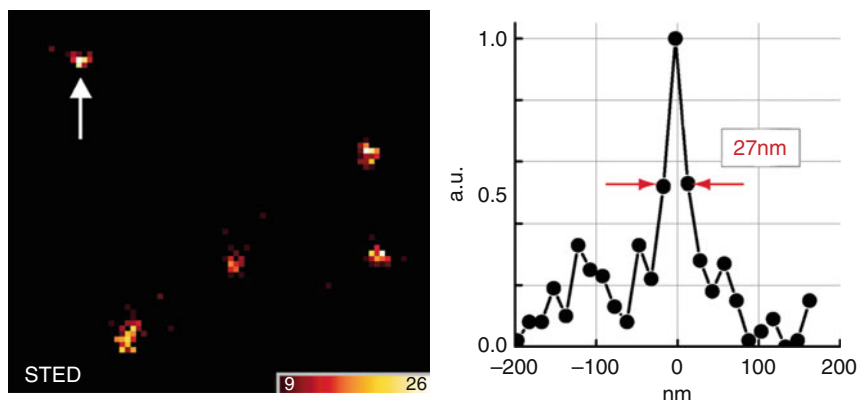
The main limitation of fluorescent techniques is their spatial resolution. For visible light, the smallest wavelength is about 400 nm, which implies that the smallest spatial scale that can be resolved is ~ 200 nm. Resolution of this size is rather poor considering that molecular phenomena take place in scales of nanometers and sizes of lipid domains with different physical properties range from a few to a few hundred nanometers. Improvements to enhance spatial resolution have

yet been developed, one of the most remarkable techniques being stimulated emission depletion (STED) (Hell 2007; Huang et al. 2009). STED is based on using two laser pulses with matching focal points to excite and de-excite fluorescent dyes. Considering labeled lipids in a flat membrane, the first laser excites the dyes, while the second laser with a local intensity minimum such as a doughnut intensity profile (where the intensity is zero in the center of a circle and evolves like a hill for increasing radial distance from the focal point) inhibits the fluorescence of all the excited dyes rendering them nonfluorescent, except for those close to the focal center. By increasing the intensity of the second de-excitation spot, the region in a membrane where dyes remain fluorescent can be made smaller. In lipid membranes, the detected region of interest has been made as small as about 20 nm (Fig. 3), which has allowed mapping proteins in cells (Donnert et al. 2006) and studying nanoscopic details of lipid membrane diffusion in living cells (Eggeling et al. 2009). In solid-state applications, the detected region can be as tiny as ~ 5 nm (Rittweger et al. 2009). Concluding, STED has potential to study the details of molecular processes under physiological conditions at \sim nanometer length scales.

Lipid Dynamics Inside Computers

Improved force fields, increasing computational power, and new multiscale modeling algorithms have not only enabled particle-based simulations to explore phenomena occurring over time and length scales once deemed inaccessible, but have also significantly boosted predictive ability. Domain formation in planar bilayers, dynamics of lipid-protein complexes, vesicle fusion, structural analysis of lipid droplets and lipoproteins, and simulations of entire viral particles are some recent examples.

A key goal in the field of particle-based simulations is to obtain simultaneous access to multiple time and length scales during the course of a simulation. Phenomena taking place over disparate time scales can be uncoupled to improve the computational efficiency of simulations without making overindulgent compromises in accuracy. In multiscale modeling, a phenomenon is investigated at various time and length scales using models of varying degree of coarseness. The procedure involves refining the courser model from simulations of finer models. Such multiscale models have facilitated simulations of



Lipid Organization, Aggregation, and Self-assembly, Fig. 3 STED microscopy on synaptotagmin I molecules on endosomes (Donnert et al. 2006). *Left*: STED recognizes sharp dots of 25–40 nm in size, highlighting its resolution and the

spatial arrangement of synaptotagmin I on the endosome. *Right*: Corresponding intensity profile, showing the spatial resolution to be in the order of ~ 20 nm (Permission granted; copyright (2011) National Academy of Sciences, USA)

vesicles of the size of 100 nm with elastic and dynamic properties that match those in real systems (Izvekov and Voth 2009). What is more, although simultaneous temporal access to all length scales yet remains elusive, it is also possible to fine grain the coarse-grained system back to atomic description for detailed studies of molecular structures. At the moment, the development of accurate algorithms that allow shuttling between course-grained and fine-grained representations of lipid systems is a very active field of work (Izvekov and Voth 2009; Rzeplia et al. 2010).

Summary

The structures of systems comprised of lipids are fascinatingly complex, and their role in biological functions is largely just beginning to be understood. What we do know is that lipids as such can function, e.g., as messengers in signaling. Lipoproteins as carriers of cholesterol and its esters include both lipids and proteins that work in unison. In cell membranes, integral proteins that take care of a great deal of cellular functions exist and work together with lipids. Meanwhile, the structure of a lipid system can also play a role, since, e.g., in liposomes the asymmetric pressure profile across a membrane contributes to the gating of mechanosensitive channels. These and many other phenomena observed in lipid systems have recently been elucidated by combination of experiments with simulations, which overall is an excellent strategy to

gain better understanding of the many lipid structures and the roles of lipids in biological functions. We hope that this short overview attracts the readers to contribute to this exciting field, to unravel the many open questions dealing with lipids' biological significance.

Cross-References

- ▶ Atomic Force Microscopy
- ▶ Chemical Diversity of Lipids
- ▶ Differential Scanning Calorimetry (DSC), Pressure Perturbation Calorimetry (PPC), and Isothermal Titration Calorimetry (ITC) of Lipid Bilayers
- ▶ Dynamic Light Scattering
- ▶ Fluorescence
- ▶ Fluorescence Correlation Spectroscopy
- ▶ Glycerolipids: Chemistry
- ▶ Lipid Domains
- ▶ Lipid Lateral Diffusion
- ▶ Lipid Signaling and Phosphatidylinositols
- ▶ Membrane Fluidity
- ▶ Membrane Proteins: Structure and Organization
- ▶ Molecular Dynamics Simulations of Lipids
- ▶ NMR
- ▶ Phase Transitions and Phase Behavior of Lipids
- ▶ Pressure Effects on Lipid Membranes
- ▶ Solid-State NMR
- ▶ Stimulated Emission Depletion (STED) Microscopy
- ▶ Thermodynamics of Lipid Interactions
- ▶ X-Ray Scattering of Lipid Membranes

References

- Bloom M, Evans E, Mouritsen OG. Physical properties of the fluid lipid-bilayer component of cell membranes: a perspective. *Q Rev Biophys*. 1991;24:293–397.
- Donnert G, Keller J, Medda R, Andrei MA, Rizzoli SO, Lührmann R, Jahn R, Eggeling C, Hell SW. Macromolecular-scale resolution in biological fluorescence microscopy. *Proc Natl Acad Sci USA*. 2006;103:11440–5.
- Eggeling C, Ringemann C, Medda R, Schwarzmann G, Sandhoff K, Polyakova S, Belov VN, Hein B, von Middendorff C, Schoenle A, Hell SW. Direct observation of the nanoscale dynamics of membrane lipids in a living cell. *Nature*. 2009;457:1159–63.
- Evans DF, Wennerström H. The colloidal domain: where physics, chemistry, biology, and technology meet. New York: Wiley; 1999.
- Feller SE, editor. Computational modeling of membrane bilayers, Current topics in membranes, vol. 60. Amsterdam: Academic; 2008.
- Hell S. Far-field optical nanoscopy. *Science*. 2007;316:1153–8.
- Hevonoja T, Pentikäinen MO, Hyvönen MT, Kovanen PT, Ala-Korpela M. Structure of low density lipoprotein (LDL) particles: basis for understanding molecular changes in modified LDL. *Biochim Biophys Acta*. 2000;1488:189–210.
- Huang B, Bates M, Zhuang X. Super-resolution fluorescence microscopy. *Annu Rev Biochem*. 2009;78:993–1016.
- Hyde S, Andersson S, Larsson K, Blum Z, Landh T, Lidin S, Ninham BW. The language of shape. The role of curvature in condensed matter: physics, chemistry and biology. Amsterdam: Elsevier; 1997.
- Izvekov S, Voth GA. Solvent-free lipid bilayer model using multiscale coarse-graining. *J Phys Chem B*. 2009;113:4443–55.
- Khandeliah H, Duelund L, Pakkanen KI, Ipsen JH. Triglyceride blisters in lipid bilayers: Implications for lipid droplet biogenesis and the mobile lipid signal in cancer cell membranes. *PLoS One*. 2010;5:e12811.
- Larsson K. Lipids – molecular organization, physical functions and technical applications. Dundee: The Oily Press; 1994.
- Lingwood D, Simons K. Lipid rafts as a membrane-organizing principle. *Science*. 2010;327:46–50.
- Mouritsen OG. Life – as a matter of fat: the emerging science of lipidomics. Berlin: Springer; 2005.
- Rittweger E, Han KY, Irvine SE, Eggeling C, Hell SW. STED microscopy reveals crystal colour centres with nanometric resolution. *Nat Photonics*. 2009;3:144–7.
- Rzepiela AJ, Schäfer LV, Goga N, Risselada HJ, de Vries AH, Marrink SJ. Reconstruction of atomistic details from coarse grained structures. *J Comput Chem*. 2010;31:1333–43.
- Science in Your Eyes 2011. <http://www.scienceinyoureyes.com/>. Accessed 20 Jan 2012.
- Serdyuk IN, Zaccai NR, Zaccai J. Methods in molecular biophysics: structure, dynamics, function. Cambridge: Cambridge University Press; 2007.
- Vattulainen I, Mouritsen OG. Diffusion in membranes. In: Heitjans P, Kärger J, editors. Diffusion in condensed matter: methods, materials, models. Berlin: Springer; 2005. p. 471–509.
- Vuorela T, Catte A, Niemelä PS, Hall A, Hyvönen MT, Marrink SJ, Karttunen M, Vattulainen I. Role of lipids in spheroidal high density lipoproteins. *PLoS Comput Biol*. 2010;6:e1000964.

Lipid Packing

- ▶ [Lipid Lateral Diffusion](#)

Lipid Phase Equilibria

- ▶ [Critical Fluctuations in Lipid Mixtures](#)
- ▶ [Hierarchically Structured Lipid Systems](#)
- ▶ [Lipid Lateral Diffusion](#)
- ▶ [Phase Transitions and Phase Behavior of Lipids](#)
- ▶ [Thermodynamics of Lipid Interactions](#)

Lipid Protocells

Anders N. Albertsen and Pierre-Alain Monnard
Department of Physics, Chemistry and Pharmacy,
FLinT center, University of Southern Denmark,
Odense, Denmark

Synonyms

[Chemoton](#); [Minimal artificial cell](#); [Minimal self-replicating chemical system](#)

Definition

Protocells are self-assembled chemical systems that are proposed either as minimal models for living cell progenitors or as artificial cells. The reductionist view of life has led to the idea that the cellular components of information, metabolism, and container are the essential pieces of living systems that work together through dynamic interconnections (Deamer 1997; Rasmussen et al. 2004; Szostak et al. 2001). These interactions lead to emergent properties within the system, such as self-maintenance and self-replication

of all parts. Thus, a protocell should be composed of at least these three components.

The container is often viewed as a self-assembled structure that has to be stable enough to contain metabolism and information components, thereby defining the protocell identity (Matsuura et al. 2002). However, it must still be rather dynamic to allow the protocell life cycle (growth and division) to occur. The metabolism of a protocell provides the components, e.g., lipids or information polymers, necessary for maintenance and reproduction of the protocell by conversion of external resources. The information molecules perform the crucial role of regulating the functions of the protocell as well as storing protocell information. The primary component that needs to be regulated, in the protocell, is the metabolism.

Certain chemical compounds named amphiphiles are capable of spontaneously self-assembling into structures defined by a fine bilayer boundary, called vesicles or liposomes. These entities possess, to a certain extent, all the desired container properties. Among amphiphiles, lipids are a broad group of natural molecules that includes fats, waxes, sterols, fat-soluble vitamins, monoglycerides, diglycerides, and phospholipids. Thus, they have often been used in protocell container design.

Introduction

Protocells have been proposed and investigated as models for progenitors of contemporary living cells (Origin of Life) (Monnard and Deamer 2002; Walde 2006) or as artificial cells (Artificial Life) (Luisi et al. 2006). In the exploration of the Origin of Life, it is necessary to consider the environment on the early Earth (i.e., 4 billion years ago) which will define the availability of chemicals. In contrast, when designing artificial cells, it is possible to assemble systems that are not necessarily biomimetic.

The importance of container structures in protocell design, as well as in contemporary cells, has been postulated very early on. Indeed, containers provide a rare opportunity to compartmentalize (i.e., spatially organize), regulate mixing of chemicals, and protect molecules from degradation. Thus, the properties of (pro)cellular networks are usually intimately linked to the presence of container structures.

In the 1920s, Oparin and Haldane (independently) proposed that life began on the early Earth as

self-assembled structures of organic material. However, the former viewed cells as a collection of aggregated colloidal particles, while the latter suggested that cells consist of numerous half-living chemical molecules suspended in water and enclosed in an oily film or membranes.

During the second half of the twentieth century, the research on protocells was greatly advanced by discoveries in cellular architecture and function, as well as by an ever-increasing understanding of the environmental conditions and potential chemistry on the early Earth. For example, as the multiple roles of membranes in cells were elucidated, it became clear that all cellular membranes are predominantly composed of lipid bilayers and that phospholipid is a nearly ubiquitous amphiphilic component of these bilayers. In 1965, Bangham and coworkers demonstrated that phospholipids alone could spontaneously form bilayer vesicles, called liposomes, having dimensions in the range of bacteria.

Analysis of chemical contents of carbonaceous meteorites, such as the Murchison meteorite (which is considered representative of those that impacted Earth during the late accretion period) established the abundant presence of lipids. Monocarboxylic acids ranging from 8 to 12 carbons in length were detected, which are now considered when protocells are constructed as models for progenitors of contemporary cells (Monnard and Deamer 2002).

Lipids Commonly Used for Protocell Compartments

Although lipids are a broad group of molecules, we will limit our enumeration to those commonly used in protocell design (see Fig. 1). These lipids originate predominantly from two types of biochemical subunits, ketoacyl and isoprene groups, and belong to the following categories: fatty acyls, glycerolipids, phospholipids, as well as isoprenol lipids. These molecules have amphiphilic character that allows them to spontaneously form various structures depending on the solubilization medium. Most significantly, they can form vesicles and liposomes (lipid bilayer membranes surrounding an aqueous core) which mimic cellular architecture.

Although the ability of phospholipids to self-assemble into membranous vesicles is common knowledge, it is less well known that bilayer structures, this

Vesicle-vesicle interactions (aggregation and fusion) can be triggered by temperature, and this is interesting from a protocell function perspective. While individuality of modern cells is necessary for evolution on a relatively long period, it may not be essential in primitive cellular systems. The exchange of internal contents as well as bilayer components could have led to increased complexity so that the emergence of new functions could be promoted.

Phospholipid Bilayer Membranes

Phospholipids, in particular phosphatidylcholines (PCs), have been used for protocell design. Their chemical or biochemical synthesis is rather complex, as it requires four enzymes, thus reducing the prebiotic likelihood.

These amphiphiles have two acyl chains, a fact that leads to properties in marked contrast with fatty acid bilayers. PC liposomes spontaneously form at CBCs as low as 10^{-6} to 10^{-9} mM. These structures are very stable over a broad pH range, resistant to high concentrations of divalent cations, and can withstand wide temperature variations. However, they tend to be rather impermeable to solutes.

Mixed Amphiphile Systems

All modern organisms use lipid mixtures to construct cell membranes and to modulate membrane chemical and physical properties. Examples include tocopherols and carotenoids (vitamins E and A) that are functional components of membranes, as well as essential fatty acids such as linoleic and arachidonic acid. Cholesterol is also used by eukaryotic cells to modulate bilayer fluidity and permeability.

Membranes composed of a pure amphiphile are often used in protocell designs although studies of mixed bilayers have demonstrated that modulation can be achieved by mixing single-chain amphiphiles. For instance, adding a secondary amphiphile, such as a fatty alcohol or a polyol (see Fig. 1(3) and (4)), to pure fatty acid bilayers can substantially lower the CBC and mitigate disruptive effects of salts, high pH, or temperature effects on fatty acid bilayers. When these vesicles are exposed to digestive enzymes, the encapsulated species remained functional, a result that establishes the relative stability of the mixed structures.

Compartmentalization of Metabolic and Information Machinery

Protocell development is often focused on three types of reactions: the synthesis of biopolymers; the synthesis of other protocell building blocks, such as amphiphiles; and the uptake of energy. The biopolymer synthesis are central to the functionality of the protocell due to their ability to catalyze reactions under mild conditions, as well as encode the information needed to construct a cell, while the synthesis of other building blocks is a prerequisite for self-maintenance and self-reproduction. Energy uptake and transduction is essential to permit the emergence of (semi)autonomous protocell.

Encapsulation

The membranous boundaries of protocells should be sufficiently impermeable to polymeric materials so that complex networks of catalyzed reactions would remain enclosed within, even though they should be more permeable than contemporary cells, to permit the uptake of nutrients.

A large number of methodologies have been developed that are usually based on the random encapsulation of solutes (Monnard et al. 2008; Walde and Ichikawa 2001). This fact renders the encapsulation of functional multiple-component catalytic systems, such as transcription and translation machinery, increasingly difficult as the number of components increase, suggesting that the protocell metabolism should be kept simple, especially considering the need for replication.

Membrane Permeability and Catalysis

Protocells will lack specialized membrane transport systems to take up substrates from their environment so that simple mechanisms such as passive diffusion will play an essential role for transmembrane transport (Mansy et al. 2008; Monnard et al. 2007). Studies of cellular membranes have however demonstrated the role of the lipid bilayer as the primary permeability barrier to free diffusion of polar and ionic solutes. Recent observations have established that the permeability to ionic solutes is inversely proportional to the length and the degree of unsaturation of the hydrocarbon chains, as well as the charge density of the solute. The permeability of PC bilayers to large ionic solutes depends on the phase of the bilayers (gel-like or liquid-crystalline phase), by extension on the

temperature and is generally lower than that of fatty acid bilayers. Permeability studies have shown that PC bilayers are not simply a barrier but also exhibit a surprising degree of selectivity. DMPC bilayers (see Fig. 1(1)) are permeable to ADP or even ATP, but impermeable to pApA. They were also more permeable to ribose than to other pentoses and hexoses.

The permeability can be further modulated by varying bilayer composition by adding cosurfactants, such as fatty acids or detergents. Mixed PC bilayers have an increased permeability to large ionic solutes, in marked contrast to the stabilization of fatty acid bilayers by alcohols. It would therefore be advantageous for protocells to have membrane boundaries composed of an amphiphilic mixture.

Energy Uptake

Three sources of energy can be harvested by protocells: chemical energy in the form of high-energy chemical bonds, oxidation-reduction reactions, and light energy (Deamer 1997). To perform synthetic reactions (e.g., to form a C-C bond), the uptake of energy and conversion into stable chemical gradients is necessary as these reactions usually require a vectorial two-electron transfer reaction. Here again, protocell membranes could play a crucial role, as their counterparts in cells do.

The question is whether protocell structures can maintain gradients during their build-up until the amplitude is large enough to drive uphill synthetic reactions. Recent studies have shown that a chemical gradient across a membrane can be created using embedded, photosensitive polycyclic aromatic hydrocarbons (PAHs). Self-assembled bilayers can also provide the framework necessary to achieve the vectorial organization in photosynthetic machinery. That is, the creation of a pH gradient strong enough to permit ATP synthesis which requires 4 protons for each ATP molecule (Steinberg-Yfrach et al. 1998).

Semiautonomous Metabolism

A minimal transcription system could be composed of RNAs that has the dual functions of catalysis and information storage (hypothesized in the “RNA world” concept). But, the required molecules, an efficient RNA-dependent RNA polymerase remains elusive. Therefore, most of the research on genetic information transfer within vesicles has been conducted using enzyme systems (see reviews

Monnard et al. 2008; Walde and Ichikawa 2001). Single polymerase enzymes, as well as transcription and translation systems (about 80 molecular components), have been successfully encapsulated in both liposomes and vesicles. These model systems can help determine how information transfer can perform in protocells.

These designs aim to creating a fully functional cell with the help of reconstituted biological architectures composed only of the necessary components for protein production (Noireaux and Libchaber 2004), but they do not represent a fully independent metabolism; thus, the protocell has to gather the missing molecules from the external medium. Interestingly, protein production within liposome can be more efficient than in bulk solution. The simultaneous expression of two membrane proteins associated with the production of a lipid, phosphatidic acid, was confirmed as their products were positively identified in the system boundaries (Kuruma et al. 2009). That is, container growth can in principle be linked with an internalized production of amphiphiles.

Considering that the encapsulation procedures used to prepare these liposomes achieves small encapsulation yields, there is a negligible probability of a simultaneous encapsulation of the many components (more than 80) in a spherical compartment with a 100-nm radius. Thus, the improvement of protein production observed is likely much higher locally.

An alternate approach to colocalization of reaction components is to anchor the entire reaction network to the structure (Rasmussen et al. 2004), i.e., on the surface of a bilayer. The advantages of this system are numerous: Nutrients and waste products can freely diffuse to and from the metabolic/informational core. It also eliminates the problem of vesicle lysis, as only the bilayer itself needs to stay intact for the protocell to survive. This system is more flexible in terms of structure types as oil droplets or reverse micelles can be also used. However, it should be noted that the type and complexity of the catalytic assemblies anchored in vesicle bilayers will be limited compared to the complexity of a transcription-translation apparatus.

One such an “interfacial” system has recently been proposed, it envisions information and catalytic molecules anchored by aliphatic hydrocarbon moieties. Furthermore, while information is typically thought of as a distant control mechanism, the information molecules in the interfacial system are not true



encoding molecules, but rather as sequence-dependent actuators of the metabolic process. The nucleic acids would play the role of an electron donor/relay in the amphiphile-precursor photofragmentation catalyzed by a ruthenium complex. The effectiveness of the electron relay function should then depend on the base sequence of the information molecule, as investigation of electron transfer in DNA has established. This approach simplifies information utilization by a protocell and should ease protocellular reproduction as small DNA fragments can be nonenzymatically replicated.

The current embodiment of this protocell with a single nucleobase, 8-oxoguanine instead of a DNA polymer, has already allowed the investigation of several processes essential for the function of a protocell: i.e., the production of building blocks from precursors using an information control and external energy (light) harvested by the protocell metabolism (Maurer et al. 2011).

Self-Reproducing Compartments

Functional protocells need to reproduce their three components in a coordinated manner. Indeed, if the rate of amphiphile formation substantially exceeds the reproduction rates of the metabolic and genetic network elements, these species will be rapidly diluted in the growing container. Consequently, newly formed vesicles will lose the parent characteristics. In contrast, an exponential replication of its internal content may lead to the release and loss of protocell identity upon bursting of the container boundary.

Luisi and coworkers at the ETH in Zürich have approached the question of self-reproducing compartments by using vesicles formed from oleic acid (Walde et al. 1994). Oleic anhydrides are used as a water-immiscible source of amphiphile precursors. Their hydrolysis provides membrane building blocks that can be used to make bilayers. Significantly, when the hydrolysis is carried out with preformed vesicles, these structures induce an autocatalytic-like behavior in the system as hydrolysis rates increase with increasing vesicle concentration.

Szostak and coworkers (Hanczyc et al. 2003) at Harvard Medical School were able to demonstrate not only growth of fatty acid vesicles containing encapsulated RNA but also a kind of division when the suspension was filtered through microscopic pores or submitted to an external shaking. They further established a detailed kinetic analysis of the growth, which demonstrated that vesicles could compete for

membrane components present in their environment, and undergo a kind of evolutionary selection (Hanczyc and Szostak 2004).

Attempts have been recently made to closely link the replication of containers to an endogenous production of amphiphiles either using simple metal catalytic systems or complex transcription and translation machinery encapsulated within amphiphilic containers, the so-called minimal cell concept (Luisi et al. 2006). These experiments indicate that in principle an internalized production of amphiphiles at rates compatible with the replication of the compartment is achievable. However, the system still lacks the possibility to replicate all its components, in particular the information part.

Summary

Much progress has been made implementing one or even multiple functions seen in living cells within artificial constructs called lipid protocells. However, the main obstacle to a truly functional protocell is the complete integration of all functions in a single self-maintaining, self-reproducing system capable of evolution, thereby possessing the emergent properties of life. Thus, it seems to be reasonable to attempt the design of protocells with a systemic approach, i.e., construct them with all their components present even in an extremely simplified manner. These self-replicating chemical systems will, however, likely remain inherently nonliving but allow us to define the requirements and limits of abridged metabolic, informational, and structural interactions.

Cross-References

- ▶ [Alkanols – Effects on Lipid Bilayers](#)
- ▶ [Chemical Diversity of Lipids](#)
- ▶ [Critical Fluctuations in Lipid Mixtures](#)
- ▶ [DNA Polymerase](#)
- ▶ [Essential Fatty Acids](#)
- ▶ [Fatty Acids, Alkanols, and Diacylglycerols](#)
- ▶ [Functional Roles of Lipids in Membranes](#)
- ▶ [Glycerolipids: Chemistry](#)
- ▶ [Lipid Bilayer Asymmetry](#)
- ▶ [Lipid Lateral Diffusion](#)
- ▶ [Lipid Organization, Aggregation, and Self-assembly](#)

- ▶ [Machinery of DNA Replication](#)
- ▶ [Membrane Fluidity](#)
- ▶ [Protein Synthesis: Translational Fidelity](#)
- ▶ [RNA Polymerases and Transcription](#)
- ▶ [Thermodynamics of Lipid Interactions](#)

References

- Deamer DW. The first living systems: a bioenergetic perspective. *Microbiol Mol Biol Rev.* 1997;61:230–61.
- Hanczyc MM, Szostak JW. Replicating vesicles as models of primitive cell growth and division. *Curr Opin Chem Biol.* 2004;8:660–4.
- Hanczyc MM, Fujikawa SM, Szostak JW. Experimental models of primitive cellular compartments: encapsulation, growth, and division. *Science.* 2003;302:618–22.
- Kuruma Y, Stano P, Ueda T, Luisi PL. A synthetic biology approach to the construction of membrane proteins in semi-synthetic minimal cells. *Biochim Biophys Acta.* 2009;1788:567–74.
- Luisi PL, Ferri F, Stano P. Approaches to semi-synthetic minimal cells: a review. *Naturwissenschaften.* 2006;93:1–13.
- Mansy SS, Schrum JP, Krishnamurthy M, Tobe S, Treco DA, Szostak JW. Template-directed synthesis of a genetic polymer in a model protocell. *Nature.* 2008;454:122–5.
- Matsuura T, Yamaguchi M, Ko-Mitamura EP, Shima Y, Urabe I, Yomo T. Importance of compartment formation for a self-encoding system. *Proc Natl Acad Sci USA.* 2002;99:7514–7.
- Maurer SE, Deamer DW, Boncella JM, Monnard P-A. Impact of glycerol monoacyl on the stability of plausible prebiotic fatty acid membranes. *Astrobiology.* 2009;9:979–87.
- Maurer SE, DeClue MS, Albertsen AN, Dörr M, Kuiper DS, Ziock H, et al. Interactions between catalysts and amphiphile structures and their implications for a protocell model. *Chem Phys Chem.* 2011;12:828–35.
- Monnard P-A, Deamer DW. Membrane self-assembly processes: steps towards the first cellular life. *Anat Rec.* 2002;268:196–207.
- Monnard P-A, Deamer DW. Preparation of vesicles from non-phospholipid amphiphiles. In: Nejat D editor. *Methods in enzymology.* New York: Academic; 2003;372:133–51.
- Monnard P-A, Luptak A, Deamer DW. Models of primitive cellular life: polymerases and templates in liposomes. *Phil Trans Roy Soc B.* 2007;362:1741–50.
- Monnard P-A, Ziock H, DeClue MS. Organic nano-compartments as biomimetic reactors, and protocells. *Curr Nanosci.* 2008;4:71–87.
- Noireaux V, Libchaber A. A vesicle bioreactor as a step toward an artificial cell assembly. *Proc Natl Acad Sci USA.* 2004;101:17669–74.
- Rasmussen S, Chen L, Deamer D, Krakauer DC, Packard NH, Stadler PF, et al. Evolution. Transitions from nonliving to living matter. *Science.* 2004;303:963–5.
- Steinberg-Yfrach G, Rigaud J-L, Durantini EN, Moore AL, Gust D, Moore TA. Light-driven production of ATP catalyzed by F_0F_1 -ATP synthase in an artificial photosynthetic membrane. *Nature.* 1998;392:479–82.
- Szostak JW, Bartel DP, Luisi PL. Synthesizing life. *Nature.* 2001;409:387–90.
- Walde P. Surfactant assemblies and their various possible roles for the origin(s) of life. *Orig Life Evol Biosphere.* 2006;36:109–50.
- Walde P, Ichikawa S. Enzyme inside lipid vesicles: preparation, reactivity and applications. *Biomol Eng.* 2001;18:143–77. Review.
- Walde P, Wick R, Fresta M, Mangone A, Luisi PL. Autopoietic self-reproduction of fatty acid vesicles. *J Am Chem Soc.* 1994;116:11649–54.

Lipid Raft

- ▶ [Lipid Lateral Diffusion](#)

Lipid Self-Organization

- ▶ [Hierarchically Structured Lipid Systems](#)
- ▶ [Phase Transitions and Phase Behavior of Lipids](#)

Lipid Shape and Curvature Stress

- ▶ [Thermodynamics of Lipid Interactions](#)

Lipid Signaling and Phosphatidylinositols

Lok Hang Mak
 Department of Chemistry, Institute of Chemical Biology, Imperial College London, London, UK

Synonyms

[Inositol lipids](#); [Phosphatidylinositol lipids](#); [Phosphoinositides](#)

Definition

Phosphatidylinositols (PI) are a class of lipids characterized by their inositol head groups which can be

phosphorylated at the 3-, 4-, and 5-positions to yield the seven naturally occurring species of phosphorylated PIs.

Basic Characteristics

Phosphatidylinositol is an important phospholipid in the cytosolic side of eukaryotic cell membranes. It is an acidic phospholipid consisting of a D-myo-inositol-1-phosphate linked via its phosphate group to diacylglycerol. Phosphatidylinositol is synthesized by the enzyme cytidine diphosphate (CDP)-diacylglycerol inositol phosphatidyltransferase from the precursors cytidine diphosphate diacylglycerol and inositol (McMaster and Jackson 2004). The inositol head group can be reversibly phosphorylated to yield phosphatidylinositol monophosphates (PIP), phosphatidylinositol bisphosphate (PIP₂), and phosphatidylinositol trisphosphate (PIP₃). Seven phosphorylated PI species have been documented in eukaryotic cells. Although they are quantitative minor components of the cell, phosphoinositides are important key players in a wide variety of cellular functions including membrane trafficking, cell proliferation, growth, and nuclear events (Di Paolo and De Camilli 2006).

Phosphatidylinositol 3-Phosphate

Phosphatidylinositol 3-phosphate (PI3P) is a monophosphorylated phosphoinositide at the 3-position of the inositol ring. It is predominantly found in early and multivesicular endosomes. PI3-kinase phosphorylates PI upon stimulation of tyrosine kinase receptor and G-protein-coupled receptors to form PI3P. PI3P can also be generated from PI(3,4)P₂ by 4-phosphatase activity (INPP4) as well as from PI(3,5)P₂ by 5-phosphatase activity (SAC3) (Sasaki et al. 2009). PI3P is dephosphorylated by the family mammalian myotubularin lipid phosphatases. It is important for the recruitment of effector proteins that contain a specific PI3P-binding domain. Specific PI3P recognition module includes the zinc-finger domains which were initially found in Fab1, YOTB, Vac1, and EEA1 proteins. These domains are collectively termed as FYVE domains. These FYVE domains containing proteins are involved in endocytic trafficking (Tatiana 2006).

PI3P plays also an important role in regulation of autophagy and cytokinesis.

Phosphatidylinositol 4-Phosphate

Phosphatidylinositol 4-phosphate (PI4P), the most abundant PI lipid is the precursor of the important signaling molecule PI(4,5)P₂, but it has its characteristic functions through interactions with a number of effectors as well. PI4P is synthesized from PI by type II and type III PI 4-kinases. Another biosynthesis route for PI4P is the turnover of PI(4,5)P₂ by type II 5-phosphatases like synaptojanin, oculocerebrorenal syndrome of lowe (OCRL), skeletal muscle and kidney-enriched inositol 5-phosphatase (SKIP), INPP5B, INPP5E, and INPP5J.

PI4P is prevalently in the Golgi apparatus, but can also be found at the plasma membrane. In the Golgi complex, PI4P has important roles in biogenesis of transport vesicles as well as maintaining the structural and functional organization of the Golgi complex (Antonietta De Matteis et al. 2005). At the plasma membrane PI4P serves mainly as the substrate for PI(4,5)P₂ synthesis. Several trans-Golgi-network-associated proteins have been identified to bind PI4P. These proteins include FAPP1, FAPP2, EpsinR, and OSBP. FAPP1, FAPP2, and OSBP bind PI4P through their PH domain (Balla et al. 2009). These PI4P effector proteins are involved in membrane trafficking upon binding to PI4P. It has been shown that endogenous and recombinant FAPPs translocate to the Golgi complex as well as to the trans-Golgi-network where transport to the plasma membrane are carried out. FAPPs are essential components in controlling the PI4P-regulated machinery for generating of post-Golgi carriers to the plasma membrane.

Phosphatidylinositol 5-Phosphate

Phosphatidylinositol 5-phosphate (PI5P) is constitutively present in many cell types, at levels roughly 100-fold less than the most abundant monophosphorylated phosphoinositide PI4P. PI5P has been shown to be present in the nucleus, Golgi complex, ER, and in the plasma membrane. In contrast to other phosphoinositides, a specific PI 5-kinase to generate PI5P from PI has not been identified to date.

Phosphatases instead play an important role in the synthesis of PI5P. PI5P can be synthesized by phosphatases of the myotubularin family from PI(3,5)P₂. It can also be generated by dephosphorylation of PI(4,5)P₂. Two human genes encoding for PI(4,5)P₂ 4-phosphatases I and II were identified to play a role in the synthesis of PI5P. In contrast to other phosphoinositides, PI5P metabolism is not controlled by dephosphorylation but phosphorylation mainly by PIP 4-kinases. PI5P plays a regulatory role in the nucleus and was found to bind the PHD finger motif of the nuclear protein ING2, which regulates p53 acetylation. Proteins with a PHD domain like ING1, ACF, and ATX1 interact with PI5P (Halstead et al. 2005).

Phosphatidylinositol 3,4-Bisphosphate

Phosphatidylinositol 3,4-bisphosphate (PI(3,4)P₂) is a minor lipid showing only trace levels in unstimulated cells. Upon stimulation the level of PI(3,4)P₂ can increase substantially, mainly by the action of 5-phosphatases SHIP, SKIP and synaptojanin by dephosphorylating PIP₃. PI(3,4)P₂ is mostly found at the plasma membrane and in the early endocytic pathway. Proteins possessing a PI(3,4)P₂-binding PH domain includes TAPP1, TAPP2, and Akt/PKB. The interactions of these proteins with PI(3,4)P₂ suggest the role of PI(3,4)P₂ in signaling stretching from plasma membrane to the nucleus. It has also been shown that the PX domain of p47PHOX is specific for PI(3,4)P₂. Disruption of the interaction between p47PHOX and PI(3,4)P₂ can cause chronic granulomatous disease (McMaster and Jackson 2004).

Phosphatidylinositol 3,5-Bisphosphate

Phosphatidylinositol 3,5-bisphosphate (PI(3,5)P₂) is mainly concentrated on late compartments of the endosomal pathway. The synthesis of PI(3,5)P₂ requires PI3P as precursor. The type III PIP kinase PIKfyve which contains a FYVE domain that is required for interaction with PI3P has been identified as the kinase for synthesizing PI(3,5)P₂. Breakdown of PI(3,5)P₂ is catalyzed by phosphatases from the myotubularin family, which dephosphorylates PI(3,5)P₂ at the 3-position of the inositol headgroup to

form PI5P. PI(3,5)P₂ has important functions in multivesicular body sorting, endosomal dynamics, and autophagy. Deficiency in PI(3,5)P₂ synthesis due to mutations in the type III PIPkins, can lead to severe neurodegeneration and early lethality (Mayinger 2012).

Phosphatidylinositol 4,5-Bisphosphate

Phosphatidylinositol 4,5-bisphosphate (PI(4,5)P₂) is enriched at the plasma membrane and is a precursor of second messengers and regulates a number of processes at the cell surface. PI(4,5)P₂ has also been detected at the Golgi as well as in the nuclear envelope. The main pool of PI(4,5)P₂ is synthesized by the action of two distinct classes of lipid kinases. Type I PIP kinase uses PI4P as substrate the main source of PI(4,5)P₂ biosynthesis. PI(4,5)P₂ is also being generated by type II PIP kinase using PI5P as substrate. It plays an important role in signal transduction through phospholipase C-mediated cleavage into IP₃ and diacylglycerol as well as substrate in the PI3-kinase-mediated synthesis of PIP₃. PI(4,5)P₂ is also important for the regulation of the actin cytoskeleton and ion channels. Additionally, it regulates clathrin-mediated endocytosis and exocytosis which is tightly controlled by the dephosphorylation of PI(4,5)P₂ through the type II phosphatase synaptojanin (McLaughlin et al. 2002).

Phosphatidylinositol (3,4,5)-Trisphosphate

Phosphatidylinositol (3,4,5)-trisphosphate is a quantitative minor PI lipid mainly localized at the plasma membrane. In unstimulated or serum-starved cells, PIP₃ exist in only trace amount which can rapidly and transiently accumulate upon a variety of external stimuli. PIP₃ is synthesized by the action of class I PI3-kinase using PI(4,5)P₂ as substrate. The cellular balance is maintained by tumor suppressor 3-phosphatase PTEN and 5-phosphatases SHIP1 and SHIP2. PIP₃ is an important effector of signaling cascade controlling cell growth and proliferation through the protein kinase Akt/PKB as a direct downstream effector. Akt possess a PIP₃-binding PH domain which induces a conformational change in the kinase upon PIP₃-binding and therefore activates the enzyme (Vanhaesebroeck et al. 2001).



Cross-References

- ▶ [Fatty Acids, Alkanols, and Diacylglycerols](#)
- ▶ [Functional Roles of Lipids in Membranes](#)
- ▶ [Glycerolipids: Chemistry](#)
- ▶ [Glycosylphosphatidylinositol](#)
- ▶ [Lipid Trafficking in Cells](#)
- ▶ [Lipids: Isolation and Purification](#)
- ▶ [Membrane Protein Function](#)
- ▶ [Membrane Proteins: Structure and Organization](#)

References

- Antonietta De Matteis M, Di Campli A, et al. The role of the phosphoinositides at the Golgi complex. *Biochimica et Biophysica Acta - Mol Cell Res.* 2005;1744(3):396–405.
- Balla T, Szentpetery Z, et al. Phosphoinositide signaling: new tools and insights. *Physiology.* 2009;24(4):231–44.
- Di Paolo G, De Camilli P. Phosphoinositides in cell regulation and membrane dynamics. *Nature.* 2006; 443(7112):651–7.
- Halstead JR, Jalink K, et al. An emerging role for PtdIns (4, 5) P₂-mediated signaling in human disease. *Trends Pharmacol Sci.* 2005;26(12):654–60.
- Mayinger P. Phosphoinositides and vesicular membrane traffic. *Biochimica et Biophysica Acta (BBA) - Mol Cell Biol Lipid.* 2012. in press. <http://dx.doi.org/10.1016/j.bbalip.2012.01.002>.
- McLaughlin S, Wang J, et al. PIP₂ and proteins: interactions, organization, and information flow. *Annu Rev Biophys Biomol Struct.* 2002;31(1):151–75.
- McMaster C, Jackson T. Phospholipid synthesis in mammalian cells. In: Daum G, editor. *Lipid Metab Membr Biogenesis.* 2004;6:105–34.
- Sasaki T, Takasuga S, et al. Mammalian phosphoinositide kinases and phosphatases. *Prog Lipid Res.* 2009;48(6): 307–43.
- Tatiana GK. Phosphatidylinositol 3-phosphate recognition and membrane docking by the FYVE domain. *Biochimica et Biophysica Acta - Mol Cell Biol Lipid.* 2006;1761(8): 868–77.
- Vanhaesebroeck B, Leever SJ, et al. Synthesis and function of 3-phosphorylated inositol lipids. *Annu Rev Biochem.* 2001;70(1):535–602.

Lipid Superstructures

- ▶ [Hierarchically Structured Lipid Systems](#)

Lipid Trafficking in Cells

Frederick R. Maxfield¹ and Mingming Hao²
¹Department of Biochemistry, Weill Cornell Medical College, New York, NY, USA
²Department of Internal Medicine, Yale University School of Medicine, New Haven, CT, USA

List of Abbreviations

BMP	bis-Monoacylglycerophosphate
CERT	Ceramide transfer protein
ER	Endoplasmic reticulum
GPI	Glycosyl-phosphatidylinositol
Insig	Insulin-induced gene
LDL	Low-density lipoprotein
NPC	Niemann-Pick disease type C
OSBP	Oxysterol-binding protein
PA	Phosphatidic acid
PC	Phosphatidylcholine
PE	Phosphatidylethanolamine
PI	Phosphatidylinositol
PI(3,4,5)P ₃	Phosphatidylinositol-(3,4,5)-triphosphate
PI(3,5)P ₂	Phosphatidylinositol-(3,5)-bisphosphate
PI(4,5)P ₂	Phosphatidylinositol-(4,5)-bisphosphate
PI3P	Phosphatidylinositol-3-phosphate
PI4P	Phosphatidylinositol-4-phosphate
PITP _S	PI/PC-transfer protein
PS	Phosphatidylserine
SCAP	SREBP cleavage-activating protein
SM	Sphingomyelin
SREBP	Sterol regulatory element-binding protein
StAR	Steroidogenic acute regulatory protein
START	StAR-related lipid transfer
TGN	trans-Golgi network

Synonyms

[Intracellular lipid transport](#); [Membrane traffic](#); [Nonvesicular transport](#)

Definition

The processes by which lipids move among organelles by vesicular trafficking processes or by diffusion through the cytoplasm in association with carrier proteins.

Introduction

Lipids play many important roles in cell physiology. Lipid bilayer membranes provide the main barrier separating the interior and exterior of a cell, restricting the transport of ions and polar molecules in and out of the cell. Lipid bilayers similarly provide a permeability barrier between the cytoplasm and the interior of organelles. The lipid composition of biological membranes must be maintained in a range that allows rapid diffusion of proteins within the bilayer while maintaining the barrier function. Several lipid species can be acted upon enzymatically to produce signaling second messengers that activate downstream signaling networks. The organization of lipids in a membrane bilayer can also affect the signaling properties of receptors and thereby modulating intracellular signal transduction. Organelles within a cell maintain lipid compositions that are individually distinct, and aspects of these lipid differences are an important component of the “identity” of the organelles that is used by proteins to interact selectively with certain organelles. The distinct lipid composition of these organelles is maintained even though there is a very robust transport of lipids between organelles. The processes regulating lipid traffic and the mechanisms for establishing and maintaining lipid composition of organelles are discussed herein. This review will focus on mammalian cells, but similar trafficking occurs in all eukaryotic cells.

Membrane Composition Varies Among Organelles

Each type of organelle maintains a distinct protein composition, which allows the organelle to carry out its specific functions. There has been considerable study of the mechanisms for trafficking membrane proteins to specific organelles, and this selective trafficking is often based on peptide sequences in the

cytoplasmic domains of proteins that are recognized by other proteins that form part of the scaffolds for budding transport vesicles or tubules from a parent organelle (Palade 1975; Bonifacino and Traub 2003). Lipid compositions also vary significantly among organelles (van Meer et al. 2008), but as discussed in a later section, the mechanisms for sorting lipids are not as well understood as for proteins. Some of the key differences in lipid composition are illustrated in Fig. 1. The plasma membrane is relatively enriched in sphingomyelin (SM), which is on the extracellular leaflet of the bilayer, and cholesterol (~30% of the lipid molecules). Phosphatidylserine (PS) is found on many organelles; on the plasma membrane, it is nearly exclusively on the cytoplasmic leaflet. External PS is found on apoptotic cells, and it is recognized by receptors on macrophages that engulf the dying cells (Savill and Fadok 2000). Phosphatidylinositol (PI), the precursor of phosphoinositides, is synthesized primarily in the endoplasmic reticulum (ER) and typically represents less than 15% of the total phospholipids found in eukaryotic cells. Phosphatidylinositol-4-phosphate (PI4P) and phosphatidylinositol-(4,5)-bisphosphate [PI(4,5)P₂] make up the bulk of phosphoinositides in mammalian cells, with PI(4,5)P₂ constituting ~1% of the phospholipids in the inner leaflet of the plasma membrane (Di Paolo and De Camilli 2006).

Many lipids are synthesized in the ER and then must be transported to other cellular organelles. The ER contains lipids with a much higher level of unsaturation than the plasma membrane, and it maintains a low level of cholesterol (~5% of lipid molecules). The ER is unusual in that it does not contain a significant transbilayer asymmetry for most of its lipids, indicating that there are mechanisms for flipping lipids across this membrane relatively rapidly (Sanyal and Menon 2009).

The lipid composition shifts along the secretory pathway, as sterols and sphingolipids increase in concentration from the ER through the Golgi to the plasma membrane. For example, trans-Golgi network (TGN)-derived secretory vesicles in yeast contain 2.3-fold more ergosterol and sphingolipids than the TGN (Klemm et al. 2009). The overall lipid composition of early endosomes is similar to that found in the plasma membrane, with some differences in the fatty acid structure. Cholesterol and SM, as well as PS, are highly enriched in the recycling endosome. Late endosomes contain large amounts of neutral lipids such as

triglycerides and cholesteryl ester, which are in the core of lipoproteins that are being digested. The membrane of late endosomes has a complex structure, with inward budding invaginations and detached internal vesicles. Bis-monoacylglycerophosphate (BMP, 15% of total lipids) is selectively enriched in the internal membranes of late endosomes (Gruenberg 2001; Kobayashi et al. 2001). Glycerolipids and sphingolipids are digested on these internal membranes to avoid damage to the limiting membrane (Kolter and Sandhoff 2010).

The lipid composition in the mitochondria varies little among different cell types, with phosphatidylcholine (PC) and phosphatidylethanolamine (PE) being the most abundant phospholipids (40% and 30% of total mitochondrial phospholipids, respectively), followed by glycerophospholipid cardiolipin (which is only found in mitochondria) and PI (10–15% of phospholipids), and phosphatidic acid (PA) and PS (5% of total mitochondrial phospholipids). Sphingolipids and sterols are not present in large amounts in mitochondrial membranes, although cholesterol, the precursor for steroid hormones, is delivered to mitochondria in steroidogenic cells (Osman et al. 2011).

Basic Mechanisms of Lipid Transport

There are two major methods for transport of lipids between organelles; they can move as part of a vesicle or tubule, or they can be transported by nonvesicular processes through the cytoplasm. Since lipids are poorly water soluble, nonvesicular transport is mediated by carrier proteins that can carry lipids between membranes. A specialized type of nonvesicular transport involves exchange of lipids between organelles at sites of close apposition (Fig. 1). Each of these transport mechanisms will be described briefly.

Vesicular Sorting

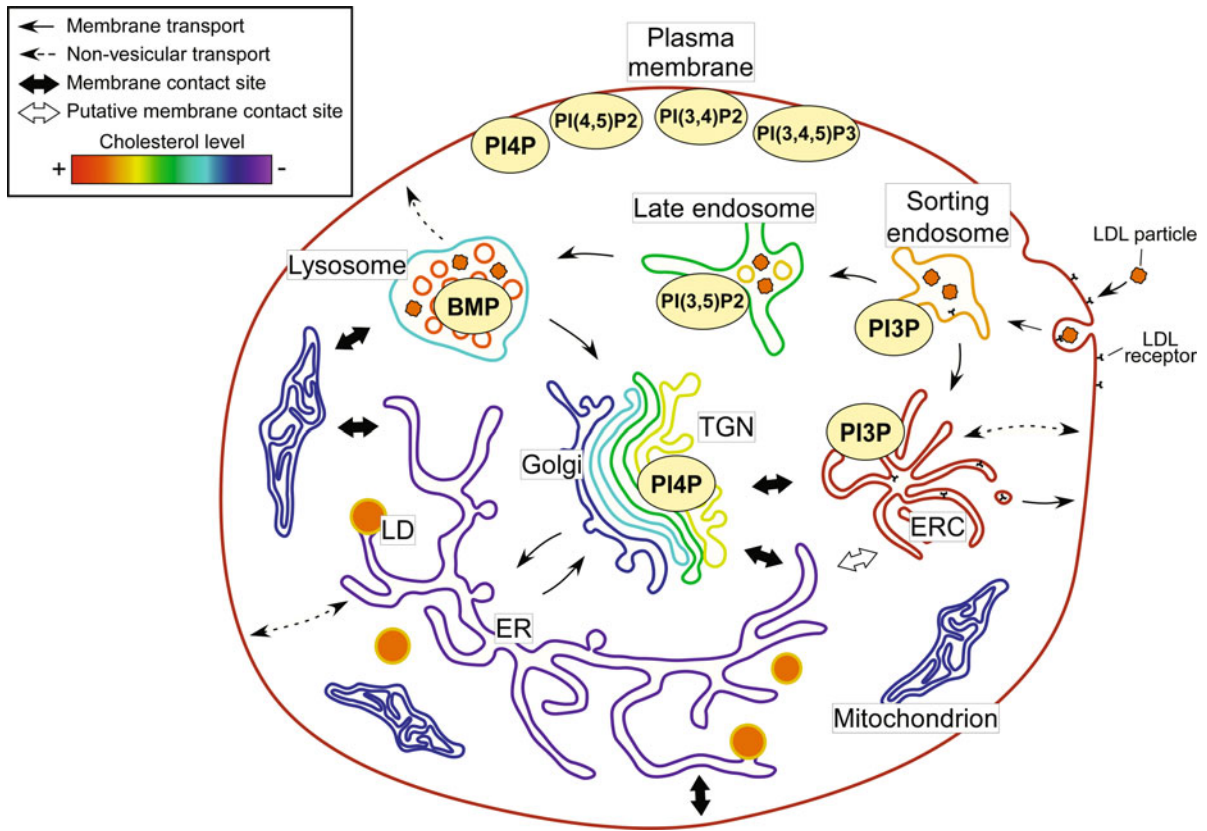
There is good evidence for sorting of lipids as vesicles and tubules bud off from a parent organelle. For example, fluorescent lipid analogs follow different endocytic routes after internalization from the plasma membrane depending upon the degree of unsaturation and the length of their hydrocarbon tails (Mukherjee et al. 1999). Lipid-anchored proteins, which are associated with membranes via

a glycosyl-phosphatidylinositol (GPI) anchor, follow different intracellular itineraries than most other lipid molecules (Mayor and Riezman 2004). Additionally, toxins (e.g., shiga or cholera toxins) bound to glycolipids follow distinctive pathways after internalization that allow the toxins to reach the ER, where they are able to use the cell's protein translocation machinery to cross into the cytoplasm (Sandvig et al. 2004).

The molecular basis for the sorting of lipids during membrane-trafficking processes is not well understood. In several cases, e.g., sorting of fluorescent lipid analogs and GPI-anchored proteins, changing cholesterol levels in cells alters the trafficking, indicating that membrane biophysical properties that are affected by cholesterol content are part of the sorting mechanism. One suggestion is that coexisting membrane microdomains are present in the parent organelle and that one type of microdomain might be preferentially incorporated into the budding vesicles or tubules. For example, if more ordered microdomains (sometimes called rafts) are enriched in a subset of proteins that are recruited by cytoplasmic coats on the budding membranes, then order-inducing lipids such as cholesterol and lipids with mostly saturated acyl chains would be selectively enriched in the budding transport vesicles (Fig. 2a). This mechanism has been suggested for lipid sorting in the biosynthetic secretory pathway (Simons and Ikonen 1997).

Another possibility is that curvature preferences play an important role in lipid sorting. Sites of vesicle and tubule budding often involve regions of high membrane curvature. Lipid molecules can be nearly cylindrical in their overall shape (i.e., the same radius at the headgroup and at the end of the acyl chain), which would lead to a preference for planar bilayers. Cone-shaped lipids (with small headgroup area) or inverted cone lipids (with large headgroups compared to the acyl chain area) will have preferences to be in curved membranes (Fig. 2b). While the preference of individual lipid molecules for curved regions does not impose a strong selection, curvature can induce phase separation in lipid mixtures in which the composition is close to a phase separation boundary (Maxfield and van Meer 2010). Thus, curvature preferences and formation of microdomains may work synergistically to promote lipid sorting during vesicle formation.

A third mechanism for lipid sorting would involve specific binding of lipid species to proteins that are incorporated into (or excluded from) forming



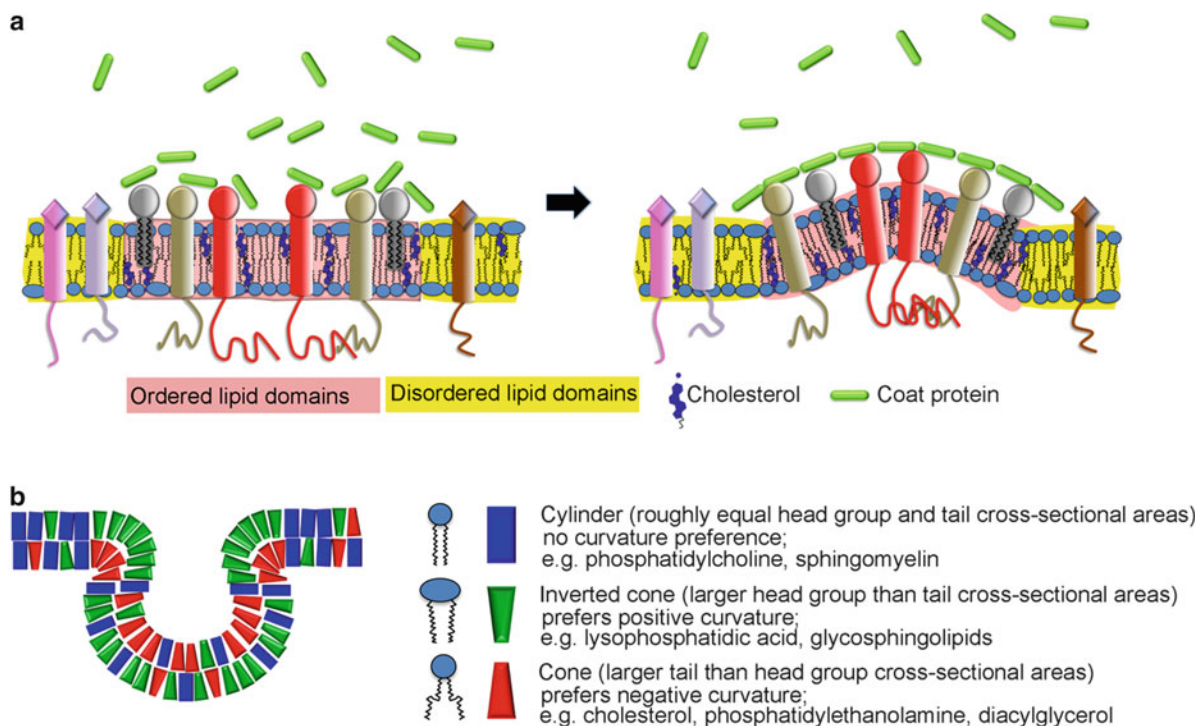
Lipid Trafficking in Cells, Fig. 1 Lipid distribution and movement among intracellular organelles. Phosphoinositides and special lipids involved in signaling and organelle recognition pathways are shown in ovals. PC, PE, PS, PI, and PA are synthesized in the ER and leave mainly by vesicular transport. SM and glycosphingolipids are synthesized in the Golgi and also move by vesicular transport. Each organelle is color-coded to reflect the relative level of cholesterol in its membranes. (The cholesterol levels for the limiting membrane of the late endosomes and lysosomes are uncertain because of the cholesterol associated with lipoproteins and internal membranes that are enriched in bis-monoacylglycerophosphate (BMP).) Circulating low-density lipoprotein (LDL) particles carrying cholesterol and cholesteryl ester are internalized through the

LDL receptors and transported to sorting endosomes. Free cholesterol, which is released upon cholesteryl ester hydrolysis in late endosomes and lysosomes, requires proteins NPC1 and NPC2 to leave these organelles. It then moves to other organelles by poorly characterized mechanisms. Excess free cholesterol is esterified, and fatty acid sterol esters are packed into lipid droplets (LD). Pathways of intracellular sterol transport, both vesicular and nonvesicular, are shown. Phosphoinositides serve as organelle identity molecules: PI3P, phosphatidylinositol-3-phosphate; PI4P, phosphatidylinositol-4-phosphate; PI(3,5)P₂, phosphatidylinositol-(3,5)-bisphosphate; PI(4,5)P₂, phosphatidylinositol-(4,5)-bisphosphate; and PI(3,4,5)P₃, phosphatidylinositol-(3,4,5)-trisphosphate. ERC, endocytic-recycling compartment

vesicles. There is little evidence that such a mechanism plays a general role in lipid sorting. However, there is mounting evidence that lipid-modifying enzymes are incorporated into forming vesicles. In particular, phosphatidylinositol kinases and phosphatases alter the phosphoinositide properties of the newly formed vesicles so that they no longer match the phosphoinositide signature of the donor membrane and begin to take on the characteristics of the target membrane with which they will fuse (Di Paolo and De Camilli 2006).

Nonvesicular Transport

Lipid molecules are held in membranes by noncovalent interactions and by the free energy associated with sequestering the hydrocarbon tails away from water. However, lipids in biological membranes are very dynamic, and they can have motions that transiently remove them partially from the bilayer, but complete spontaneous desorption is energetically unfavorable. It requires ~50 kJ/mol to remove cholesterol from membranes (Zhang et al. 2008) and ~80 kJ/mol to remove phospholipids (Marrink et al. 2009).



Lipid Trafficking in Cells, Fig. 2 *Lipid sorting by vesicular mechanisms.* This figure illustrates two *putative* mechanisms for sorting lipids during the vesicle-budding process in membrane transport. (a) Proteins associated with a particular type of microdomain, in this illustration cholesterol-enriched ordered lipid domains (*pink*), may also associate with coat proteins that form a budding vesicle. This would enrich the new vesicle in the types of lipids in the microdomain. (b) The shape of lipids can

affect their ability to be accommodated in regions of high curvature present at sites of vesicle budding. Cone-shaped lipids (*red*) might be accommodated in the cytoplasmic leaflet of the neck region of a vesicle bud, whereas inverted cone lipids (*green*) might be better accommodated in the luminal leaflet of the neck region. Different curvature (and the associated lipid preferences) are found in the more distal parts of the budding vesicle or tubule

Because of their poor solubility in water, lipid molecules, including cholesterol, must be associated with carrier proteins for efficient nonvesicular transport between organelles. Several such transport proteins have been identified. Members of the steroidogenic acute regulatory (StAR) protein-related lipid transfer (START) domain family of proteins have been shown to bind and transport cholesterol and some other lipids. The founding member of this family, StARD1, transports cholesterol to the inner membrane of mitochondria, where it can be converted to steroid hormones in steroidogenic tissues (Strauss et al. 2003; Miller and Auchus 2011). Other members of the START family have been shown to bind cholesterol (Alpy and Tomasetto 2005; Lavigne et al. 2010) and may play an important role in transport. Another member of this family, ceramide transfer protein (CERT), binds and transports ceramide (Hanada et al. 2009).

The oxysterol-binding protein (OSBP) was identified as a protein that binds 25-hydroxycholesterol. A related family of proteins (Osh proteins) contains OSBP homology domains, and many of these can bind sterols and transport them between membranes *in vitro*. The significance of this transport in cells is not known (Fair and McMaster 2008). A family of PI/PC-transfer proteins (PITPs) can transfer lipids between membranes, but their main function is to coordinate lipid traffic and lipid metabolism (Mousley et al. 2010).

With their lower free energy for desorption from the membrane, sterols are a good candidate for nonvesicular transport, and there is evidence for substantial nonvesicular sterol transport in yeast and in mammalian cells. For example, sterol in the endocytic recycling compartment, which contains about 35–40% of the cholesterol in a cultured fibroblast line, exchanges with other sterol pools in the cell with a $t_{1/2}$ of about 2–3 min (Hao et al. 2002). This suggests that

nonvesicular transport is the largest component of intracellular sterol transport. Similar conclusions were reached by studying the transport of newly synthesized cholesterol from the ER to the plasma membrane (Maxfield and Menon 2006). In yeast and in mammalian cells, treatments that block vesicular transport did not greatly alter transport of sterol from the ER to the plasma membrane. Unfortunately, the identity of the major cholesterol carriers has not been elucidated.

This rapid equilibration among organelles raises a question about how large differences in the sterol content of different organelle membranes is maintained (Mesmin and Maxfield 2009). Other membrane components of the various organelles can stabilize sterols to varying degrees, and this allows different concentrations of sterol to coexist in different organelles. For example, lipids with saturated acyl chains stabilize cholesterol in the membrane, and this type of lipid is enriched in the plasma membrane (high cholesterol) while unsaturated lipids predominate in the ER (low cholesterol).

The ER is the most important organelle for sterol regulation (Brown and Goldstein 2009). Cholesterol is synthesized in the ER. Esterification of cholesterol for storage in lipid droplets is the cellular high capacity, rapid response system for dealing with excess cholesterol, and acyl CoA cholesteryl acyltransferase, the enzyme that esterifies cellular cholesterol, resides in the ER. The complexes containing Insig, sterol regulatory element-binding protein (SREBP), and SREBP cleavage-activating protein (SCAP) also reside in the ER, and these proteins sense cholesterol levels and regulate the transcription of proteins involved in the uptake and synthesis of sterols. In high-cholesterol conditions, cholesterol binds to SCAP and Insig, leading to retention of SREBP in the ER. When cholesterol levels fall, SCAP and SREBP are recruited to transport vesicles and delivered to the Golgi apparatus. Two sequential proteolytic cleavages of SREBP in the Golgi lead to release of a cytoplasmic fragment of SREBP, which contains a transcriptional regulator that increases transcription of genes involved in cholesterol synthesis and the gene for the LDL receptor. In order for this system to work effectively, the ER must be able to sense the cholesterol levels in other organelles such as the plasma membrane. Since there is little vesicular transport from the plasma membrane to the ER, it is likely that nonvesicular sterol transport is an

important component of this regulation, but the identity of the sterol carriers remains uncertain.

Endocytic Uptake of Lipoproteins

Nucleated cells can synthesize cholesterol and take it up by endocytosis of lipoproteins. Outside the central nervous system, LDLs are the main cholesterol carriers; the core of LDL is packed with cholesteryl esters, and the outer surface contains the protein (mainly apoB) and a monolayer of lipids and cholesterol. LDL binds to the LDL receptor and enters the cell by receptor-mediated endocytosis (Brown and Goldstein 1986). The LDL dissociates from its receptor in an acidified endosome, and the LDL receptor is recycled to the plasma membrane while the LDL is delivered to late endosomes and lysosomes and is degraded. Cholesteryl esters are hydrolyzed by lysosomal acid lipase. The unesterified cholesterol, which is very poorly soluble in water, is transported out of the lysosomes by a process that requires the proteins NPC1 and NPC2. It appears that cholesterol is first bound by NPC2, a soluble protein in the lumen of late endosomes. The cholesterol is then transferred to an N-terminal cholesterol-binding site on NPC1, a polytopic membrane protein in the late endosomes. It is unclear how NPC1 then facilitates the transport of cholesterol out of the late endosomes and lysosomes, but defects in either NPC1 or NPC2 cause Niemann-Pick disease type C, a severe lysosomal storage disorder in which cholesterol and other lipids accumulate in lysosomal storage organelles (Mesmin and Maxfield 2009).

Transport of Newly Synthesized Lipids

Most lipids are synthesized in the ER in mammalian cells, although significant lipid synthesis and remodeling also occurs in the Golgi apparatus and in mitochondria. An excellent review of transport of newly synthesized lipids has been presented recently (Blom et al. 2011). The predominant transport pathway for newly made phospholipids is by vesicular transport. (This must operate in such a way that the lipids with more saturated acyl chains are continually returned to the ER to maintain that organelle's membrane characteristics.)

An important exception is ceramide, which can be transported by CERT, which has a ceramide-binding START domain. CERT also has a pleckstrin homology domain for targeting to Golgi membranes and a FFAT motif that binds the ER protein, VAP. Thus, CERT is able to efficiently shuttle ceramide from the cytoplasmic side of the ER, where it is made to the cytoplasmic side of the Golgi, where it can be converted to glucosylceramide. It is not entirely clear how the glucosylceramide is flipped to the luminal leaflet of the biosynthetic organelles, which is essential to conversion to more complex glycolipids. One proposal (Halter et al. 2007) is that glucosylceramide is returned to the ER by nonvesicular transport on FAPP2 and that it is then flipped in the ER membrane and transported by vesicular transport to the Golgi. This somewhat baroque pathway may be used to regulate SM and glycolipid synthesis since the activity of the nonvesicular transport processes can modulate proteins that are involved in other aspects of lipid metabolism (D'Angelo et al. 2008).

Summary

Lipids move rapidly among cellular organelles by a combination of vesicular and nonvesicular transport processes. Despite all of this trafficking, organelles maintain very different lipid compositions. The maintenance of the unique lipid compositions of organelles requires sorting of lipids at many steps of vesicle formation. The underlying mechanisms for this lipid sorting are only partially understood. Some lipids (especially cholesterol) are transported by soluble carrier proteins among organelles.

Acknowledgment We are grateful to Dr. Bruno Mesmin for preparation of Fig. 1.

Cross-References

- ▶ [Chemical Diversity of Lipids](#)
- ▶ [Functional Roles of Lipids in Membranes](#)
- ▶ [Glycerolipids: Chemistry](#)
- ▶ [Glycosylphosphatidylinositol](#)
- ▶ [Lipid Bilayer Asymmetry](#)
- ▶ [Lipid Domains](#)
- ▶ [Lipid Flip-Flop](#)

- ▶ [Lipid Lateral Diffusion](#)
- ▶ [Lipid Signaling and Phosphatidylinositols](#)
- ▶ [Lipidomics](#)
- ▶ [Sphingolipids and Gangliosides](#)

References

- Alpy F, Tomasetto C. Give lipids a START: the StAR-related lipid transfer (START) domain in mammals. *J Cell Sci.* 2005;118:2791–801.
- Blom T, Somerharju P, Ikonen E. Synthesis and biosynthetic trafficking of membrane lipids. *Cold Spring Harb Perspect Biol.* 2011;3(8):a004713. doi:10.1101/cshperspect.a004713
- Bonifacino JS, Traub LM. Signals for sorting of transmembrane proteins to endosomes and lysosomes. *Annu Rev Biochem.* 2003;72:395–447.
- Brown MS, Goldstein JL. A receptor-mediated pathway for cholesterol homeostasis. *Science.* 1986;232:34–47.
- Brown MS, Goldstein JL. Cholesterol feedback: from Schoenheimer's bottle to Scap's MELADL. *J Lipid Res.* 2009;50(Suppl):S15–27.
- D'Angelo G, Vicinanza M, De Matteis MA. Lipid-transfer proteins in biosynthetic pathways. *Curr Opin Cell Biol.* 2008;20:360–70.
- Di Paolo G, De Camilli P. Phosphoinositides in cell regulation and membrane dynamics. *Nature.* 2006;443:651–7.
- Fairn GD, McMaster CR. Emerging roles of the oxysterol-binding protein family in metabolism, transport, and signaling. *Cell Mol Life Sci.* 2008;65:228–36.
- Gruenberg J. The endocytic pathway: a mosaic of domains. *Nat Rev Mol Cell Biol.* 2001;2:721–30.
- Halter D, Neumann S, van Dijk SM, Wolthoorn J, de Maziere AM, Vieira OV, Mattjus P, Klumperman J, van Meer G, Sprong H. Pre- and post-Golgi translocation of glucosylceramide in glycosphingolipid synthesis. *J Cell Biol.* 2007;179:101–15.
- Hanada K, Kumagai K, Tomishige N, Yamaji T. CERT-mediated trafficking of ceramide. *Biochim Biophys Acta.* 2009;1791:684–91.
- Hao M, Lin SX, Karylowski OJ, Wustner D, McGraw TE, Maxfield FR. Vesicular and non-vesicular sterol transport in living cells. The endocytic recycling compartment is a major sterol storage organelle. *J Biol Chem.* 2002;277:609–17.
- Klemm RW, Ejsing CS, Surma MA, Kaiser HJ, Gerl MJ, Sampaio JL, de Robillard Q, Ferguson C, Proszynski TJ, Shevchenko A, Simons K. Segregation of sphingolipids and sterols during formation of secretory vesicles at the trans-Golgi network. *J Cell Biol.* 2009;185:601–12.
- Kobayashi T, Yamaji-Hasegawa A, Kiyokawa E. Lipid domains in the endocytic pathway. *Semin Cell Dev Biol.* 2001;12:173–82.
- Kolter T, Sandhoff K. Lysosomal degradation of membrane lipids. *FEBS Lett.* 2010;584:1700–12.
- Lavigne P, Najmanivich R, Lehoux JG. Mammalian StAR-related lipid transfer (START) domains with specificity for cholesterol: structural conservation and mechanism of reversible binding. *Subcell Biochem.* 2010;51:425–37.
- Marrink SJ, de Vries AH, Tieleman DP. Lipids on the move: simulations of membrane pores, domains, stalks and curves. *Biochim Biophys Acta.* 2009;1788:149–68.

- Maxfield FR, Menon AK. Intracellular sterol transport and distribution. *Curr Opin Cell Biol.* 2006;18:379–85.
- Maxfield FR, van Meer G. Cholesterol, the central lipid of mammalian cells. *Curr Opin Cell Biol.* 2010;22:422–9.
- Mayor S, Riezman H. Sorting GPI-anchored proteins. *Nat Rev Mol Cell Biol.* 2004;5:110–20.
- Mesmin B, Maxfield FR. Intracellular sterol dynamics. *Biochim Biophys Acta.* 2009;1791:636–45.
- Miller WL, Auchus RJ. The molecular biology, biochemistry, and physiology of human steroidogenesis and its disorders. *Endocr Rev.* 2011;32:81–151.
- Mousley CJ, Trettin KD, Tyeryar K, Ile KE, Schaaf G, Bankaitis VA. Sphingolipid metabolism in trans-golgi/endosomal membranes and the regulation of intracellular homeostatic processes in eukaryotic cells. *Adv Enzyme Regul.* 2010;50:339–48.
- Mukherjee S, Soe TT, Maxfield FR. Endocytic sorting of lipid analogues differing solely in the chemistry of their hydrophobic tails. *J Cell Biol.* 1999;144:1271–84.
- Osman C, Voelker DR, Langer T. Making heads or tails of phospholipids in mitochondria. *J Cell Biol.* 2011;192:7–16.
- Palade G. Intracellular aspects of the process of protein synthesis. *Science.* 1975;189:347–58.
- Sandvig K, Spilsberg B, Lauvrak SU, Torgersen ML, Iversen TG, van Deurs B. Pathways followed by protein toxins into cells. *Int J Med Microbiol.* 2004;293:483–90.
- Sanyal S, Menon AK. Flipping lipids: why an' what's the reason for? *ACS Chem Biol.* 2009;4:895–909.
- Savill J, Fadok V. Corpse clearance defines the meaning of cell death. *Nature.* 2000;407:784–8.
- Simons K, Ikonen E. Functional rafts in cell membranes. *Nature.* 1997;387:569–72.
- Strauss 3rd JF, Kishida T, Christenson LK, Fujimoto T, Hiroi H. START domain proteins and the intracellular trafficking of cholesterol in steroidogenic cells. *Mol Cell Endocrinol.* 2003;202:59–65.
- van Meer G, Voelker DR, Feigenson GW. Membrane lipids: where they are and how they behave. *Nat Rev Mol Cell Biol.* 2008;9:112–24.
- Zhang Z, Lu L, Berkowitz ML. Energetics of cholesterol transfer between lipid bilayers. *J Phys Chem B.* 2008;112:3807–11.

Lipid, Protein Interactions

- ▶ [Membrane Proteins: Folding and Stability](#)

Lipid–Cholesterol Interactions

- ▶ [Thermodynamics of Lipid Interactions](#)

Lipid–Lipid Interactions

- ▶ [Thermodynamics of Lipid Interactions](#)

Lipidomics

Thomas Kolter

LiMES – Program Unit Membrane Biology & Lipid Biochemistry, Universität Bonn, Bonn, Germany

Synonyms

[Mass action](#); [Mass spectrometry](#)

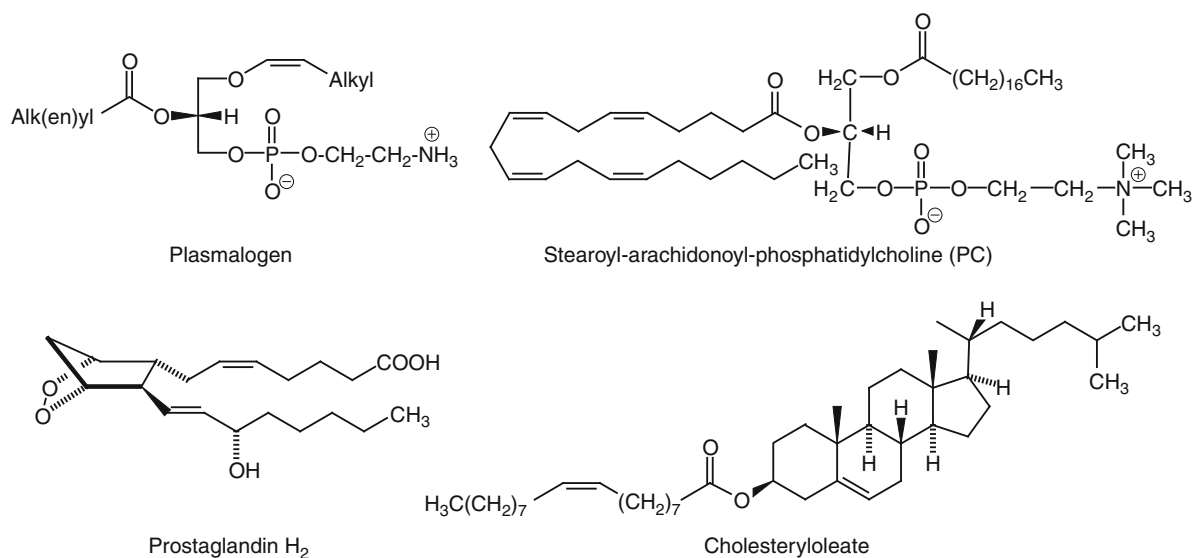
Definition

Systems level analysis and characterization of lipids and their interacting moieties (Wenk 2005).

Introduction

Lipidomics is a mass-spectrometry-based systems level analysis of cellular lipids (Ivanova et al. 2009). This requires the identification and quantitation of thousands of lipid molecular species. In addition, function, interaction, and dynamics of lipids are in the focus of this discipline and also the understanding of the changes in lipid profiles that occur in response to perturbation of the system, such as diseases, pharmacological treatment, or the targeted disruption of certain genes.

As a discipline of systems biology, lipidomics attempts to obtain, analyze, and integrate complex data on the lipidome of cells, tissues, organs, biofluids, or organisms (“systems”). Together with other metabolites such as amino acids, carbohydrates, and nucleotides, lipids form the metabolome of the system (▶ [Metabolomics](#)). The knowledge of lipid profiles should allow correlations with genome (DNA), transcriptome (RNA), proteome (proteins), and other metabolites of a system. As a technological platform, lipidomics faces the problem to determine levels of a large and structurally very heterogeneous group of



Lipidomics, Fig. 1 Structures of selected lipids: a plasmalogen and a phosphatidylcholine as membrane lipids, a prostaglandin as a lipid mediator, and a cholesterol ester as a storage lipid

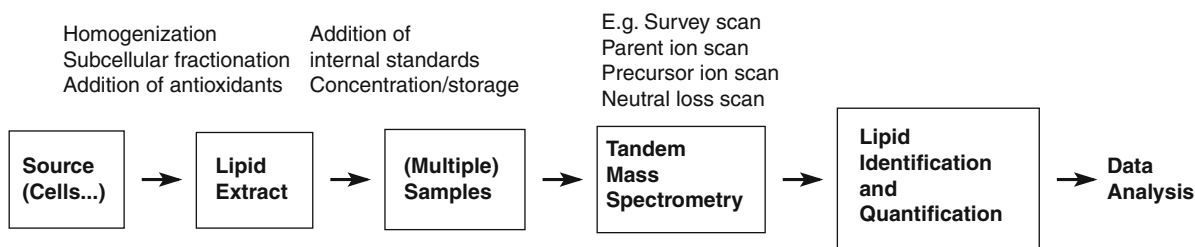
metabolites (Fig. 1) that can differ drastically in their abundance and their physical and functional properties (► [Chemical Diversity of Lipids](#)). Also, the subcellular distribution of a certain lipid can be critical for its function (van Meer 2005), for example, it can be necessary to determine its level in an intracellular compartment like the endoplasmic reticulum, a nerve ending, or the nucleus. Even if it is present on the inner or outer leaflet of a membrane might be important.

Lipids

Lipids are usually defined by common solubility properties: The majority of lipids is only slightly soluble in water and can be extracted from biological sources with organic solvents. Efforts for standardization by the LIPIDMAPS consortium (www.lipidmaps.org) led to a definition of lipids according to their biosynthetic origin and to their classification into eight different groups: fatty acyls (► [Fatty Acids, Alkanols, and Diacylglycerols](#)), glycerolipids (► [Glycerolipids: Chemistry](#)), glycerophospholipids, sphingolipids (► [Sphingolipids and Gangliosides](#); ► [Glycolipids](#)), sterol lipids, prenol lipids, saccharolipids, and polyketides (Fahy et al. 2005, 2009).

Membrane Lipids

Lipids differ not only in their chemical structures but also in the types of aggregates that they form in the aqueous environment of a living system (► [Hierarchically Structured Lipid Systems](#)). Amphiphilic lipids with cylindrical shape like phosphatidylcholines and sphingomyelins form lamellar phases and are found together with cholesterol as components of biological membranes (► [Functional Roles of Lipids in Membranes](#)). Membranes can contain more than 1,000 different lipid species, and different cellular membranes maintain different lipid compositions (van Meer 2005). When embedded in bilayers, cone-shaped lipids with small head groups such as phosphatidylethanolamine (PE) or phosphatidic acid (PA) can induce concave phase frontiers and a more dense packing in planar bilayers. Dependent on their species or subcellular origin (► [Lipid Trafficking in Cells](#)), membranes differ in their total lipid composition, but can show different lipid compositions of their two leaflets (► [Lipid Bilayer Asymmetry](#); ► [Lipid Flip-Flop](#)) and also between the apical and basolateral membranes of a polarized cell. Lateral differences in lipid compositions give rise to transient microdomains that account, for example, for differences in bilayer thickness and, subsequently, protein transport (► [Lipid Domains](#)). Although information on the spatial distribution of



Lipidomics, Fig. 2 Schematic diagram of a representative shotgun lipidomics approach

membrane lipids can be important, most attempts in lipidomics aim currently at the determination of the total lipid composition of cells, tissues, or organelles and apply techniques where this information is lost.

Mediator Lipids

Distinguished from membrane lipids are highly bioactive lipids that are transiently formed in often minute concentrations. These can be extracellular mediators such as the eicosanoids, lysophospholipids, platelet activating factor, or in part, structurally very complex metabolites that arise from the oxidation of fatty acids. Structure elucidation of these lipids and determination of their concentration in complex matrices is a technological challenge in lipidomics and usually addressed in so-called targeted approaches. Assignment of structures can often not be achieved by MS alone, such as absolute configurations or double-bond geometries.

Storage Lipids

Triacylglycerols are used as storage forms of metabolic energy, and cholesterol esters are the storage forms of cholesterol. These lipids aggregate to lipid globules in an aqueous environment, and within cells, they are deposited in specialized storage organelles, the lipid droplets. These occur in large amounts in the cytoplasm of adipocytes, differ in size and lipid composition, and are highly relevant for human diseases such as obesity, diabetes, and metabolic syndrome.

Lipid Analysis

Especially, the new developments in mass spectrometry (MS; ► [Mass Spectrometry](#)) had a huge impact on lipid analysis and enabled lipidomics as a large-scale

approach. They allowed not only the rapid quantification of different lipid classes but also the determination of complex molecular lipid species that arise by combination of different acyl (more general: “radyl”) chains (Fahy et al. 2005). Structure determination and quantification by MS occurs after different steps of sample preparation, lipid extraction, and eventually, one or more separation steps (Fig. 2).

Sample Preparation

Sample preparation includes steps like determination of wet- or dry weights of organs or tissues, of cell numbers, or protein- or DNA content for normalization purposes. To ensure reproducible results, sample preparation should be standardized and might rely on advanced methods that can be conducted in parallel, like immunomagnetic cell separation. Various methods for homogenization and subcellular fractionation are available. In special cases, also derivatization of the analyte can be carried out, for example, the formation of methyl esters of fatty acids for separation by GC.

Lipid Extraction

Since lipids can have different physicochemical properties including polarities, a comprehensive extraction of all lipid classes is not possible with only one solvent system. A popular method for lipid extraction has been established by Folch in 1957: Lipids are extracted by a mixture of chloroform and methanol followed by a partition step against an aqueous solvent. Under these conditions, most lipids are found in the organic phase, but more hydrophilic lipids like gangliosides are separated into the aqueous phase. Another method for lipid extraction that was introduced by Bligh and Dyer in 1959 is carried out by a monophasic mixture of chloroform, methanol, and water (1:2:0.8 v/v/v).

Changing the ratio to 2:2:1.8 (v/v/v) leads to a phase separation, where most lipids can be recovered from the organic phase. Quantitative lipid extraction by either of these or other methods is not always achieved; for example, the recovery of acidic lipids like phosphatidic acid (PA) and phosphatidylglycerol (PG) can be less than 30% in classical Folch and Bligh-Dyer extraction, where these lipids can become tightly bound to proteins. Lipids can also be covalently bound to proteins; for example, ω -hydroxylated ceramides are bound to protein of the cornified envelope of the human skin (► [Skin Lipids](#)). Such lipids are only released after chemical cleavage of the lipid-protein linkage. Special conditions are required for extraction of more polar lipids. For example, phosphatidylinositol-phosphates (► [Lipid Signaling and Phosphatidylinositols](#)) are not easily extractable, sensitive to harsh conditions, and adhere tightly to most materials used in the procedures of lipid analysis like glassware and metals.

Lipid Standards

The addition of internal standards can be required for lipid quantification or measurement of lipid dynamics (Postle and Hunt 2009). Standard lipids (Moore et al. 2007) that can be distinguished from endogenously occurring lipids contain rare alkyl chain combinations or the stable isotopes ^2H or ^{13}C so that their m/z values do not overlap with those of the analyte. For the analysis of structurally complex lipids like complex glycosphingolipids or gangliosides, standards have to be chemically prepared in a laborious manner and are still not available for a number of analytes.

Separation Techniques

Lipid classes can be separated from crude lipid extracts by different methods. If ESI-MS is used as the key analytical technique, also, the direct infusion of unseparated lipid extracts into the mass spectrometer is common in the so-called shotgun lipidomics approach. Separation can be achieved by chromatographic techniques which are coupled online or offline to MS, such as GC/MS, LC/MS, and LC/MS/MS. This allows identification of lipids by their accurately determined masses and retention times. A very robust technique is thin layer chromatography (Fuchs et al. 2011), by which lipid classes are easily separated and quantified after staining by densitometry.

Sample Storage

Samples are stored at low temperatures in an inert atmosphere, lipid extracts in diluted solutions. Exposure to air or enzyme sources might lead to lipid alteration or decomposition; especially, cholesterol is highly sensitive toward oxidation by oxygen with formation of oxysterols.

Mass Spectrometry

Instrumentation

In MS, mass to charge ratios (m/z values) are determined with instruments that contain an ion source, a mass analyzer (or combinations of them), and an ion detector (► [Mass Spectrometry](#)). Time-of-flight mass (TOF) spectrometers use a mass analyzer in which m/z values are determined by measuring their flight time through an evacuated tube of a defined length. Ion-trap mass spectrometers allow tandem MS and MS^n analyses of lipids. Limitations of this technique, such as limited mass accuracy and resolving power, are in part overcome by Orbitrap mass spectrometers. Triple quadrupole mass spectrometers were especially valuable for lipidomics since they allowed precursor ion- and neutral loss scanning and quantitative analyses using the multiple reaction monitoring (MRM) mode (Blanksby and Mitchell 2010). Limitations are low resolving power, precision, and accuracy in m/z determination and that they are not suitable to perform MS^n experiments with $n > 2$. Also, hybrid combinations of analyzers such as quadrupole-time of flight (Q-TOF) are in use. Specialized instruments applied to lipidomics are, for example, Fourier transform ion cyclotron resonance spectrometers, instruments for secondary ion MS (SIMS), or for ion mobility MS, which gives information about the molecular shape of the analyte (► [Ion-Mobility Mass Spectrometry: Biological Applications](#)).

Ionization Methods

The ionization technique most frequently applied to lipid analysis is electrospray ionization (ESI), but also other methods are used.

Electrospray Ionization (ESI)

ESI is a “soft” ionization method that can operate without fragmentation of the analyte molecules. While it is suitable for the analysis of many

amphiphilic membrane lipids, less polar lipids show generally poorer ionization efficiencies in classic ESI so that additional measures like adduct formation, chemical derivatization, or application of nano-ESI are required. Typical drawbacks of ESI include signal suppression in complex matrices and varying adduct patterns. Nano-ESI is a miniaturization of ESI with enhanced sensitivity and reduced signal suppression. Many lipids have been analyzed using ESI and nano-ESI also in automated and high-throughput applications.

Atmospheric Pressure Chemical Ionization (APCI) and Atmospheric Pressure Photoionization (APPI)

In APCI, charge is transferred onto the analyte by reaction with ionized carrier gas molecules. The ionization conditions are less mild than ESI, and sensitive molecules show in-source fragmentation. APCI is suitable for lipids of lower polarity, and the solvent plays a less dominant role for ionization than in ESI. This allows measurement of lipids dissolved in organic solvents such as chloroform or hexane. APPI is a modification of APCI, which has been reported to be more sensitive and efficient than APCI.

Matrix-Assisted Laser Desorption/Ionization (MALDI)

In MALDI, the analyte is placed onto an UV-absorbing solid matrix of aromatic acids, which are cocrystallized with the sample. Irradiation of suitable positions on the target with a laser of appropriate wavelength causes analyte desorption and ionization. MALDI has also been applied to the analysis of lipids and in particular glycolipids (Fuchs et al. 2010). MALDI is a qualitative method that normally provides no quantitative results. However, it is more tolerant to salts and other disturbing components and also allows imaging MS from tissue sections.

Imaging Techniques

Imaging MS is a technique to visualize the distribution of molecules within tissue sections. Disadvantages of MALDI are the limited lateral resolution of 20–50 μm , unfavorable signal to noise ratio for low molecular weight analytes, and long acquisition times. Secondary ion MS (SIMS) is suitable for imaging MS of lipids with lateral resolution in the submicrometer range.

Desorption electrospray ionization (DESI) has been used to create two-dimensional images of the distribution of lipid species in human tissues. In addition to MS approaches, also coherent anti-Stokes Raman scattering (CARS) microscopy ([► Infrared Spectroscopy of Membrane Lipids](#)) is used to determine the special distribution of nonlabeled lipids (Rinia et al. 2008).

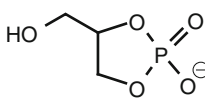
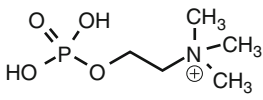
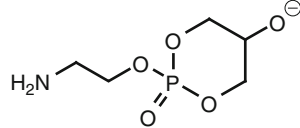
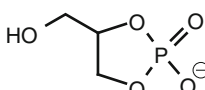
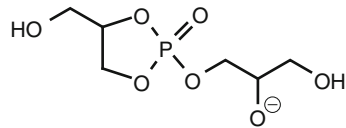
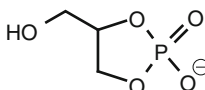
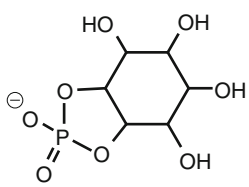
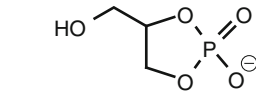
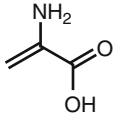
Tandem Mass Spectrometry

The generation of fragment ions for structure elucidation and quantification is called tandem MS. It can be carried out either as tandem-in-space using combinations of a quadrupole and another mass analyzer, such as a triple quadrupole, or as tandem-in-time using an ion trap. Ion traps allow multiple MS (MS^n), and a triple quadrupole (TQ) allows different MS/MS scan modes, especially product ion scans, precursor or parent ion scans, and neutral loss scans. TQ mass spectrometers have been frequently used for lipid analysis. The second of their three quadrupoles can be filled with an inert collision gas for collision-induced dissociation (CID) of the analyte molecules. This setup allows product ion or daughter ion scans, which produce fragments from a defined parent ion. In a parent (or precursor) ion scan, all parent ions that give rise to a certain fragment are registered. This scan mode is used to identify lipids with common head groups or backbones (Fig. 3). In a neutral loss scan, m/z values of parent ions that produce daughter ions by the loss of a defined uncharged molecule are registered. This can be the loss of a certain fatty acid in the analysis of phospholipids, or the loss of a sugar in the analysis of glycolipids. These scan modes or combinations of them are also used for quantification of lipids in comparison usually to isotope-labeled standard substances of known concentration.

Multiple parent ion scan (MPIS) of head group and backbone (fatty acids) fragments are used for the determination of phospholipid molecular species from crude lipid extracts. Another important feature for lipid quantification by LC/MS/MS approaches is multiple reaction monitoring (MRM). Here, multiple combinations of specific precursor ion/product ion transitions can be monitored and used for the rapid and sensitive quantification of molecular lipid species.

Lipidomics,

Fig. 3 Diagnostic fragments for the identification of selected phospholipid classes by tandem MS. Phospholipids: phosphatidic acid (PA), phosphatidylcholine (PC), phosphatidylethanolamine (PE), phosphatidylglycerol (PG), phosphatidylinositol (PI), and phosphatidylserine (PS). Ion mode (+ or -), scan mode (PIS, parent ion scan; NL, neutral loss scan), and structure of fragments are given. For details, see (Hsu and Turk 2005)

PA	$[M-H]^{-}$	PIS	153 <i>m/z</i>	
PC	$[M+H]^{+}$	PIS	184 <i>amu</i>	
PE	$[M-H]^{-}$	PIS	196 <i>m/z</i>	
PG	$[M-H]^{-}$	PIS	153 <i>m/z</i>	
PG	$[M-H]^{-}$	PIS	227 <i>m/z</i>	
PI	$[M-H]^{-}$	PIS	153 <i>m/z</i>	
PI	$[M-H]^{-}$	PIS	241 <i>m/z</i>	
PS	$[M-H]^{-}$	PIS	153 <i>m/z</i>	
PS	$[M-H]^{-}$	NL	87 <i>amu</i>	

Shotgun Lipidomics

The combination of electrospray ionization and tandem MS is frequently used for direct lipid quantitation from crude extracts. Changing the experimental conditions during ESI enables intrasource separation of lipid classes (Han and Gross 2005) and the structural and quantitative analysis of molecular lipid species. Limitations are signal suppression effects during MS ionization.

Bioinformatics

The complexity of the lipidome and its regulation requires bioinformatic approaches for data processing and lipid quantitation, statistical data analysis, pathway analysis, and modeling of systems (Niemelä et al. 2009). For example, isotope correction of peak intensities is needed to get more accurate and precise data for monoisotopic masses.

Applications

Although the “lipidome” comprises the complete lipid profile, it is still not possible to identify and quantify the whole structural variety of the different lipids present in most systems by one or few methods. Nearly complete lipid compositions were determined in synaptic vesicles or viruses, and a growing number of lipids were determined in yeasts and many other sources using shotgun approaches or LC/MS. Targeted lipidomics using LC/MS/MS in combination with totals synthesis (to determine stereochemistry) and bioinformatics led to the identification of specialized proresolving mediators of inflammation, the resolvins, protectins, and maresins (Bannenberg and Serhan 2010). Many studies have become available that correlate lipid profiles with human diseases and physiological processes (Oresic et al. 2008; Bou Khalil et al. 2010), and challenges for an improved understanding of the biological role of lipids are currently addressed (Wenk 2010).

Acknowledgment Support from the European Community (seventh framework program “LipidomicNet,” proposal No. 202272) is gratefully acknowledged.

Cross-References

- ▶ [Chemical Diversity of Lipids](#)
- ▶ [Fatty Acids, Alkanols, and Diacylglycerols](#)
- ▶ [Functional Roles of Lipids in Membranes](#)
- ▶ [Glycerolipids: Chemistry](#)
- ▶ [Glycolipids](#)
- ▶ [Hierarchically Structured Lipid Systems](#)
- ▶ [Infrared Spectroscopy of Membrane Lipids](#)
- ▶ [Ion-Mobility Mass Spectrometry: Biological Applications](#)
- ▶ [Lipid Bilayer Asymmetry](#)
- ▶ [Lipid Domains](#)
- ▶ [Lipid Flip-Flop](#)
- ▶ [Lipid Signaling and Phosphatidylinositols](#)
- ▶ [Lipid Trafficking in Cells](#)
- ▶ [Mass Spectrometry](#)
- ▶ [Metabolomics](#)
- ▶ [Skin Lipids](#)
- ▶ [Sphingolipids and Gangliosides](#)

References

- Bannenberg G, Serhan CN. Specialized pro-resolving lipid mediators in the inflammatory response: an update. *Biochim Biophys Acta*. 2010;1801:1260–73.
- Blanksby SJ, Mitchell TW. Advances in mass spectrometry for lipidomics. *Annu Rev Anal Chem*. 2010;3:433–65.
- Bou Khalil M, Hou W, Zhou H, Elisma F, Swayne LA, Blanchard AP, Yao Z, Bennett SA, Figeys D. Lipidomics era: accomplishments and challenges. *Mass Spectrom Rev*. 2010;29:877–929.
- Fahy E, Subramaniam S, Brown HA, Glass CK, Merrill Jr AH, Murphy RC, Raetz CR, Russell DW, Seyama Y, Shaw W, Shimizu T, Spener F, van Meer G, Van Nieuwenhze MS, White SH, Witztum JL, Dennis EA. A comprehensive classification system for lipids. *J Lipid Res*. 2005;46:839–62.
- Fahy E, Subramaniam S, Murphy RC, Nishijima M, Raetz CR, Shimizu T, Spener F, van Meer G, Wakelam MJ, Dennis EA. Update of the LIPID MAPS comprehensive classification system for lipids. *J Lipid Res*. 2009;50(Suppl):S9–14.
- Fuchs B, Süss R, Schiller J. An update of MALDI-TOF mass spectrometry in lipid research. *Prog Lipid Res*. 2010;49:450–75.
- Fuchs B, Süss R, Teuber K, Eibisch M, Schiller J. Lipid analysis by thin-layer chromatography—A review of the current state. *J Chromatogr A*. 2011;1218:2754–74.
- Han X, Gross RW. Shotgun lipidomics: electrospray ionization mass spectrometric analysis and quantitation of cellular lipidomes directly from crude extracts of biological samples. *Mass Spectrom Rev*. 2005;24:367–412.
- Hsu FF, Turk J. Electrospray ionization with low-energy collisionally activated dissociation tandem mass spectrometry of complex lipids: structural characterization and mechanisms of fragmentation. In: Byrdwell WC, editor. *Modern methods for lipid analysis by liquid chromatography/mass spectrometry and related techniques*. Champaign: AOCS; 2005.
- Ivanova PT, Milne SB, Myers DS, Brown HA. Lipidomics: a mass spectrometry based systems level analysis of cellular lipids. *Curr Opin Chem Biol*. 2009;13:526–31.
- Moore JD, Caufield WV, Shaw WA. Quantitation and standardization of lipid internal standards for mass spectroscopy. *Meth Enzymol*. 2007;432:351–67.
- Niemelä PS, Castillo S, Sysi-Aho M, Oresic M. Bioinformatics and computational methods for lipidomics. *J Chromatogr B*. 2009;877:2855–62.
- Oresic M, Hänninen VA, Vidal-Puig A. Lipidomics: a new window to biomedical frontiers. *Trends Biotechnol*. 2008;26:647–52.
- Postle AD, Hunt AN. Dynamic lipidomics with stable isotope labeling. *J Chromatogr B Analyt Technol Biomed Life Sci*. 2009;877:2716–21.
- Rinia HA, Burger KN, Bonn M, Müller M. Quantitative label-free imaging of lipid composition and packing of individual cellular lipid droplets using multiplex CARS microscopy. *Biophys J*. 2008;95:4908–14.
- van Meer G. Cellular lipidomics. *EMBO J*. 2005;24:3159–65.
- Wenk MR. The emerging field of lipidomics. *Nat Rev Drug Discov*. 2005;4:594–610.
- Wenk MR. Lipidomics: new tools and applications. *Cell*. 2010;143:888–95.

Lipid-Protein Interactions

- ▶ [Thermodynamics of Lipid Interactions](#)

Lipids

- ▶ [Chemical Diversity of Lipids](#)
- ▶ [Critical Fluctuations in Lipid Mixtures](#)
- ▶ [Electron Microscopy of Membrane Lipids](#)
- ▶ [Infrared Spectroscopy of Membrane Lipids](#)
- ▶ [Phase Transitions and Phase Behavior of Lipids](#)
- ▶ [Supported Lipid Bilayers](#)

Lipids: Isolation and Purification

C. Wolf

Applied Lipidomics Investigation, APLIPID Sarl,
Laboratoire de Lipidomique, Faculté de Médecine P et
M Curie, UPMC, Paris, France

Introduction

Pure lipid preparations in the range of 1–100 mg are commonly required for biophysical studies. This contrasts with the microgram requirements of analytical and biochemical methods. Structure studies by X-ray (Caffrey 1989) and NMR (▶ [X-Ray Scattering of Lipid Membranes](#), ▶ [NMR](#)) are especially demanding regarding the lipid amounts. As a result, scarce lipid sources such as cell cultures, which are appropriate using the microscale procedures in biochemical studies, cannot be applied. The capability to purify abundant and sufficiently purified mg samples is a critical prerequisite for biophysical biological lipid studies.

For amounts required by biophysical studies, the extraction of lipids from biological sources is challenged by chemical synthesis, which can be scaled up into the range of several hundreds of milligram. However, synthetic lipids form a single molecular species in contrast with biological lipids which are

comprised of a variety of molecular species with different fatty acyl chains. Indeed, a single molecular structure exhibits clear-cut phase cooperativity at the thermotropic and lyotropic transition lines of the phase diagram, in contrast with the broad transitions undergone by polydisperse lipid classes extracted from biological sources (Koynova and Caffrey 1994; Caffrey 1989; for example, see www.lipidat.tcd.ie) (▶ [Differential Scanning Calorimetry \(DSC\), Pressure Perturbation Calorimetry \(PPC\), and Isothermal Titration Calorimetry \(ITC\) of Lipid Bilayers](#)). The interpretation of biophysical observations for synthetic lipids takes great advantage of the characteristic values detected in the narrow intervals upon which the molecular regime is changed. However, studies conducted with synthetic lipids may not be reliable to judge the behavior of a biological material. Comparison and confirmatory studies are required to establish the relevance of synthetic lipids to more complex mixtures.

A first step in the preparation of biological lipids is the selection of appropriate sources. Ideally, the source should be abundant, commercially available, and sufficiently enriched in the lipid of interest (Christie 1993). The conditions are fulfilled for most neutral lipids extracted from oil, milk, or storage tissues (e.g., white adipose tissue, oil processed from seeds and nuts). Polar lipids may be prepared as by-products of “degumming” these crude oils prepared for neutral lipids extraction in a prepurified grade on an industrial scale. Technologies of soybean, canola, and sunflower are examples of trait-enhanced oilseeds with alteration of the molecular species profile (Flickinger 2007). Preparation from animal tissues with a particular lipid metabolism may be also a potential source. For an example, fatty fishes of cold oceanic areas have been investigated for their rich content in polyunsaturated omega-3 lipids (▶ [Essential Fatty Acids](#)), lipophilic vitamins A and D, and antioxidants (Cabrini et al. 1992). To identify a source of particular lipids, the empiric knowledge of an activity of many crude lipid preparations is generally taken in historical and medicinal practices. Interesting physicochemical activities can be also traced back with the specialist eye in the empiric usages of the culinary practices and recipe, cosmetics, lubricants, and even as partially defined reagents in the laboratory. The use of lipids extracted from their biological source points to remarkable biophysical properties. Rich sources have been identified,

and a list would provide a historical perspective on the efforts of the preparative biochemistry of lipids during the last two centuries. A few examples are illustrative of such efforts as egg yolk containing lecithin used as an emulsifier; spermaceti with cosmetics usage (spermaceti is a mixture of palmitoyl-cetyl ester and triglycerides which acts to modify the buoyancy in the sperm whale head during diving) (Clarke 1970; Clarke 1978); the central nervous system white matter used as a binder of sauces which contains the heat-resistant sphingomyelin of myelin sheath (their usage has been proscribed after the bovine spongiform encephalitis episode); the so-called cephalin, a mixture of phosphatidylethanolamine and phosphatidylserine extracted from the central nervous gray matter which was used mixed with kaolin or cholesterol for coagulation tests (Pohle and Stewart 1941; Chargaff 1937); gangliosides named after extraction from the spinal ganglia (Burmester 1946); cerebrosides from a dry extract called “protagon” comprised in the “mechanical mixture” of lipids prepared from the ox brain (Gamgee and Blankenhorn 1879; Pearson 1914; Robson 1951) (► [Glycosphingolipids](#)); beef liver lipid extracts containing most of the glycerophospholipid classes (Spencer and Schaffrin 1964; Youngs and Cornatzer 1963), sterol intermediate metabolites (e.g., the precursor of cholesterol, 7-dehydrocholesterol), and bile acids; and adrenal glands that have also been a long-time source for crude steroid preparations cited in the pharmacopeia before the “BSE” epizooty.

The selection of unexpected sources of lipids with a potential biophysical application requires a detailed review of the literature. For this purpose, the query in the large medical data banks for storage diseases (OMIM www.ncbi.nlm.nih.gov/omim and Orphanet <http://www.orpha.net>) is especially fruitful for identifying the multigram accumulation of glycolipids (e.g., preparation of GM2 from the spleen of Gaucher patients affected by lysosomal deficit). Similarly, the accumulation of very long-chain fatty acids (24–26 carbon atoms) or branched fatty acid such as phytanic acid can be exploited in the peroxisomal deficits. Fluorescence studies with lipid molecular probes (e.g., parinaric acid) have also benefited from the availability of botanical data banks to pinpoint a particular

source (e.g., the nut of *Parinarium glaberrimum* from Fiji and Palau Islands as a rich source of the conjugated tetraene fatty acid (Sklar et al. 1981)).

Hemi-synthesis starting from prepurified biological lipid is an alternative workflow combining the advantages of abundant starting material with efficient enzyme transformation. The method may be illustrated by two examples: (1) phosphatidyl-ethanolamine, -glycerol, -ethanol, and -butanol can be prepared by trans-phosphatidylation from the abundant egg yolk phosphatidylcholine by phospholipase D (Yu et al. 1996) and (2) asymmetric molecular species of PC can be prepared by phospholipase A2 deacylation followed by reacylation with a short-chain fatty acid (Huang 1990). The asymmetric phosphatidylcholine shows various interdigitated bilayer arrangements (► [Lipid Bilayer Asymmetry](#)). Noticeably, hemi-synthesis preserves the stereochemistry characteristics of the biological compound.

Extraction using Soxhlet methodology is appropriate for milligram to gram lipid preparations. The derived methods are iterative processes where a solvent heated continuously to reflux is condensed and repeatedly drained through the lipid containing sample (Luque de Castro and Priego-Capote 2010). A broad variety of devices are available commercially to allow small and large solvent volumes and warm or hot extraction. Importantly, a variety of solvents with safe and minimum volumes (chloroform, hexane or cyclohexane, petroleum ether, diethyl ether) can be used under an inert atmosphere preventing oxidation of the unsaturated lipids. The hydrolysis of the raw homogenized lipid-containing material as well as microwave- and ultrasound-assisted extraction can be processed in the same vessel that is eventually used for solvent extraction. The process can be automated and monitored by a computer to allow the unattended and time-consuming (several hours) repetitive operation. The functioning is depicted in the website of equipment providers (e.g., see <http://www.buchi.com> and <http://www.foss.dk>).

Methods derived from “solvent partition” allow many research laboratory-scaled preparations of microgram to mg lipid amounts with a clear-cut preference. The partition into apolar solvent of amphiphilic



lipids (e.g., anionic phospholipids) is favored by changing pH and salt composition of the hydroalcoholic mixture separating after the more apolar solvent partition. Because a concentrated homogenate may be used as a starting material for a “quantitative” preparation, a difficulty arises if abundant tissue proteins accumulate at the interface (Folch et al. 1957). The method has been adapted to diluted aqueous suspensions (Bligh and Dyer 1959). Chloroform (and chlorinated solvents) partition, although established as a reference method, requires unacceptable volumes of toxic solvent for scaling up to a preparative scale (Matyash et al. 2008). An alternative method has been proposed, using the nonchlorinated solvent methyl-*tert*-butyl ether as the apolar phase (Matyash et al. 2008). In contrast with chloroform, the low density of this solvent allows the extraction of lipids from the upper layer that can be collected easily by automated robot pipette without risk of a contamination by proteins around the needle pipette.

Specific methods have been also set up for industrial preparation of particular lipids. For example, the soy lecithin fraction is obtained in the process of degumming crude soy oil with a purity around 20% phosphosphatidylcholine, 20% phosphatidylethanolamine, and 10% phosphatidylinositol. The phospholipids are mixed with mucilaginous compounds to form the so-called gum of soybean oil. The world production of soy lecithin fraction is estimated between 200,000 and 300,000 t (<http://www.soyinfocenter.com>) with major industrial uses related to their physical property as a food additive in margarine for antispatter and as an emulsifier, in chocolates, caramels, and coatings, to control viscosity, crystallization, and sticking, and in instant foods such as cocoa powders, coffee creamer, and instant breakfast for wetting, dispersing, and emulsifying. The crude lecithin surfactant preparation is also used in cosmetics, pharmaceuticals, coatings (paints, magnetic tape coatings, waxes), plastic and rubber industry, glass and ceramic processing, paper and printing, masonry and asphalt products, petroleum industry, metal processing, pesticides, adhesives, textiles, and leathers. Such a broad spectrum of applications underlines the usefulness of pilot biophysical studies

conducted on the biological lipid extracts at a low grade of chemical purity, in contrast with research-oriented studies.

Conclusions

For detailed methodological information, the reader is referred to the book collection entirely dedicated to lipids such as the Oily Press Lipid Library (published by PJ Barnes & Associates, PO Box 200, Bridgwater TA7 0YZ, UK). A few websites are also carefully maintained and are highly recommended for their pages describing preparation methods: www.cyberlipid.org (Ed. C. Leray), www.lipidlibrary.aocs.org (Ed. W.W. Christie), www.lipidomicnet.org (European Lipidomics Initiative), and www.lipidmaps.org (Ed. E.A. Dennis).

References

- Bligh EG, Dyer WJ. A rapid method of total lipid extraction and purification. *Can J Biochem Physiol.* 1959;37:911–7.
- Burmester CF. A comparison of brain cephalin fractions. *J Biol Chem.* 1946;165(2):577–83.
- Cabrini L, Landi L, Stefanelli C, Barzanti V, Sechi AM. Extraction of lipids and lipophilic antioxidants from fish tissues – a comparison among different methods. *Comp Biochem Physiol.* 1992;101B:383–6.
- Caffrey M. The study of lipid phase transition kinetics by time-resolved X-ray diffraction. *Annu Rev Biophys Biophys Chem.* 1989;18:159–86.
- Chargaff E. The occurrence in mammalian tissue of a lipid fraction acting as inhibitor of blood clotting. *Science.* 1937;85:548–9.
- Christie WW. Preparation of lipid extracts from tissues. In: Christie WW, editor. *Advances in lipid methodology - Two.* Dundee: Oily Press; 1993. p. 195–213.
- Clarke MR. Function of the spermaceti organ of the sperm whale. *Nature.* 1970;228:873–4.
- Clarke MR. *J Mar Bio Ass UK.* 1978;58:1–17.
- Flickinger BD. Utilizing biotechnology in producing fats and oils with various nutritional properties. *J AOAC.* 2007; 90:1465–9.
- Folch J, Lees M, Sloane Stanley GH. A simple method for the isolation and purification of total lipids from animal tissues. *J Biol Chem.* 1957;226:497–509.
- Gangee A, Blankenhorn E. On protagon. *J Physiol.* 1879;2: 113–31.
- Huang C. Mixed-chain phospholipids and interdigitated bilayer systems. *Klin Wochenschr.* 1990;68:149–65.



- Koynova R, Caffrey M. Phases and phase transitions of the glycolipids. *Chem Phys Lipids*. 1994;69:181–207.
- Luque de Castro MD, Priego-Capote F. Soxhlet extraction: past and present panacea. *J Chromatogr A*. 2010;1217:2383–9.
- Matyash V, Liebisch G, Kurzchalia TV, Shevchenko A, Schwudke D. Lipid extraction by methyl-tert-butyl ether for high-throughput lipidomics. *J Lipid Res*. 2008;49:1137–46.
- Pearson AL. A comparison between the molecular weights of protagon and of the phosphatide and cerebrosides obtainable from it. *Biochem J*. 1914;8:616–27.
- Pohle FJ, Stewart JK. The cephalin cholesterol flocculation test as an aid in the diagnosis of hepatic disorders. *J Clin Invest*. 1941;20:241–7.
- Robson JT. Protagon granules in the normal sciatic nerve with some observations on the greater splanchnic nerve. *J Neuropathol Exp Neurol*. 1951;101:77–81.
- Sklar LA, Hudson BS, Simoni RD. Parinaric acid from *Parinarium glaberrimum*. *Methods Enzymol*. 1981;72:479–82.
- Spencer WA, Schaffrin R. The isolation of beef sphingomyelins. *Can J Biochem Physiol*. 1964;42:1659–75.
- Youngs JN, Cornatzer WE. Phospholipid composition of mouse, beef pig, cat and hamster tissues. *Comp Biochem Physiol*. 1963;16:257–9.
- Yu CH, Liu SY, Panagia V. The transphosphatidylase activity of phospholipase D. *Mol Cell Biochem*. 1996;157:101–5.

Lipopolysaccharides: Physical Chemistry

Klaus Brandenburg and Thomas Gutschmann
Research Center Borstel, LG Biophysics, Borstel,
Germany

Synonyms

[Endotoxins](#); [LPS](#)

Definition

Lipopolysaccharides (LPS) belong to the class of glycolipids and are membrane-forming constituents of the outer membrane of Gram-negative bacteria.

Basic Characteristics

Basics

Whereas in most cellular membranes the main amphiphilic compounds constituting the lipid matrix are phospholipids, in many membrane systems also, other lipid species are found. To this class belong glycolipids, which have a sugar moiety as head group, ranging from mono- to polysaccharides. Due to their particular physicochemistry, these molecules might have a variety of different functions such as cell recognition, adhesion, and signaling. One important glycolipid is lipopolysaccharide (LPS, endotoxin) from Gram-negative bacteria, which constitutes the outer leaflet of their outer membrane. LPS is made responsible for the high permeability barrier of the outer membrane, in particular against hydrophobic drugs, and is – after the release from the bacteria due to cell division or the action of components of the defense system or antibiotics – one of the strongest stimulators of the human immune system known. This property may be beneficial at low LPS concentrations but lead to severe pathophysiological effects at high LPS concentrations such as sepsis, severe sepsis, and endotoxic shock with high death rates at critical care units (Rietschel et al. 1994).

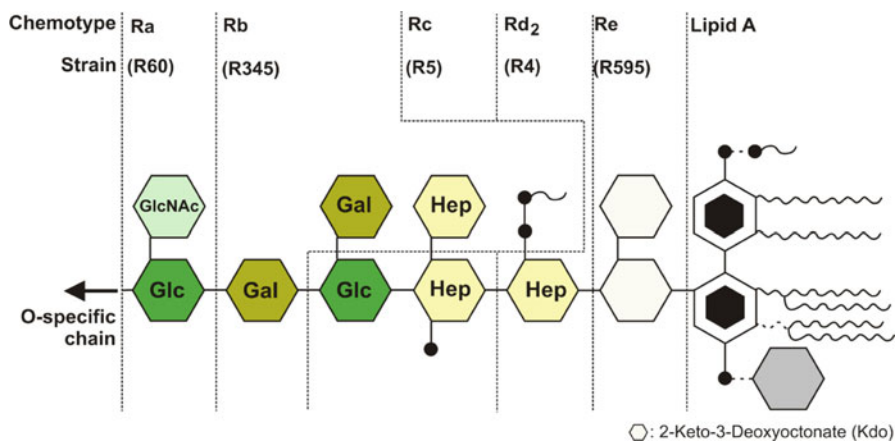
LPS Chemistry

The chemical structure of enterobacterial LPS can be divided into three parts, the lipid A moiety, the “endotoxic principle” of LPS, the oligosaccharide core differing for the various rough mutant LPS (R-LPS) and the O-antigen (smooth form S-LPS, see [Fig. 1](#) for strains from *Salmonella enterica* serovar Minnesota). The chemical heterogeneity is low for the first part (“conservative structure”), medium for the second part, and high for the latter. The immunostimulatory activity is nearly identical for all rough mutant and S-LPS, which implies that the lipid A moiety is the decisive unit for bioactivity (Rietschel et al. 1994). Lipid A from enterobacterial LPS consists of a diglucosamine moiety phosphorylated at



Lipopolysaccharides: Physical Chemistry,

Fig. 1 Chemical structures of lipopolysaccharides from rough mutant Re through Ra from *Salmonella enterica* serovar Minnesota (parenthesis: strains). Linked to LPS is a polysaccharide portion (O-antigen) having a high heterogeneity for different strains and genera

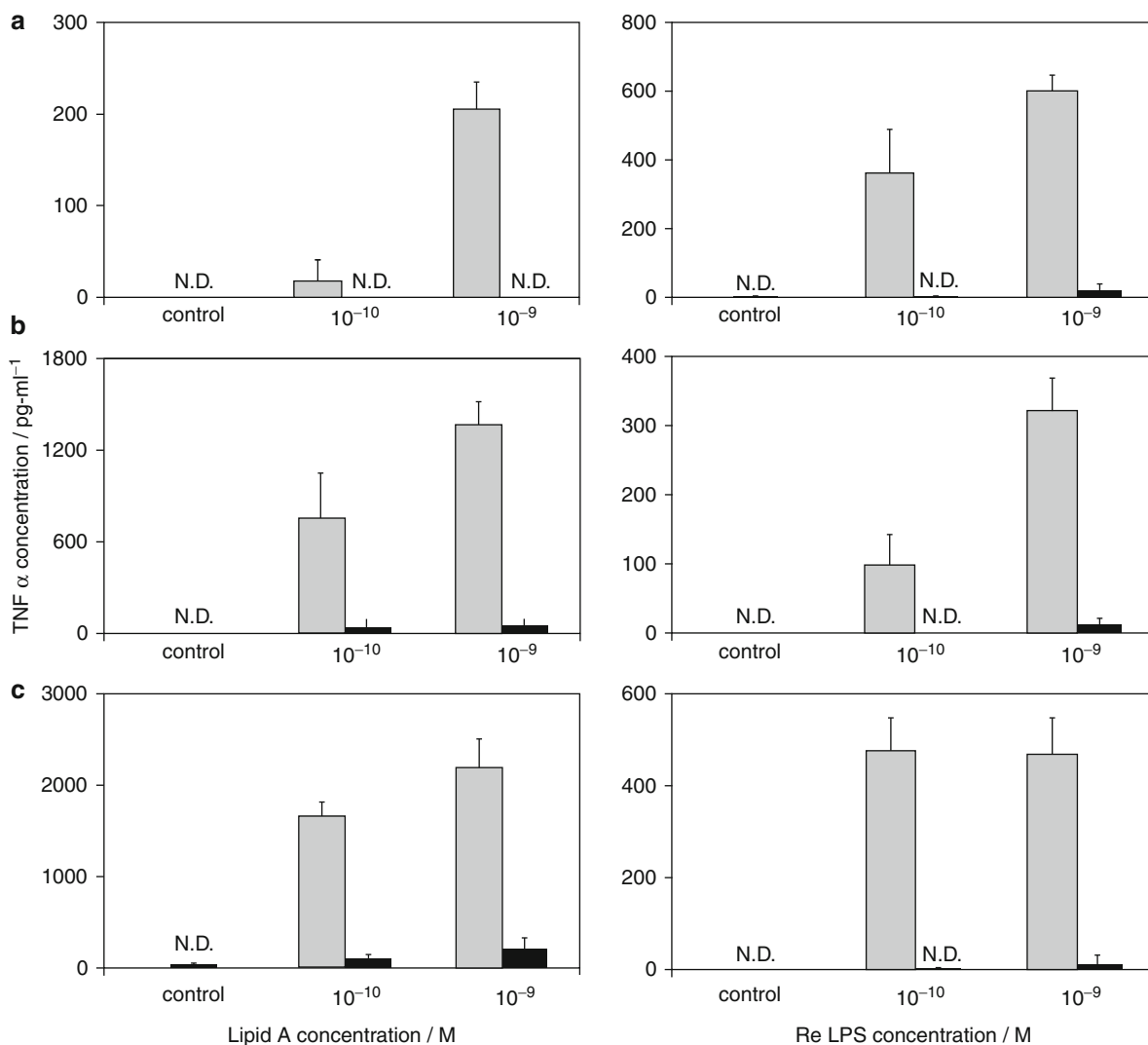


position 1 and 4' and acylated in positions 2, 3, and 2',3' with up to seven hydroxyl fatty acids, mostly of length C14.

LPS Physicochemistry

The critical micellar concentration (CMC), i.e., the concentration at which the aggregates dissolve into monomers, can be estimated to be lower than the nanomolar range (Gutsmann et al. 2007). Since at these concentrations the biological activities start, it can be concluded that an aggregated state of LPS is the prerequisite for bioactivity. This has been proven actually, as shown in Fig. 2, in which the tumor-necrosis-factor- α -inducing capacities in human mononuclear cells of lipid A (left) and deep rough mutant LPS (right) as monomers and as aggregates are compared, under different conditions of serum and also in the presence of lipopolysaccharide-binding protein (LBP) (Mueller et al. 2004). Differing results in literature, in which monomers were described to be the active unit, were obtained with inadequate methods, e.g., by using metabolically ³H-labeled LPS, which has severe restrictions due to radiation damage. The details of these investigations are discussed in reviews (Gutsmann et al. 2007; Brandenburg et al. 2010).

The number of acyl chains governs decisively the bioactivity of LPS, with complete activity for hexa- and hepta-acyl lipid A, only very low activity for penta-acyl lipid A and no activity for tetra-acyl lipid A. For an explanation of these surprising results, the molecular conformation of the different species must be considered: It could be shown that hexa- and hepta-acyl lipid A adopt cubic inverted aggregate structures, leading to a conical shape of the single molecules within the aggregates – the hydrophobic part has a higher cross section than the hydrophilic part. The two lower acylated lipid A adopt multilamellar aggregate structures characteristic for a cylindrical shape of the single molecules, concomitant with absence of agonistic, but exerting antagonistic, activity against the action of agonistic LPS. In conically shaped lipid A, the diglucosamine backbone has a high inclination angle with respect to the direction of the acyl chains, whereas in cylindrically shaped lipid A, there is no or only a small inclination angle. Also the binding of the acyl chains to the two glucosamines is of relevance, the 4/2 binding pattern (4 to the non-reducing and 2 to the reducing glucosamine part) leads to high, whereas the 3/3 configuration leads to no agonistic, but antagonistic, activity (Fig. 3). A summary of these interrelationships is demonstrated in Fig. 3 for selected compounds with variations in the lipid



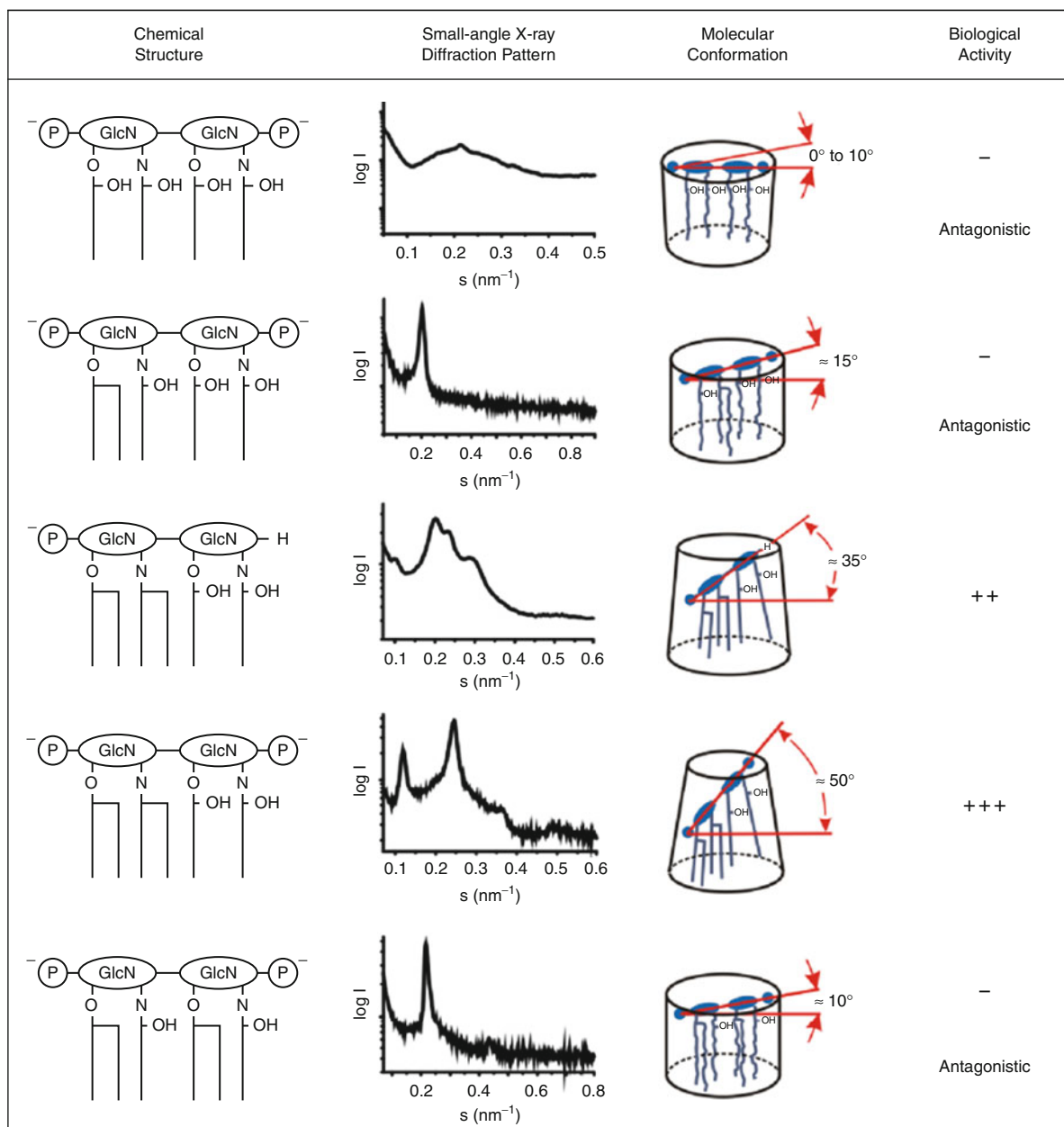
Lipopolysaccharides: Physical Chemistry, Fig. 2 Induction of tumor-necrosis-factor- α in human mononuclear cells by lipid A and LPS Re from *Salmonella enterica* serovar Minnesota Re (strain R595) by monomers (dark bars) and aggregates (light bars) at concentrations of 0.1 and 1 mM. N. D. not

detectable. (a) Serum-free, (b) in the presence of 100 ng/ml LBP, (c) in the presence of 4% AB serum. The monomers were produced by a dialysis chamber (With permission by ASBMB)

A acylation pattern (Gutsmann et al. 2007; Brandenburg et al. 2010).

A further physicochemical parameter possibly relevant for biological activity is the acyl chain melting behavior. It was found that a gel to liquid crystalline phase transition of the acyl chains in the range

30–37°C takes place for all enterobacterial LPS, whereas it lies at 45°C for free lipid A. This behavior could explain the observation that lipid A has a lower bioactivity than parent LPS of one to two orders of magnitude due to the much lower mobility or “fluidity” of its acyl chains at 37°C, impeding the interaction



Lipopolysaccharides: Physical Chemistry, Fig. 3 Chemical structure, small-angle X-ray scattering patterns, molecular conformation, and agonistic and antagonistic activity of various lipid A with different acylation patterns

with binding proteins (Brandenburg et al. 2010). However, a high fluidity per se does not necessarily lead to biological activity; the basic prerequisite is the conical molecular conformation as illustrated in Fig. 3.

Cross-References

- ▶ [Bacterial Lipopolysaccharide, OPS, and Lipid A](#)
- ▶ [Lipid Organization, Aggregation, and Self-assembly](#)

- ▶ [Membrane Fluidity](#)
- ▶ [Polarized Infrared Spectroscopy](#)
- ▶ [X-Ray Scattering of Lipid Membranes](#)

References

- Brandenburg K, Schromm AB, Gutschmann T. Endotoxins: relationship between structure, function, and activity. In: Wang X, Quinn PJ (eds.), *Endotoxins: structure, function, and recognition*, Subcellular biochemistry, vol. 53. Dordrecht: Springer; 2010. p. 53–67.
- Gutschmann T, Schromm AB, Brandenburg K. The physicochemistry of endotoxins in relation to bioactivity. *Int J Med Microbiol.* 2007;297:341–52.
- Mueller M, Lindner B, Kusumoto S, Fukase K, Schromm AB, Seydel U. Aggregate are the biologically active units of endotoxin. *J Biol Chem.* 2004;279:26307–13.
- Rietschel ETh, Kirikaie T, Schade FU, Mamat U, Schmidt G, Loppnow H, Ulmer AJ, Zähringer U, Seydel U, Di Padova F, Schreier M, Brade H. Bacterial endotoxin: molecular relationships of structure to activity and function. *FASEB J.* 1994;8:217–25.

Live-Cell Single-Molecule Imaging

Julie S. Biteen
Department of Chemistry 2533 Chemistry,
University of Michigan, Ann Arbor, MI, USA

Synonyms

[In vivo imaging](#); [Single-molecule imaging](#)

Definition

Live-cell single-molecule imaging refers to the investigation of single fluorescent molecules in living cells. This process can be used to determine the localization, dynamics, and structure of biomolecules in cells.

Basic Characteristics

The first single molecules were observed by absorption (Kador et al. 1999) and fluorescence emission (Orrit and Bernard 1990) over 20 years ago. The possibility of examining one molecule at a time has

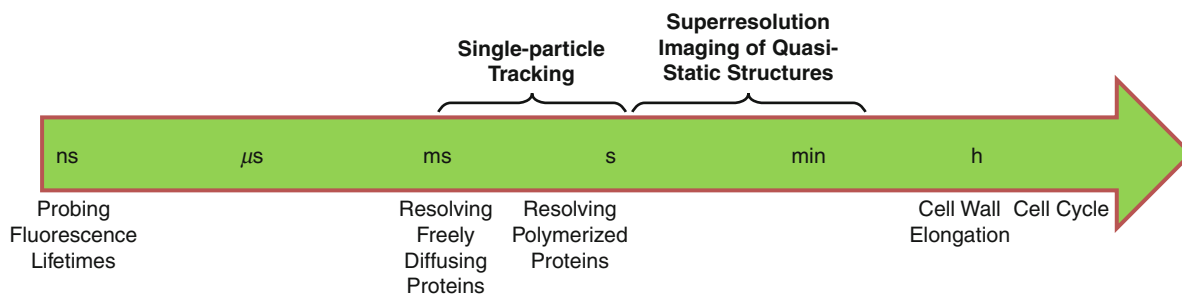
enabled investigations of properties free from ensemble averaging in heterogeneous systems, as well as sub-diffraction-limited (superresolution) imaging of dynamics and structure. With information attainable on the scale of a few nanometers, one very important application of single-molecule fluorescence (SMF) imaging has emerged as the ability to investigate biological samples, and in particular, to examine molecules within live cells.

Advantages

Fluorescence imaging, which can be performed in an optical microscope under ambient conditions, is an important instrument for cell biology as light can be used to noninvasively probe a sample with relatively small perturbation of the specimen. A host of bright probes and attachment schemes have been developed to label biomolecules with high specificity (cf. ▶ [Protein Fluorescent Dye Labeling](#); ▶ [Fluorescence Labeling of Nucleic Acids](#)); these labels include genetically encoded fluorescent proteins and organic dyes. Identifying specific molecules of interest is therefore relatively straightforward in fluorescence microscopy. Live-cell SMF imaging is often done in a ▶ [total internal reflection fluorescence microscopy \(TIRFM\)](#) configuration, though bacteria cells, with their thinner diameter, can be visualized in a widefield setup.

Live-cell imaging has several important advantages for biological studies. In particular, it enables investigations of dynamics within the physiologically relevant, crowded environment of the cell. The dynamics that have been studied in live cells range from tracking the movement of single proteins (▶ [Single-Particle Tracking](#)) to visualizing morphological changes in superstructures such as polymerized proteins (▶ [Photoactivated Localization Microscopy \(PALM\)](#)). By enabling dynamical investigations, live-cell imaging can also elucidate responses to stimuli and expression of novel proteins during the course of the cell cycle. Furthermore, even when looking at quasi-static structures in cells, live-cell imaging is free from the artifacts that have been found to plague chemically fixed cells or the ice damage that can arise from plunge-freezing.

The dynamics in a cell can be used to improve experimental conditions. When SMF imaging is combined with single-particle tracking, a mobile molecule is localized in several distinct positions over the course of an experiment, reducing the need for overexpression



Live-Cell Single-Molecule Imaging, Fig. 1 Relevant timescales for single-molecule fluorescence imaging in live bacterial cells

of that molecule. In addition, the dynamics of molecules can be used in post-processing algorithms to differentiate between highly mobile particles (e.g., freely diffusing cytoplasmic proteins) and less rapidly moving particles (e.g., membrane- or structure-bound proteins).

Challenges

Live-cell SMF experiments require some particular controls and considerations. In particular, it is of utmost importance to verify that the labeling and imaging conditions in a living cell are non-perturbative. Significant overexpression must be avoided; fortunately this is simple in SMF experiments where only a small number of fluorescently tagged molecules is desired. However, even at low expression levels, labeling can lead to mislocalizations, which must be ruled out, at the very least, by comparing live-cell results to results obtained in bulk-level antibody-stained fixed cells, electron microscopy, biochemical studies, etc. SMF investigations generally use low-intensity continuous-wave (CW) lasers, but one must still determine that these conditions do not heat or damage cells. In prokaryotic cells, this can be done by verifying that the bacteria still grow and divide following imaging.

While preparing a live-cell sample, the options for labeling are more limited than in vitro or in fixed cells. Fluorescent tags must be genetically encoded or penetrate the cell membrane. In particular, antibodies, which are very large and can polymerize, are not generally suitable for live-cell imaging. Most work to date on SMF imaging in live cells is enabled by fusions between a protein of interest and a fluorescent protein tag. Such a labeling scheme provides high specificity,

but careful attention must be paid to the effect of the fluorescent protein, which can be as large as the protein of interest, and which may tend to dimerize with other fluorescent proteins. Several small-molecule labeling schemes have emerged, including some that are compatible with live-cell imaging, yet it certainly remains a challenge in live cells to investigate biomolecules other than proteins because of the limited number of labeling schemes.

Timescales

Because the sample is a dynamic entity, the timescale of a live-cell experiment must be taken into careful consideration. There exists a trade-off between the spatial resolution for single-molecule localizations, which improves beyond the standard diffraction limit roughly as one over the square root of the number of detected photons (Thompson et al. 2002; ► [Fluorescence Imaging with One Nanometer Accuracy](#)), and the time resolution. This trade-off is further compounded for single-molecule-based superresolution imaging, such as photoactivated localization microscopy (PALM), where the resolution of an image is defined as the separation distance between neighboring localization events; this resolution is improved by increasing the number of fluorophores that are localized and therefore the number of imaging frames. Therefore, though the electron-multiplying charge-coupled detector (EMCCD) cameras typically used can operate as fast as ~ 50 frames/s, very fast processes may not be resolved with SMF imaging. However, slower (longer-exposure) experiments are not possible in live-cell imaging as most processes are dynamic and a compromise must therefore be found. [Figure 1](#) shows the timescales of some typical processes in bacterial cell



imaging; SMF experiments can resolve events that occur on the timescale of approximately 10 ms–10 min.

Applications

Live-cell single-molecule imaging has been successfully applied to prokaryotic and eukaryotic cells. Experiments on bacterial cell imaging (Biteen and Moerner 2010), protein expression in bacterial cells (Xie et al. 2008), and single-particle tracking in mammalian cells (Patterson et al. 2010) have been reviewed extensively. The majority of these experiments are done on proteins genetically fused to a fluorescent protein, which may be photoswitchable to permit high-resolution structural reconstructions (Biteen et al. 2008) or tracking of multiple single particles (Shroff et al. 2008). These experiments have led to discoveries including quantifying protein motion and diffusion, measuring superstructures, investigating the expression of low copy-number proteins, and evaluating transport in membranes and cells.

Cross-References

- ▶ [Fluorescence Imaging with One Nanometer Accuracy](#)
- ▶ [Fluorescence Labeling of Nucleic Acids](#)
- ▶ [Photoactivated Localization Microscopy \(PALM\)](#)
- ▶ [Protein Fluorescent Dye Labeling](#)
- ▶ [Single-Particle Tracking](#)
- ▶ [Total Internal Reflection Fluorescence Microscopy for Single-Molecule Studies](#)

References

- Biteen JS, Moerner WE. Single-molecule and superresolution imaging in live bacteria cells. *Cold Spring Harb Perspect Biol.* 2010;2:a000448.
- Biteen JS, Thompson MA, Tselentis NK, Bowman GR, Shapiro L, Moerner WE. Super-resolution imaging in live *Caulobacter crescentus* cells using photoswitchable EYFP. *Nat Methods.* 2008;5:947–9.
- Kador L, Latychevskaia T, Renn A, Wild UP. Absorption spectroscopy on single molecules in solids. *J Chem Phys.* 1999;111:8755–8.
- Orrit M, Bernard J. Single pentacene molecules detected by fluorescence excitation in a p-terphenyl crystal. *Phys Rev Lett.* 1990;65:2716–9.
- Patterson G, Davidson M, Manley S, Lippincott-Schwartz J. Superresolution imaging using single-molecule localization. *Annu Rev Phys Chem.* 2010;61:345–67.

Shroff H, Galbraith CG, Galbraith JA, Betzig E. Live-cell photoactivated localization microscopy of nanoscale adhesion dynamics. *Nat Methods.* 2008;5:417–23.

Thompson RE, Larson DR, Webb WW. Precise nanometer localization analysis for individual fluorescent probes. *Biophys J.* 2002;82:2775–83.

Xie XS, Choi PJ, Li GW, Lee NK, Lia G. Single-molecule approach to molecular biology in living bacterial cells. *Annu Rev Biophys.* 2008;37:417–44.

LOV Proteins: Photobiophysics

Aba Losi

Department of Physics, University of Parma,
Parma, Italy

Synonyms

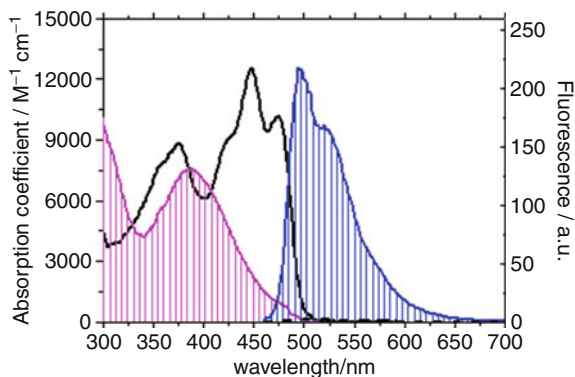
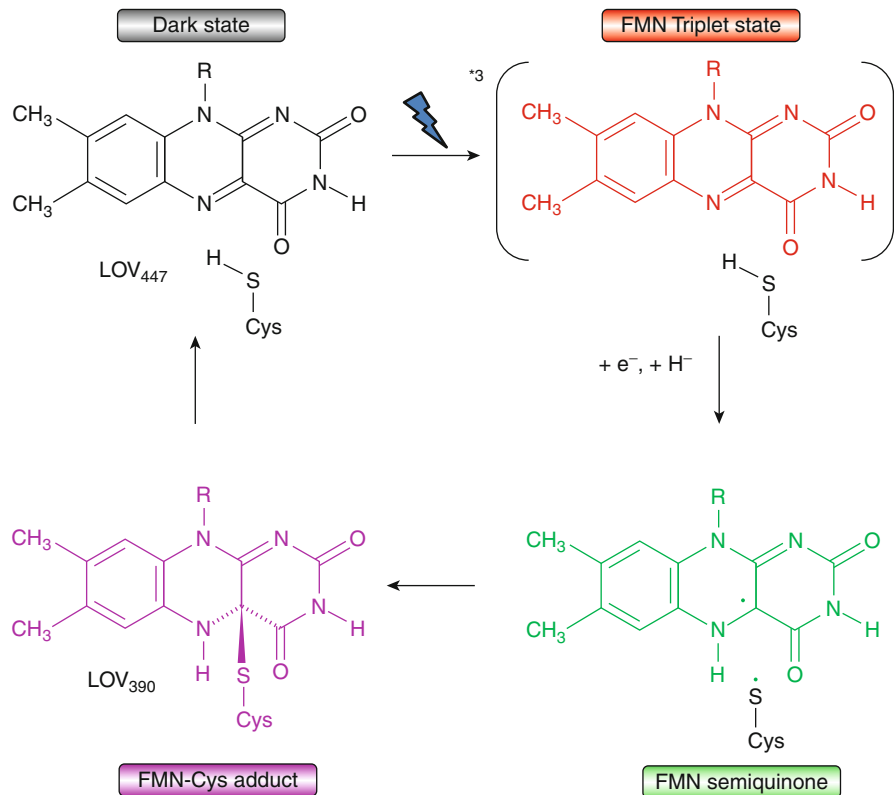
[Light, oxygen, or voltage domains \(LOV\)](#)

Definition

LOV proteins are UVA/Blue-light photoreceptors employing LOV (light, oxygen, voltage) domains as photosensory modules. They are wide spread among plants, fungi, bacteria, and archaea. LOV domains are α/β folds of ca. 110 amino acids and bear a fully oxidized FMN (flavin mononucleotide) chromophore, noncovalently bound in the dark-adapted state of the protein. Upon photoexcitation, FMN forms a covalent bond with a nearby cysteine (between the cys-SH group and position 4a of the flavin) during the decay of the FMN triplet state (Fig. 1). According to its absorption maximum, the adduct is referred to as LOV₃₉₀ (Fig. 2) and is supposed to be the signaling state in vivo. In most LOV proteins, LOV₃₉₀ thermally recovers to the dark-adapted state, LOV₄₄₇. Signal propagation from the LOV core to effector domains or protein partners occur via the antiparallel β -scaffold and helical caps flanking the LOV core (Fig. 3). The peculiar photobiophysics of LOV proteins can be exploited for advanced biotechnological applications, such as fluorescence imaging, super-resolution microscopy, and optogenetics (Fig. 4).

LOV Proteins: Photobiophysics,

Fig. 1 Proposed photocycle of LOV domains after blue-light excitation of the dark-adapted state. Subscripts indicate the absorption maxima as shown in Fig. 2



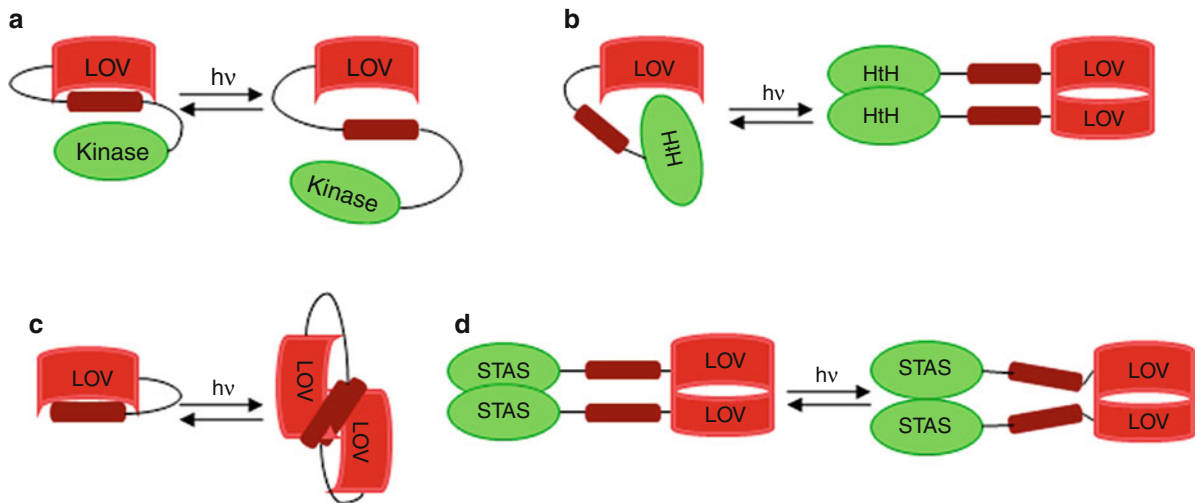
LOV Proteins: Photobiophysics, Fig. 2 Spectral properties of a LOV domain (here the *Bacillus subtilis* protein YtvA) in the dark-adapted state (*dark line*) and in the FMN-Cys adduct. In *blue*, the fluorescence spectrum of the dark-adapted state. Fluorescence is totally lost in the adduct

Basic Characteristics

The Photocycle of LOV Proteins

A LOV (Light, Oxygen, Voltage) domain is a small-sized (ca. 110 aa) UVA/blue-light sensing module, first characterized in the plant photoreceptor phototropin,

a light-activated kinase (Briggs 2006). LOV domains, photosensitive thanks to a bound flavin chromophore (Edwards 2006; Kritsky et al. 2010; ► [Flavins](#)), are largely distributed in the living world, identified in plants, bacteria, archaea, and fungi (Herrou and Crosson 2011). In prokaryotes they are present in 10–12% of the sequenced genomes (Losi and Gärtner 2012). LOV domains, belonging to the PAS (PerArntSim) superfamily, present a characteristic α/β fold, where the secondary structure elements are named $A\beta B\beta C\beta D\alpha E\alpha F\alpha G\beta H\beta I\beta$, starting from the N-terminus (Zoltowski and Gardner 2011). The five β -strands form an extended and twisted antiparallel β -scaffold (Losi 2007), in most cases flanked by helical regions, located N- and/or C-terminally to the LOV core. The photocycle of LOV domains starts from the dark-adapted state LOV₄₄₇, in which flavin mononucleotide (FMN) is noncovalently bound in its fully oxidized state. The photocycle involves the formation a covalent bond between FMN (position 4a) and a conserved cysteine (LOV₃₉₀), also referred to as adduct or photoadduct, via the short μ s decay of the FMN triplet state. Formation of LOV₃₉₀ involves the



LOV Proteins: Photobiophysics, Fig. 3 Signal propagation mechanisms in LOV proteins. (a) In Asphot1 (*Avena sativa* phototropin 1), light relieves inhibition of the kinase activity by promoting undocking of the J-linker helix, mostly clamped at the β -scaffold of LOV2 in the dark; (b) in ELOV-HtH (*Erythrobacter litoralis* LOV-HelixTurnHelix) protein, dimerization is blocked in the dark by direct contact between the LOV

and HtH domains. Light promotes dimerization by weakening this contact, allowing HtH binding to target DNA; (c) in the short-LOV protein NcVVD (*Neurospora crassa* Vivid), light promotes dimerization by partial undocking of the helical Ncap; (d) In BsYtvA (*Bacillus subtilis* YtvA) a torquing of the J-linker helix might activate the effector/secondary switch STAS domain in the protein dimer

establishment of new C(4a)-S and N-H(5) bonds, most probably via the fast decay of a FMNH⁻-H₂CS^{*} radical pair (Fig. 1). With few exceptions, for which the photoaddition reactions is virtually irreversible, LOV₃₉₀ thermally decays to the parent state with breakage of the covalent bond, on the s-to-h timescale at room temperature (Losi and Gärtner 2012). The driving force for the dark-recovery reaction results from the high energy content of LOV_{Lit}, ca. 110–140 kJ/mol, indicative for a strained protein conformation. As an example, Fig. 2 reports photocycle and spectral parameters of the bacterial LOV protein YtvA. The dynamics of the photocycle can be regulated by introducing mutations in the vicinity of the chromophore, chiefly involved in the hydrogen bonds network stabilizing FMN in the cavity (Raffelberg et al. 2011), but also by changing more peripheric amino acids (Losi and Gärtner 2012).

Besides thermal recovery, there are evidence for photochromicity in LOV domains, whereby LOV₃₉₀ can be photoexcited, yielding the parent state in a fast but poorly efficient process (vide infra).

Signal Transmission in LOV Proteins

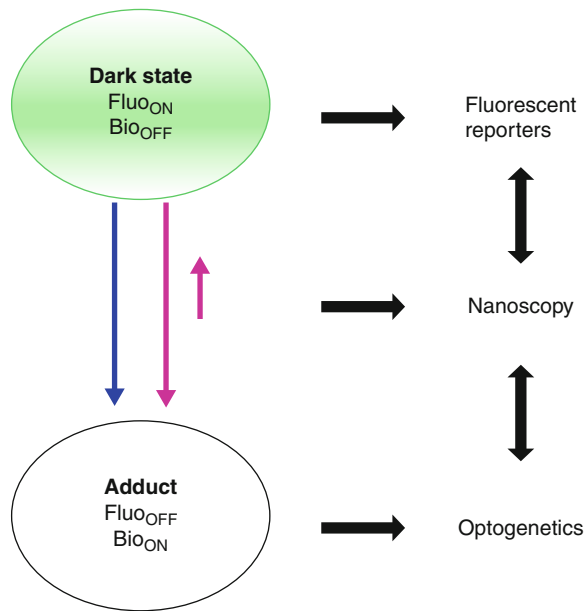
LOV proteins are highly modular, with diverse effector domains linked to the LOV core, including kinases,

phosphatases, second-messenger regulators, or DNA-binding motifs (Herrou and Crosson 2011; Zoltowski and Gardner 2011; Losi and Gärtner 2012). Standalone, extended LOV domains are also present in many instances. The photochemical event triggers intraprotein signal propagation via conformational changes that travel from the chromophore cavity to molecular surfaces, where they affect interdomain or protein-protein interactions.

The extended, antiparallel β -sheet of the LOV core is a chromophore/environment interface: on one side it hosts residues directly interacting with the isoalloxazine ring of FMN (Raffelberg et al. 2011), and on the other side it communicates with helical regions flanking the LOV core (N-terminal cap and/or J α -linker) or it interacts directly with effector domains (Zoltowski and Gardner 2011; Losi and Gärtner 2012).

Photo-perturbation of the LOV core β -sheet mediates signal propagation via different mechanisms, involving the N-terminal cap and/or J α -linker to effector domains by, e.g., undocking of the J α -linker and torquing (Fig. 3).

The β -scaffold surface also participates in LOV-LOV dimerization, which in solution may be a highly dynamic phenomenon (► [Transient Grating Spectroscopy: Dynamics of Photoreceptors](#)). For example, the



LOV Proteins: Photobiophysics, Fig. 4 LOV domains biotechnology applications. The *fluorescence* of the dark-adapted state can be exploited to engineer reporter genes. *Blue-light* excitation results in adduct formation, i.e., the signaling state, that may in turn regulate a variety of metabolic processes. This feature is exploited in optogenetics. The adduct is biologically active and nonfluorescent ($\text{Fluo}_{\text{OFF}}/\text{Bio}_{\text{ON}}$), but the system can be driven into a photoequilibrium by means of *violet/UVA* light, with a very low yield for recovery of *fluorescence*. This photoswitching feature has potential application in super-resolution *fluorescence* microscopy (nanoscopy)

fungal LOV protein VVD (Vivid) is monomeric in the dark and tends to undergo a light-driven dimerization, but the lit form itself appears to be a rapid monomer-dimer equilibrium (Fig. 3c).

Advanced Biophysical Applications: Microscopy, Nanoscopy, and Optogenetics

The fluorescence of the dark-adapted state, LOV_{447} , allows applications of LOV proteins in fluorescence imaging (► [Flavin Mononucleotide-Binding Fluorescent Proteins](#)). As fluorescence is lost upon formation of the LOV_{390} adduct, this last process can be annihilated by mutating the reactive cysteine. Compared with green fluorescent proteins and its derivatives, where chromophore formation is oxygen dependent, LOV domains are advantageous for applications in anaerobic or microaerobic environments as well as for investigating viral infections of plants. Since the latter is considered to be the biologically active (signaling) state, it may be stated that fluorescence is ON when

the biological photoresponses are OFF, and vice versa, i.e., LOV_{Dark} and LOV_{Lit} can be labeled $\text{Fluo}_{\text{ON}}\text{Bio}_{\text{OFF}}$ and $\text{Fluo}_{\text{OFF}}\text{Bio}_{\text{ON}}$, respectively (Fig. 4).

Interestingly, an early report on the LOV2 domain from the phy3 receptor of *Adiantum* indicated that for this protein the light adapted species can be photoconverted in good yield to the dark adapted, fluorescent state, by shining near UV-violet light on the photoreceptor (Kennis et al. 2004). The finding of photoswitching phenomena in LOV domain proteins went largely unnoticed and the potential of this property was almost completely unexplored. The availability of genetically encodable fluorescent reporters with photochromic properties is of fundamental relevance to super-resolution microscopy (nanoscopy) studies, based on the stochastic photoactivation of single molecules, like in FPALM (Patterson et al. 2010; ► [Photoactivated Localization Microscopy \(PALM\)](#)).

Optogenetics indicates the use of light-gated proteins originally designed by nature as tools to photomodulate cell activities. Prompted by the success of the retinal-protein channelrhodopsin that provides a nontoxic, inheritable mechanism for the selective manipulation of cell membrane potential, optogenetics applications are now also becoming available with LOV proteins and other flavin-binding photoreceptors (Losi and Gärtner 2012). Given the modularity of LOV proteins, a number of light-regulated functions are at hand, such as turnover of second messengers, kinase and phosphatase activities, gene activation.

It is also noted that LOV proteins have the potential to function at the same time as optogenetic tools (initiating a biological function, e.g., enzyme activities) AND as photoswitchable proteins in super-resolution microscopy, given the possibility to establish a photoequilibrium between the LOV_{447} and LOV_{390} . Although this opportunity needs to be demonstrated in living cells, it represents a novel potential application of LOV proteins.

Cross-References

- [Flavin Mononucleotide](#)
- [Flavin Mononucleotide-Binding Fluorescent Proteins](#)
- [Flavins](#)
- [Photoactivated Localization Microscopy \(PALM\)](#)
- [Photoadduct](#)

- ▶ [Riboflavin](#)
- ▶ [Riboflavin 5'-phosphate \(FMN\)](#)
- ▶ [Transient Grating Spectroscopy: Dynamics of Photoreceptors](#)

References

- Briggs WR. Blue/UV-A: historical overview. In: Schäfer E, Nagy F, editors. Photomorphogenesis in plants and bacteria. 3rd ed. Dordrecht: Springer; 2006. p. 171–97.
- Edwards AM. General properties of flavins. In: Silva E, Edwards AM, editors. Flavin photochemistry and photobiology. Cambridge: RSC Publishing; 2006. p. 1–11.
- Herrou J, Crosson S. Function, structure and mechanism of bacterial photosensory LOV proteins. *Nat Rev Microbiol*. 2011;9:713–23.
- Kennis JTM, van Stokkum IHM, Crosson S, Gauden M, Moffat K, van Grondelle R. The LOV2 domain of phototropin: a reversible photochromic switch. *J Am Chem Soc*. 2004;126:4512–3.
- Kritsky MS, Telegina TA, Vechtomova YL, Kolesnikov MP, Lyudnikova TA, Golub OA. Excited flavin and pterin coenzyme molecules in evolution. *Biochemistry (Mosc)*. 2010;75:1200–16.
- Losi A. Flavin-based blue-light photosensors: a photobiophysics update. *Photochem Photobiol*. 2007;83:1283–300.
- Losi A, Gärtner W. The Evolution of flavin-binding photoreceptors: an ancient chromophore serving trendy blue-light sensors. *Annu Rev Plant Biol*. 2012;63. doi:10.1146/annurev-arplant-042811-105538.
- Patterson G, Davidson M, Manley S, Lippincott-Schwartz J. Superresolution imaging using single-molecule localization. *Annu Rev Phys Chem*. 2010;61:345–67.
- Raffelberg S, Mansurova M, Gärtner W, Losi A. Modulation of the photocycle of a LOV domain photoreceptor by the hydrogen bonding network. *J Am Chem Soc*. 2011;133:5346–56.
- Zoltowski BD, Gardner KH. Tripping the light fantastic: blue-light photoreceptors as examples of environmentally modulated protein–protein interactions. *Biochemistry*. 2011;50:4–16.

Low Angle Neutron Scattering

- ▶ [Small Angle Neutron Scattering](#)

Low Q Neutron Scattering

- ▶ [Small Angle Neutron Scattering](#)

Low-Resolution Diffraction Data

- ▶ [CNS \(Crystallography and NMR System\)](#)

LPS

- ▶ [Bacterial Lipopolysaccharide, OPS, and Lipid A](#)
- ▶ [Lipopolysaccharides: Physical Chemistry](#)

LPSVD

- ▶ [Linear Prediction in NMR Spectroscopy](#)

Lysozyme – Computational Studies

Anna Louise Bowman

Center for Drug Discovery, The Bouvé College of Health Sciences, Northeastern University, Boston, MA, USA

Synonyms

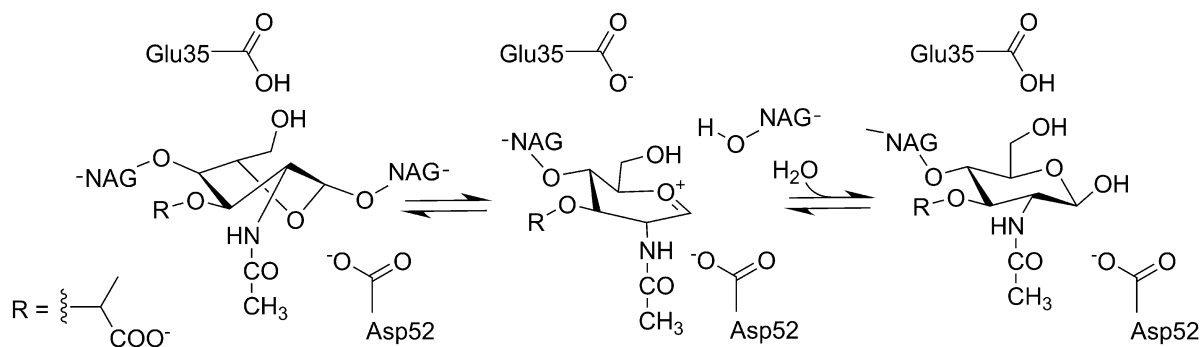
[Muramidase](#); [N-acetylmuramide glycanhydrolase](#)

Definition

Lysozyme is an enzyme (EC 3.2.1.17) which catalyzes hydrolysis of the $\beta(1-4)$ glycosidic bond between *N*-acetyl-muramic acid and *N*-acetyl-D-glucosamine and serves as an important model system for many fields of study.

Introduction

Lysozyme is a model system for many studies; hen egg white lysozyme (HEWL) was the first protein to be sequenced that contains together all the 20 amino acids, the first enzyme to have its 3D structure determined by X-ray crystallography, the first enzyme for



Lysozyme – Computational Studies, Fig. 1 The catalytic mechanism for HEWL proposed by Phillips via an oxocarbenium ion intermediate

which a detailed chemical mechanism was proposed, and the first enzyme to be studied with QM/MM methods. HEWL can be considered as one of the most influential enzymes in the field of biochemistry (Jollés 1996).

HEWL consists of a single polypeptide chain containing 129 amino acids and is linked by four disulphide bonds. A deep crevice or cleft containing the active site divides the molecule into two domains: one of them is almost entirely β -sheet structure (residues 40–85), whereas the other is comprised of the N and C-terminal segments (residues 1–39 and 101–129) and is more alpha helical in nature. The two domains are linked by an α -helix (residues 89–99).

Lysozyme hydrolyzes a component of the polysaccharide cell wall in Gram-positive bacteria, cleaving the $\beta(1-4)$ glycosidic bond between *N*-acetyl-muramic acid (NAM) and *N*-acetyl-D-glucosamine (NAG). The enzyme binds the polysaccharide in a cleft six saccharide units long, traditionally designated sites A–F (or in more systematic nomenclature –4 to +2). From X-ray crystallography (subsites A, B, and C) and model building studies (subsites E and F) most sugars were found to fit perfectly, however, the D (–1) site NAM suffered bad steric contacts with enzyme. It is thought that the D site NAM is distorted away from the chair conformation when bound to minimize this steric strain (Frey and Hegeman 2007).

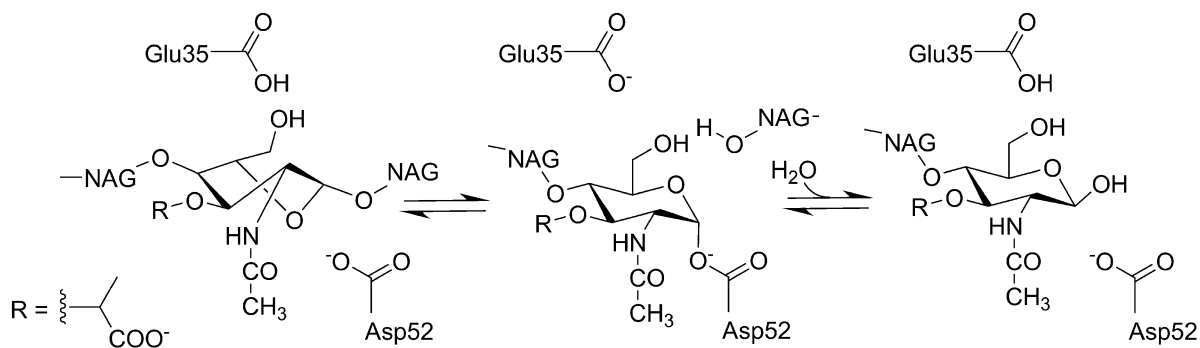
Proposed Mechanisms

The determination of the structure of HEWL led directly to the proposal of a dissociative (S_N1 -type) mechanism involving an oxocarbenium ion

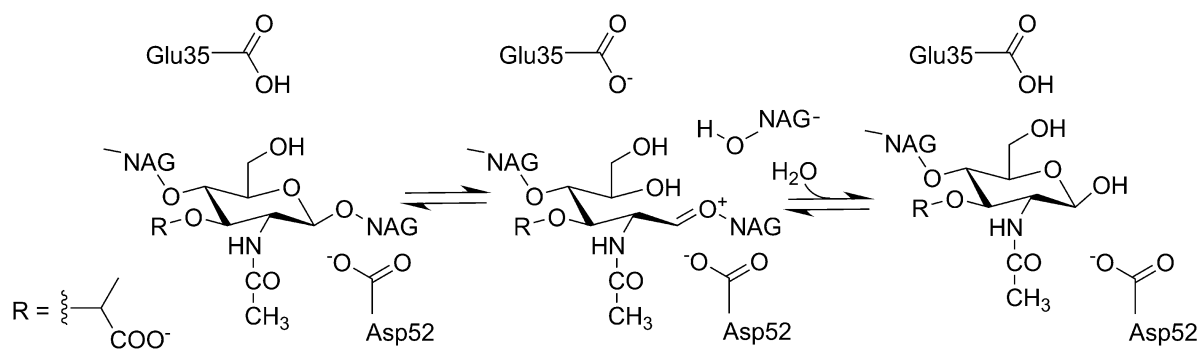
intermediate; Fig. 1. The carboxylic acid group of glutamic acid 35 was proposed to donate a hydrogen to the glycosidic oxygen atom between rings D and E (–1 and +1). This results in cleavage of the glycosidic bond and, according to Phillips, yields an ionic (oxocarbenium) intermediate. The positive charge was proposed to be stabilized by the lone pair of electrons of the ring oxygen and electrostatically by the negative charge of the carboxylate group of the neighboring Asp52. The oxocarbenium ion then reacts with a solvent water molecule and Glu35 becomes reprotonated. This mechanism had been a textbook example mainly because historical importance of lysozyme and the coherent message the structure seemed to provide.

Evidence from crystallography and electrospray ionization mass spectrometry indicates that catalysis proceeds via a covalent intermediate (Vocadlo et al. 2001). However, these results required the use of a (catalytically less competent) mutant HEWL or an unnatural substrate. The mechanism is an S_N2 -type reaction: after cleavage of the glycosidic bond the D site NAM forms a covalent intermediate with Asp52. The transition state for this S_N2 -type reaction would be an oxocarbenium ion analogous to that envisaged as the intermediate in the mechanism proposed by Phillips. In this transition state electron donation from the ring oxygen would stabilize most of the positive charge that would otherwise develop at C1. This mechanism, originally proposed by Koshland, is the generally accepted mechanism for most retaining β -glycosidases; Fig. 2.

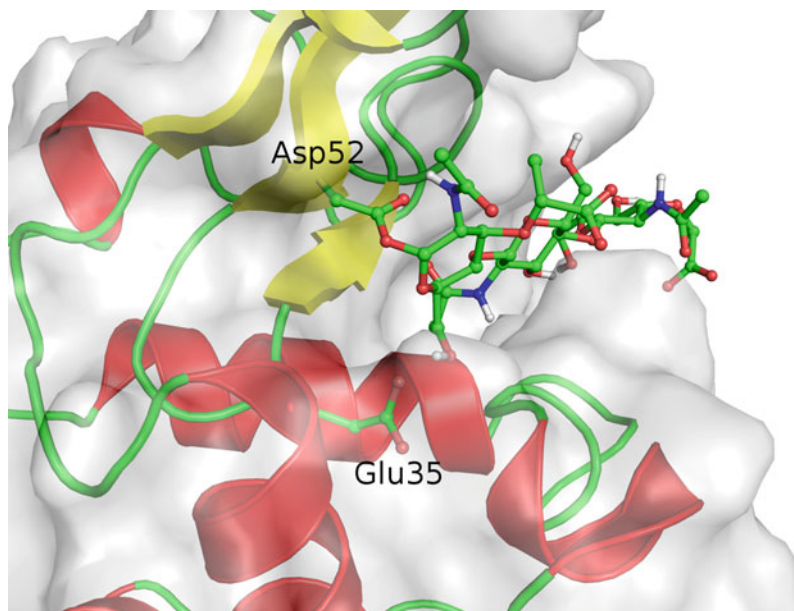
A third mechanism for HEWL in which an endocyclic bond is broken was proposed by Post and Karplus, on the basis of a 55 ps molecular dynamics



Lysozyme – Computational Studies, Fig. 2 The catalytic mechanism for HEWL proposed by Koshland via a covalent intermediate



Lysozyme – Computational Studies, Fig. 3 The catalytic endocyclic mechanism for HEWL proposed by Post and Karplus



Lysozyme – Computational Studies, Fig. 4 The covalent intermediate formed in HEWL from QM/MM molecular dynamics simulations (Bowman et al. 2008)



simulation of a lysozyme complex with NAM₆. This mechanism does not require distortion of the NAM D site ring. The initial step is protonation of the ring oxygen O5 by Glu35. Cleavage of the endocyclic C1–O5 bond then forms the acyclic oxocarbenium ion intermediate, which is stabilized by Asp52 (Stote et al. 1997); Fig. 3.

Reaction Modeling

The first QM/MM study of HEWL focused on the oxocarbenium ion and concluded that electronic stabilization would be paramount for formation of this proposed intermediate (Warshel and Levitt 1976). Density functional theory calculations on a small model system did not support the mechanism proposed by Phillips, and suggested that both the mechanism proposed by Koshland and that by Post/Karplus were energetically feasible (Bottoni et al. 2005). QM/MM molecular dynamics simulations on the wild-type HEWL with the natural substrate provided evidence that the reaction proceeds via a covalent intermediate (Bowman et al. 2008); Fig. 4. The transition state to breakage of the glycosidic bond resembled an oxocarbenium ion. The endocyclic mechanism was also simulated, but was found to be prohibitively high in energy compared with the exocyclic protonation mechanism.

The simulations of Bowman et al. indicate that the findings for a mutant HEWL with a fluorinated substrate (Vocadlo et al. 2001) are indeed relevant for the wild-type enzyme with its natural substrate (Bowman et al. 2008). Together experimental and computational methods indicate that the reaction in HEWL proceeds

via a covalent intermediate contrary to the previously widely accepted mechanism.

Cross-References

- ▶ [QM/MM Methods](#)
- ▶ [Quantum Mechanical Simulations of Biopolymer Vibrational Spectra](#)
- ▶ [X-Ray Diffraction and Crystallography of Oligosaccharides and Polysaccharides](#)

References

- Bottoni A, Miscione GP, De Vivo M. A theoretical DFT investigation of the lysozyme mechanism: computational evidence for a covalent intermediate pathway. *Proteins*. 2005;59: 118–30.
- Bowman AL, Grant IM, Mulholland AJ. QM/MM simulations predict a covalent intermediate in the hen egg white lysozyme reaction with its natural substrate. *Chem Commun*. 2008;37:4425–7.
- Frey PA, Hegeman AD. Lysozyme. In: *Enzymatic reaction mechanisms*. New York: Oxford University Press; 2007. p. 589–94.
- Jollés J. *Lysozymes: model enzymes in biochemistry and biology*. Basel: Birkhäuser; 1996.
- Stote RH, Dejaegere A, Karplus M. Molecular mechanics and dynamics simulations of enzymes. In: Náray-Szabó G, Warshel A, editors. *Computational approaches to biochemical reactivity*. Dordrecht: Kluwer Academic; 1997. p. 164–7.
- Vocadlo DJ, Davies GJ, Laine R, Withers SG. Catalysis by hen egg-white lysozyme proceeds via a covalent intermediate. *Nature*. 2001;412:835–8.
- Warshel A, Levitt M. Theoretical studies of enzymic reactions: dielectric, electrostatic and steric stabilization of the carbonium ion in the reaction of lysozyme. *J Mol Biol*. 1976;103:227–49.



